Chromatin Structure in Cell Differentiation, Aging and Cancer

Sima Kheradmand Kia

The research presented in this thesis was performed at the Department of Biochemistry within the Erasmus Medical Center, Rotterdam, The Netherlands.

The research has been supported by a European Commission (EC) grant "Epigenetic plasticity of the genome".

Financial support by the Erasmus MC and SSCD for the publication of this thesis is gratefully acknowledged.

Cover Design: Gazelle Pezeshkmehr

Layout: Parham & Kourosh

Printed by Wöhrmann Print Service, Zutphen

Chromatin Structure in Cell Differentiation, Aging and Cancer

Chromatine Structuur in Cel Differentiatie, Veroudering en Kanker

Proefschrift

ter verkrijging van de graad van doctor aan de
Erasmus Universiteit Rotterdam
op gezag van de rector magnificus

Prof. dr. S. W. J. Lamberts
en volgens besluit van het College voor Promoties

De openbare verdediging zal plaatsvinden op
Woensdag 3 juni 2009 om 11.45

door

Sima Kheradmand Kia

geboren te Tehran, Iran

Promotie commissie

Promotor:	Prof.dr. C.P. Verrijzer
Overige leden:	Prof.dr. F.G. Grosveld Prof.dr. R. Fodde Prof.dr. J.N.J. Philipsen

It does not matter where I am.
The sky is always mine.
Windows, ideas, air, love,
earth, all mine.
So who cares if sometimes the leaves of solitude
may grow all around.

The Footsteps of Water (Seday-e Pay-e Ab) by Sohrab Sepehri, Iranian poet (1928 - 1980)

To my elder sister
Simin

Contents

Chapter1	Introduction	9
	Outline of the thesis	26
Chapter2	Global Gene Expression Regulation by hSNF5	27
Chapter3	Cancer-associated mutations in chromatin remodeller hSNF5 promote chromosomal instability by compromising the mitotic checkpoint	45
Chapter4	SWI/SNF mediates polycomb eviction and epigenetic reprogramming of the INK4b-ARF-INK4a locus	53
Chapter5	An EZH2-Dependent Repressive Chromatin Loop Controls Human INK4a and INK4b Expression During Cell Differentiation, Aging and Senescence	63
Chapter6	Discussion and Future Prospects	83
	Summary	97
	Samenvatting	99
	Curriculum Vitae	101
	Publication list	102
	PhD portfolio	103
	Acknowledgement	104
	List of Abbreviations	106

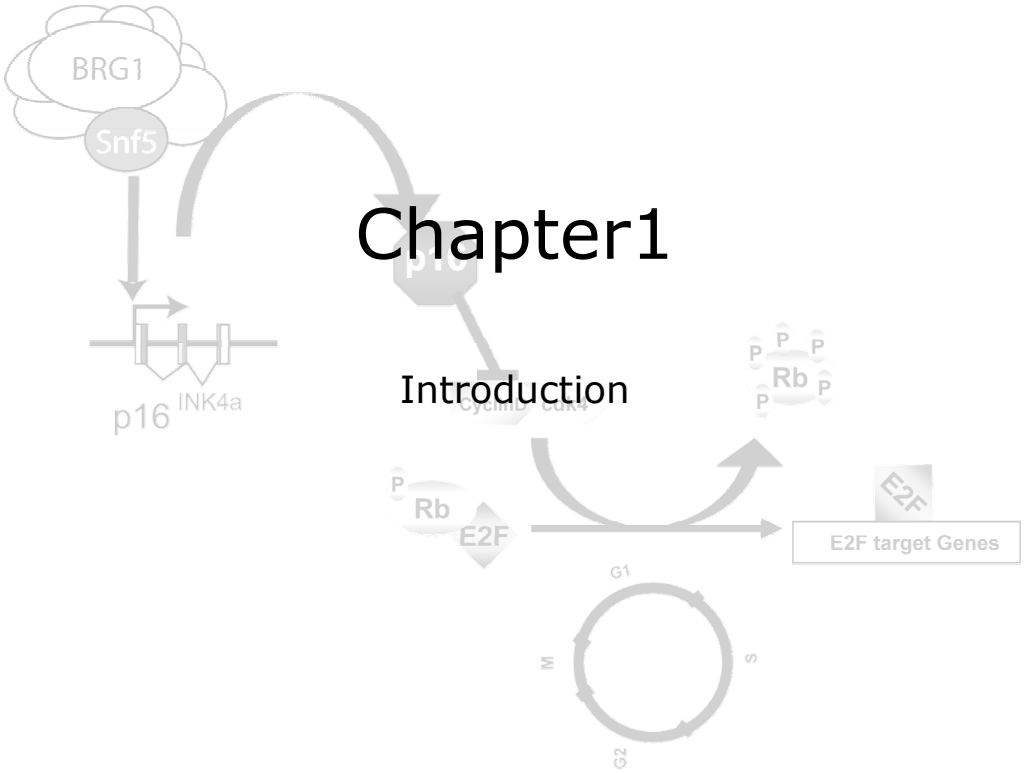

Chapter1

Introduction

Chromatin structure

Chromatin is the structure that the eukaryotic genome is packaged into, allowing over a metre of DNA to fit into the small volume of the nucleus. It is composed of DNA and proteins, most of which are histones. This DNA-protein complex is the template for a number of essential cell processes including transcription and replication. The basic structural unit of chromatin is the nucleosome. Nucleosomes comprise around 146 base pairs of DNA wrapped in a left-handed superhelix 1.7 times around a core histone octamer. This 11nm fibre is often referred to as 'beads on a string' (Figure 1A). Chromatin assembly involves wrapping of DNA around histone octameres producing repetitive nucleosomal array followed by folding of chromatin fibre into solenoid-like structure and deposition of non-histone proteins (19, 25, 52, 55).

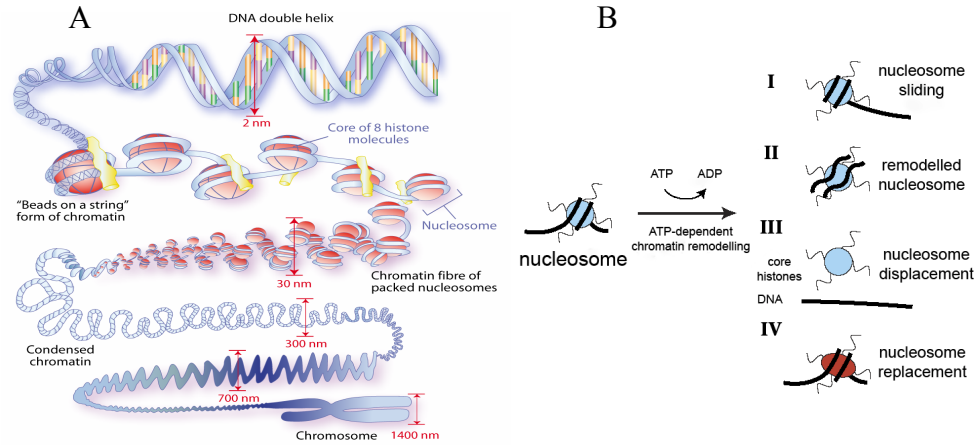

Figure1. Schematic model for Chromatin Structure and ATP-dependent Chromatin remodelling.
(A) Each DNA strand wraps around groups of small protein molecules called histones, forming a series of bead-like structures, called nucleosomes, connected by the DNA strand. Under the micros-cope, uncondensed chromatin has a "beads on a string" appearance. The string of nucleosomes, already compacted by a factor of six, is then coiled into an even denser structure known as a solenoid that compacts the DNA by factor of 40. The solenoid structure then coils to form a chromosome (Figure adapted from www.epitron.eu). **(B**) ATP-dependent chromatin remodelling complexes use the energy derived from ATP hydrolysis to alter histone-DNA contacts in such a way that (I) nucleosomes slide to another position, (II) a remodelled state is created in which the DNA becomes more accessible but histone remain bound, (III) DNA and histone dissociate completely, or (IV) histone (variant) replacement (figure adapted from Ref.28).

Chromatin is a dynamic structure that modulates the access of regulatory factors to the genetic material of eukaryotes and hence controls at a high level the machinery of DNA replication, transcription and repair. For this reason, chromatin needs to be remodelled. The regulated alteration of chromatin structure, termed remodelling can be accomplished by covalent modification of histones or by the action of ATP-dependent remodelling complexes. Remodellers are DNA-translocating motors that utilize the energy of ATP to disrupt histone-DNA contacts (26, 50, 72, 73, 95, 100, 102). ATP-dependent chromatin remodelling factors (remodellers) expose DNA to be accessible for transcription regulators. There are several

possible outcomes of the ATP-dependent chromatin remodelling reaction including nucleosome sliding, creation of DNA loops on the surface of nucleosomes, nucleosome displacement and histone exchange (Figure1B)(26, 50, 72, 73, 95, 100, 102). A precise coordination of events in opening and closing of the chromatin is crucial to ensure that the correct spatial and temporal epigenetic code is maintained within the eukaryotic genome.

ATP-dependent chromatin remodelling factors

Remodellers are typically large, multiprotein complexes assembled around the SNF2-like ATPase 'engine' protein(20-22, 24, 86). The SNF2 superfamily of chromatin remodelling ATPases can be divided into various families based on the presence of additional domains(24). Four different classes of remodelling complexes have been recognized: SWI/SNF, ISWI, Mi-2 and Ino80. Recent survey of SNF2 superfamily members reveals 24 distinct groups, suggesting a large structural variety among ATP-dependent chromatin remodelling enzymes(24). We will focus on the highly conserved SWI/SNF family of ATP-dependent chromatin remodelling factors.

The SWI/SNF complex

The first chromatin remodelling factor identified was ySWI/SNF. It contains 11 known subunits, including SWI2/SNF2. Subunits of the ySWI/SNF were initially identified based on two independent screens for mutants affecting either mating type switching or growth in sucrose, thereby SWI stands for SWItching defective and SNF – for Sucrose Non-Fermenting. In agreement with the phenotypes caused by mutations in the ySWI/SNF subunits, this complex is required for the activation of a number of specific genes such as HO endonuclease, SUC2, GAL1 and GAL10, which are involved in mating-type switch and sucrose and galactose fermenting(63). The SWI/SNF complex is evolutionary highly conserved and homologous complexes have been identified in Drosophila and mammals. The SWI/SNF group of remodellers can be subdivided further into two distinct highly conserved subclasses, yeast SWI/SNF, fly BAP, mammalian BAF or yeast RSC, fly PBAP and mammalian PBAF (Figure 2).

In mammals, BAF and PBAF complexes share most core subunits except the two SWI2/SNF2-type ATPases: BRG1 (Brahma-Related Gene 1) and hBrm (human Brahma). BAF subfamily contains either BRG1 or BRM (hBRM in human and mBRM in mice) as well as the distinct BAF250 subunit, whereas the PBAF subfamily is uniquely built on BRG1 ATPase(47, 57, 97, 98) and also distinctly contains BAF180 and BAF200 subunits. In addition to this, several tissue specific subunits can be identified(58). In Drosophila, RNAi knockdown of the BAP subunits results in accumulation of the cells in G2/M phase of the cell cycle, whereas depletion of the PBAP specific subunits has no significant effect on growth and cell cycle progression(56).

Together, BAP and PBAP have a critical role for both SWI/SNF complexes in the recruitment of the basal transcription machinery(2). The core subunits and the BAP-specific

subunit OSA have been implicated in the regulation of expression of homeotic genes, repression of the Wingless target genes and regulation of the genes involved in the Notch signalling pathway during development(3, 16, 85). In mammals it has been shown that both BAF and PBAF complexes regulate expression of distinct interferon-responsive genes(98). Furthermore, both complexes seem to cooperate with distinct nuclear hormone receptors.

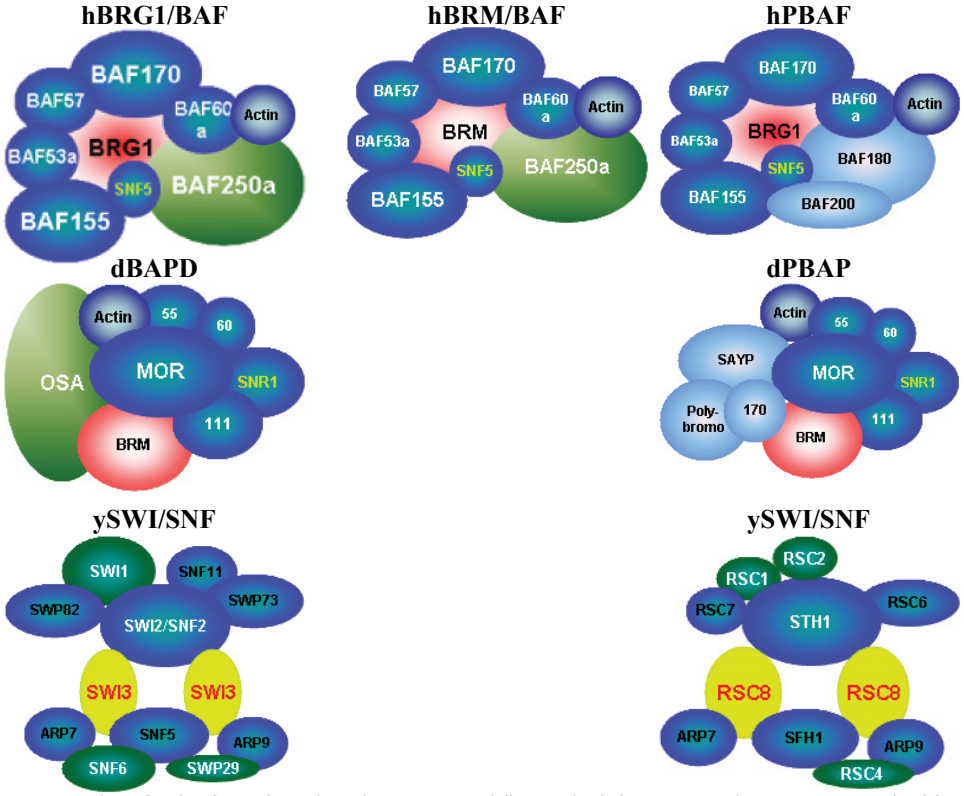

Figure 2. SWI/SNF family of ATP-dependent chromatin remodellers is divided into two evolutionary conserved subfamilies characterized by the presence of subfamily specific signature subunits (shown for human "h", Drosophila – "d"–and yeast "y")

Knockout (KO) mice for PBAF specific subunit BAF180 show only mild effect on embryonic development like defects in placental trophoblast and heart development(94). Depletion of the BAF-specific subunit BAF250 results in more severe developmental defects similar to those obtained after knockout of one of the core subunits (94). This further substantiates the idea that, unlike yeast ySWI/SNF complex, metazoan BAP/BAF complex plays more prominent function in cell proliferation and viability than PBAP/PBAF complex. In mice, targeted disruption of SWI/SNF core subunits usually results in embryonic lethality with the exception of BRM; this is thought to be due to up regulation of and compensation by BRG1(14, 28, 38,

41, 67, 68). BRG1 knockout results in severe developmental defects. $BRG1^{-/-}$ embryos dye at pre-implantation stage and neither trophectoderm nor inner cell mass of blastocysts survives(14). These results suggest that BRG1-containing BAF complex is critical for early embryo development and cell viability and reveal further functional diversification between mammalian BRM and BRG1-containing BAF complexes. The requirement of the SWI/SNF complex for heart development, embryonic brain development, regulation of neuronal differentiation and vascular development during murine embryogenesis, embryonic and adult β-globin transcription and erythropoiesis and T-cell development has been shown and reviewed in (17, 42).

The SWI/SNF complex and Cancer

Thus far there is strong evidence supporting a role for SWI/SNF complexes in cancer development, as several subunits possess intrinsic tumour suppressor activity or are required for the activity of other tumour suppressor genes (8, 18, 34, 66, 76, 77, 91, 96). Inactivating mutations or aberrant expression of the genes encoding SWI/SNF core subunits have been found in different human tumour cell lines and primary tumours (18). BRG1 and BRM mutations are frequently observed in various tumour cell lines including pancreatic, breast, lung and prostate cancer cells. Lack of expression of both SWI/SNF ATPase subunits BRG1 and hBRM correlate with poorer prognosis in patients with non-small-cell lung cancer (66). Human SNF5 (hSNF5, INI1 or SMARCB1) located in the chromosomal region 22q11.2, is a core component of the hSWI/SNF and it has been implicated in gene regulation, cell division and tumourigenesis (32). Mice heterozygous for SNF5 are predisposed to tumours with features similar to the human Malignant Rhabdoid tumours (MRTs), which are frequently metastatic to the lung and/or lymph node. SNF5-deficient tumours undergo loss of heterozygosity (LOH), which results in SNF5 depletion (14, 28, 41, 68). Unlike SNF5-deficient tumours, BRG1-mutated tumours occur at different locations such as the neck or inguinal regions, display different features of epitheloid origin, and appear not to undergo LOH (96).

The SWI/SNF complex associates directly with cancer-related molecules such as BRCA1 and c-Myc and beta-catenin (4, 9, 15, 84). BRCA1 activates p53-dependent transcription, which is abrogated by a dominant-negative mutant form of BRG1 (9). SNF5 also interacts directly with c-Myc and this interaction is important for trans-activating the function of c-Myc (15). SWI/SNF complex has been shown to interact directly with myeloid/lymphoid or Mixed-Lineage Leukaemia (MLL), human homolog of Drosophila trithorax (trxG), through SNF5 subunit. SWI/SNF and MLL activate oncogenesis through different mechanisms, such as inhibition of GADD34 induced apoptosis and aberrant activation of MLL target genes (reviewed in [70]). Collectively these observations point to the function of SWI/SNF complexes as tumour suppressors.

Malignant rhabdoid tumour and Atypical teratoid rhabdoid tumour

The term malignant rhabdoid tumour (MRT) has been used to describe a heterogeneous group of neoplasms, having in common distinct so-called "rhabdoid" cytologic features. The rhabdoid cell is a medium-sized, round-to-oval cell with distinct borders, an eccentric nucleus, and a prominent nucleolus. The cell of origin of malignant rhabdoid tumour remains an enigma. Malignant rhabdoid tumour may arise either de novo from non-neoplastic cells or through tumour progression from other types of neoplasms. These latter tumours, in which other nonrhabdoid tumour components are identified, may be termed composite MRT. Rhabdoid tumours were reported in many tissues including the kidney, the liver, soft tissue, and the central nervous system (8, 71, 77, 91). The cerebellum is the most common location for primary intracerebral MRT. Malignant rhabdoid tumour (MRT) of the CNS is known as Atypical teratoid/rhabdoid tumour (AT/RT). In the United States, three children per 1,000,000 or around 30 new AT/RT cases are diagnosed each year. AT/RT represents around 3% of pediatric cancers of the central nervous system (CNS). ATRT/MRTs are highly aggressive cancer of early childhood and despite intensive therapies 80-90% of children die within first year of diagnosis. About 50% of atypical teratoid/rhabdoid tumours arise in the posterior fossa, 40% are supratentorial, and the rest are pineal, spinal, or multifocal. Both ATRTs and MRTs are characterized by the presence of rhabdoid cells carrying vacuolated nuclei and Periodic Acid-Shiff (PAS) cytoplasmic inclusions, however the histological diagnosis can be difficult (29). Biallelic inactivating mutations and deletions of the SWI/SNF core subunit SNF5/INI1 have been identified in the majority of kidney malignant rhabdoid tumours (MRT) and brain atypical teratoid/rhabdoid tumours (ATRT) However, at least 20% of cases do not have genomic alterations of *hSNF5*, despite showing loss of immunostaining for the SNF5 protein (8, 76, 77, 91). In several cases germline mutations in SNF5/INI1 gene accompanied by somatic loss or mutation of the remaining allele were documented in patients with ATRT/MRTs indicating that SNF5/INI1 is a classical tumour suppressor gene (8, 77). Loss of SNF5/INI1 has been also detected in a number of tumours histologically distinct from ATRT/MRTs such as paediatric choroid plexus carcinoma, meningioma, medulloblastoma (70).

hSNF5 is a tumour suppressor gene

The SWI/SNF complex is also involved in various cellular processes that are potentially associated with tumour formation including DNA synthesis, virus integration, DNA repair, and mitotic gene regulation (70). Numerous studies to dissect the connection between these activities and tumour formation are currently in progress. The molecular mechanisms underlying tumour development in mice with inactivation of BRG1 or SNF5 are still unclear. A mouse strain carrying reversibly inactivating SNF5/INI1 allele by applying LoxP-Cre recombination system has been generated to find the mechanisms of tumourigenesis caused by loss of SNF5/INI1 (69). 100% of the resultant mice develop short latency highly aggressive tumours such as $CD8^+$ T cell lymphomas and rhabdoid tumours (69). Paradoxical observations

that phenotypes induced by BRG1 or SNF5 deficiency in mouse embryonic fibroblasts (MEFs) are very similar to those of cancer cells whose BRG1 or SNF5 are ectopically over-expressed. Both cell lines undergo cell cycle arrest, cell death, or senescence (69).

Although the molecular mechanisms for SNF5/INI1 function in cell survival in normal cells is not yet known for mammals, in recent years significant progress has been made in understanding of SNF5/INI1 role in tumour suppression. It appeared, that re-expression of SNF5/INI1 in human MRT cell lines leads to an accumulation in G0/G1 phase, cellular senescence and in some cases apoptosis (1, 7, 60, 90, 93, 101). We have shown that SNF5/INI1 binds to the promoter of *p16^{ink4a}* tumour suppressor gene and recruits BRG1-containing SWI/SNF complex resulting in transcription activation (Figure 2, chapter 3) (37, 60).

p16^{ink4a} gene encodes a specific cyclin-dependent kinase (CDK)4/CDK6 inhibitors, which targets retinoblastoma (pRb) protein for phosphorylation (51). Hyperphosphorylated pRb dissociates from E2F transcription factor allowing S phase specific genes expression and promoting cell proliferation. Therefore, increased p16^{ink4a} expression upon SNF5/INI1 induction in MRT cells (lacking hSNF5) results in pRb hypophosphorylation and inhibits cell cycle progression (Figure 2). Interestingly, MRT cell lines lacking *p16^{ink4a}* activity or expressing *p16^{ink4a}*-insensitive mutant of CDK4 continue to grow after SNF5/INI1 re-expression supporting a role of SNF5/INI1 in p16^{ink4a}-CDK4/Cyclin D1-pRB/E2F pathway (60, 93). Several groups have also shown that SNF5/INI1 can repress Cyclin D1 expression in ATRT/MRTs by recruiting HDACs to the promoter, or it can function in the repression of E2F target genes via direct association with pRb, thereby causing cell-cycle arrest in G1 phase (99, 101). In agreement with a role of SWI/SNF ATP-dependent chromatin remodellers in the regulation of pRb/E2F transcriptional circuitry, genome-wide expression profiling revealed down regulation of some of the E2F-target genes in MRT cell lines, including mitotic checkpoint gene Mad2 (93)(and chapter2). Over-expression of Mad2 leads to chromosomal instability and tumourigenesis (81, 89).

The Ink4-Arf locus

The Ink4b-Arf-Ink4a locus, spanning an approximately 40 kb stretch of the human chromosome 9p21 (chromosome 4 in mouse), encodes three distinct tumour suppressors, *p15^{Ink4b}*, *p16^{Ink4a}* and *p14^{ARF}* (*p19^{ARF}*in mice) whose expression enhances the growth-suppressive functions of the retinoblastoma (Rb) and p53, respectively (Figure 3). Both p15^{Ink4b} and p16^{Ink4a} are able to induce cell cycle arrest in G1 by inhibiting cyclin dependent kinase CDK4 and CDK6 to inactivate retinoblastoma (RB)(59). Because only p16^{Ink4a} can form stable, binary complex with both CDK4 and CDK6, p16^{Ink4a} is likely the most effective inhibitor of CDK4 and CDK6 (61). The unrelated p14^{ARF} protein acts via MDM2 to activate the key check point protein TRP53, thereby inducing either cell cycle arrest (both in G1 and G2) or apoptosis

(65). The locus *p14*^{ARF} (named ARF because it uses the second exon of Ink4a in an Alternative translational Reading Frame) is implicated in various types of cancer (reviewed in (27, 78)).

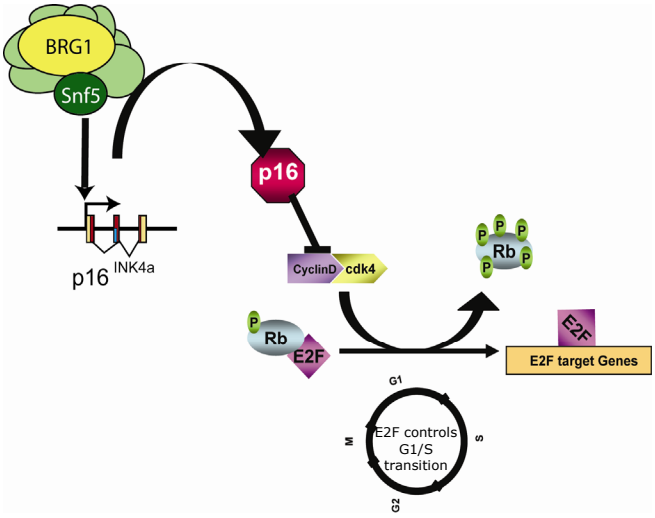

Figure 2. Mammalian ATRT/MRT tumour cells lack SNF5/INI1 function resulting in increased CDK4/cyclin D1 activity. This triggers pRb hyperphosphorylation and unleashes transcription of E2F-dependent genes causing increased proliferation, chromosomal instabilities and cancer. Re-expression of SNF5/INI1 reverses cell proliferation and leads to G0/G1 arrest, senescence and apoptosis primarily due to activation of p16INK4a tumour suppressor gene expression and repression of cyclin D1 gene expression.

In mice, ectopic expression of FOXO transcription factor (which regulates cell cycle progression, cell survival and DNA-repair pathways) cause increased level of Ink4b and Arf but not Ink4a(36). In a variety of tumours, *p16*^{INK4a} is inactivated through epigenetic silencing, involving PcG (Polycomb groups) proteins and DNA methylation (27, 33, 82). Significantly, the PcG protein BMI1 promotes oncogenesis in mice through silencing of the *Ink4a-Arf* locus (31). Both the PRC1 and PRC2 PcG complexes directly bind and silence the *Ink4a-Arf* locus (12, 37, 43). In MRT cells, human embryonic fibroblasts (TIG3) and human neonatal fibroblast, both Polycomb-Repressive Complexes (PRC1 and PRC2) bind to Ink4a and Ink4b (this thesis). It has been shown that depletion of EZH2 subunit of the PRC2 in response to stress causes the loss of H3K27me3, displacement of BMI1 subunit of the PRC1 and transcription activation of INK4a (12). In agreement with this we showed depletion of EZH2 during aging and differentiation causes displacement of BMI1 and activation of Ink4a and Ink4b (This thesis).

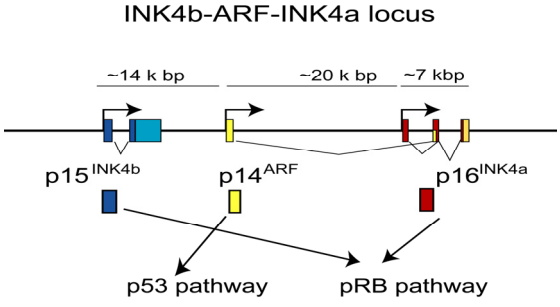

Figure 3. Organization of the human INK4b-ARF-INK4a locus (not drawn to scale). The genomic locus spans approximately 40 Kbp of human chromosome 9, and encodes three distinct proteins, p15^{INK4b}, p14^{ARF} and p16^{INK4a}. The 5′ and 3′ untranslated regions (yellow boxes), the coding sequences of p15^{INK4b} (green), p14^{ARF} (blue) and p16^{INK4a} (red) are indicated.

Numerous studies showed that promoter hypermethylation of CpG island (CGI) sequences is the most frequent pathway for inactivation of $p16^{INK4a}$ in human carcinomas, including those that arise in the lung, oropharynx, bladder, cervix, liver, colon, pancreas, and other sites (5). The H3K36 demethylase JmjC domain-containig histone demethylase 1b in primary MEFs regulates cell proliferation and senescence through Ink4b (30). The *Ink4/Arf* locus is normally expressed at very low levels in most tissues of young organisms(45). It is well established that the *Ink4/Arf* locus is activated during organismal ageing in both rodents and humans, and the levels of p16INK4a constitute an impressively good overall biomarker of ageing(40). These observations point to $p16^{Ink4a}$ both serving as a brake for the proliferation of cancer cells, and also limiting the long-term renewal of stem cells. The Ink4a-Arf locus responds to stress signals, limiting cell proliferation and modulating oncogene-induced apoptosis (reviewed in (51)). A challenging issue which remains is to understand the interplay between signalling and PcG control of InK4b-Arf-Ink4a locus.

Polycomb group complex

Polycomb group proteins were first identified in *Drosophila melanogaster* as mutants deregulating Hox gene expression pattern during fly early development. The PcG are required to maintain chromatin in a repressed state while the trithorax-group (trxG) proteins (including the hSWI/SNF complex) are necessary for the maintenance of transcriptional activity of several developmental genes. The PcG is a diverse group of proteins that form at least three different complexes: Polycomb repressive complex 1 and 2 (PRC1 and PRC2) and pleiohomeotic (Pho) repressive complex (PhoRC) (75). A list of the proteins pertaining to any of the complexes, the respective human and mouse homologues and some of the known function can be found in table1 (adapted from(54)).

The main function of the PRC1 proteins is to inhibit chromatin remodelling and maintain the repressed state of chromatin by out-competing the trxG protein complexes such as SWI/SNF chromatin-remodelling complex. PRC2 on the other hand is known to be the initiator of the suppression process in which chromatin and or DNA are marked for repression. The key component of PRC2 is the SET domain H3 methyltransferase protein enhancer of Zeste (E(Z)). E(Z), when assembled in the complex methylates H3K27. In human cells, PRC2 can physically associate with HDACs 1 and 2. HDACs can deacetylate H3K27 to make it available for methylation by PRC2 (46). In vivo, trimethylation of H3K27 is characteristic of PcG target genes (74). The H3K27me3 mark is thought to act as a docking site for chromo-domain of the CBX family proteins, which recruit other members of the PRC1 complex (6). Genome wide mapping of Polycomb target genes revealed only depletion of EZH2 causes induction of Ink4b(11).

Table1. PCG Componets in Drosophila Melanogaster (Dm) and their Human Orthologues

Complex	Dm	Human	Domains	Function
PRC1	Pc	HPC1, HPC2, HPC3	Chromodomain	Methyl-lysine binding
	Ph	HPH1, HPH2, HPH3	Zinc-finger SPM domain	
	Sce	Ring1A, RING1B		
	Psc	BMI1, PCGF2, ZNF134	Ringfinger domain	Ubiquitin ligase
	Scm	SCML1	Zinc-finger SPM domain	
PRC2	Esc	EED	WD repeats	
	E(Z)	EZH1, EZH2	SET domain	Histone methyltarnsferase
	Su(Z)12	SUZ12	Zinc-finger domain	
	Caf1	RBAP48, RBAP46	WD repeats	Histone binding
	Pc1	PHF1	PHD-finger domain	
PhoRc	Pho	YY1	Zinc-finger domain	Sequence- specific DNA binding
	Pho1	YY1		DNA binding
	DSfmbt	SFMBT1, SFMBT2	MBT-repeat	Methyl-lysine binding

Polycomb complexes function as global enforcers of epigenetically repressed states, balanced by an antagonistic state that is mediated by trithorax. These epigenetic states must be reprogrammed when cells become committed to differentiation. Mammalian Polycomb group (PcG) proteins are essential transcription silencers that control multiple development processes, including stem cell self-renewal, cell differentiation
and have been implicated in several types of cancers (10, 49, 53, 88).

EZH2 a key for differentiation, aging and cancer

EZH2 is the catalytic subunit of PRC2, which is a highly conserved histone methyltransferase that targets lysine-27 of histone H3. This methylated H3-K27 chromatin mark is commonly associated with silencing of differentiation genes in organisms ranging from flies to human. EZH2 is frequently over-expressed in wide variety of cancerous tissue types including prostate, breast, lymphoma, myeloma, bladder, colon, skin, liver, endometrial, lung, gastric (80). EZH2 and EED co- immunoprecipitate with all three human DNMTs (DNA methyl-transfrases) and silencing of certain target genes requires both EZH2 and DNMTs (92). *EZH2* and *EED* are targets of the pRB-E2F pathway, and deregulation of the pathway, as is frequently observed in human cancer, would result in higher levels of EZH2 and EED. The EZH2 and EED promoters are direct targets of the E2F transcription factors *in vivo.* Over-expression of EZH2 shortens the G_1 phase of the cell cycle, results in accumulation of cells in the S phase of the cell cycle, and confers a proliferative advantage when ectopically expressed in primary MEFs. The role of E2F and pRB in the control of embryonic development is likely related to their ability to regulate the abundance of the PRC2 complex (13). EZH2 is accumulated in undifferentiated progenitor cell population, such as haematopoietic cells(83).

Genome wide mapping of PRC2 target genes in different cells in human, mouse and Drosophila by ChIP-on-ChIP method have been performed by different groups. These studies revealed that PRC2 target genes are highly enriched for transcription factors and signalling components that control cell differentiation (reviewed in (80). Correspondence between silenced genes bound by Oct4, Sox2 and Nanog, which promote expression of proliferation genes and silencing of differentiation genes, with PRC2 target genes suggests that PRC2 is a key co-repressor in ES cells(49, 62). Recently it has been shown that epidermal basal cells like ES cells are rich in EZH2 and other PcG proteins, but as they differentiate EZH2 expression is turned off and the cells exit the cell cycle concomitant with induction of *INK4b/a*. Loss of PcG function makes the binding site available for AP1 transcription factors, which are major effectors of the expression of epidermal genes associated with terminal differentiation, and thereby permits the expression of terminal differentiation genes(23, 64). How PcG genes themselves are regulated still remains unresolved. It is not mechanistically clear how PcG proteins repress their targets, PcG and histone marks may silence target genes through the looping process. It has been shown recently that PcG-occupied region can form chromatin loops and physically interact in cis around a single gene in mammalian cells. EZH2 knock down was shown to affect this long-range interaction(87).

References

1. **Ae, K., N. Kobayashi, R. Sakuma, T. Ogata, H. Kuroda, N. Kawaguchi, K. Shinomiya, and Y. Kitamura.** 2002. Chromatin remodelling factor encoded by ini1 induces G1 arrest and apoptosis in ini1-deficient cells. Oncogene **21:**3112-20.
2. **Armstrong, J. A., O. Papoulas, G. Daubresse, A. S. Sperling, J. T. Lis, M. P. Scott, and J. W. Tamkun.** 2002. The Drosophila BRM complex facilitates global transcription by RNA polymerase II. Embo J **21:**5245-54.
3. **Armstrong, J. A., A. S. Sperling, R. Deuring, L. Manning, S. L. Moseley, O. Papoulas, C. I. Piatek, C. Q. Doe, and J. W. Tamkun.** 2005. Genetic screens for enhancers of brahma reveal functional interactions between the BRM chromatin-remodelling complex and the delta-notch signal transduction pathway in Drosophila. Genetics **170:**1761-74.
4. **Barker, N., A. Hurlstone, H. Musisi, A. Miles, M. Bienz, and H. Clevers.** 2001. The chromatin remodelling factor Brg-1 interacts with beta-catenin to promote target gene activation. Embo J **20:**4935-43.
5. **Baylin, SB., J.G. Herman. J.R Graff, P.M. Vertino, and J.P. Issa.** 1998. Alterations in DNA methylation: a fundamental aspect of neoplasia. Adv Cancer Res. **72:**141-96.
6. **Bernstein, E., E. M. Duncan, O. Masui, J. Gil, E. Heard, and C. D. Allis.** 2006. Mouse Polycomb Proteins Bind Differentially to Methylated Histone H3 and RNA and Are Enriched in Facultative Heterochromatin, p. 2560-2569, vol. 26.
7. **Betz, B. L., M. W. Strobeck, D. N. Reisman, E. S. Knudsen, and B. E. Weissman.** 2002. Re-expression of hSNF5/INI1/BAF47 in pediatric tumour cells leads to G1 arrest associated with induction of p16ink4a and activation of RB. Oncogene **21:**5193-203.
8. **Biegel, J. A., J. Y. Zhou, L. B. Rorke, C. Stenstrom, L. M. Wainwright, and B. Fogelgren.** 1999. Germ-line and acquired mutations of INI1 in atypical teratoid and rhabdoid tumours. Cancer Res **59:**74-9.
9. **Bochar, D. A., L. Wang, H. Beniya, A. Kinev, Y. Xue, W. S. Lane, W. Wang, F. Kashanchi, and R. Shiekhattar.** 2000. BRCA1 is associated with a human SWI/SNF-related complex: linking chromatin remodelling to breast cancer. Cell **102:**257-65.
10. **Boyer, L. A., K. Plath, J. Zeitlinger, T. Brambrink, L. A. Medeiros, T. I. Lee, S. S. Levine, M. Wernig, A. Tajonar, M. K. Ray, G. W. Bell, A. P. Otte, M. Vidal, D. K. Gifford, R. A. Young, and R. Jaenisch.** 2006. Polycomb complexes repress developmental regulators in murine embryonic stem cells. Nature **441:**349-353.
11. **Bracken A.P., N. Dietrich, D. Pasini, K.H. Hansen, K. Helin.** 2006. Genome-wide mapping of Polycomb target genes unravels their roles in cell fate transitions. Genes Dev **20:**1123-36.
12. **Bracken, A. P., D. Kleine-Kohlbrecher, N. Dietrich, D. Pasini, G. Gargiulo, C. Beekman, K. Theilgaard-Monch, S. Minucci, B. T. Porse, J.-C. Marine, K. H. Hansen, and K. Helin.** 2007. The Polycomb group proteins bind throughout the INK4A-ARF locus and are disassociated in senescent cells. Genes Dev **21:**525-530.
13. **Bracken AP, D. Pasini, M. Capra, E. Prosperini, E. Colli, K. Helin.** 2003. EZH2 is downstream of the pRB-E2F pathway, essential for proliferation and amplified in cancer. EMBO J. **22:**5323-35.
14. **Bultman, S., T. Gebuhr, D. Yee, C. La Mantia, J. Nicholson, A. Gilliam, F. Randazzo, D. Metzger, P. Chambon, G. Crabtree, and T. Magnuson.** 2000. A Brg1 null mutation in the mouse reveals functional differences among mammalian SWI/SNF complexes. Mol Cell **6:**1287-95.
15. **Cheng, S. W., K. P. Davies, E. Yung, R. J. Beltran, J. Yu, and G. V. Kalpana.** 1999. c-MYC interacts with INI1/hSNF5 and requires the SWI/SNF complex for transactivation function. Nat Genet **22:**102-5.
16. **Collins, R. T., and J. E. Treisman.** 2000. Osa-containing Brahma chromatin remodelling complexes are required for the repression of wingless target genes. Genes Dev **14:**3140-52.
17. **de la Serna, I. L., Y. Ohkawa, and A. N. Imbalzano.** 2006. Chromatin remodelling in mammalian differentiation: lessons from ATP-dependent remodellers. Nat Rev Genet **7:**461-473.
18. **Decristofaro, M. F., B. L. Betz, C. J. Rorie, D. N. Reisman, W. Wang, and B. E. Weissman.** 2001. Characterization of SWI/SNF protein expression in human breast cancer cell lines and other malignancies. J Cell Physiol **186:**136-45.
19. **Dorigo, B., T. Schalch, A. Kulangara, S. Duda, R. R. Schroeder, and T. J. Richmond.** 2004. Nucleosome arrays reveal the two-start organization of the chromatin fiber. Science **306:**1571-3.

20. **Durr, H., A. Flaus, T. Owen-Hughes, and K. P. Hopfner.** 2006. Snf2 family ATPases and DExx box helicases: differences and unifying concepts from high-resolution crystal structures. Nucleic Acids Res **34:**4160-7.
21. **Durr, H., C. Korner, M. Muller, V. Hickmann, and K. P. Hopfner.** 2005. X-ray structures of the Sulfolobus solfataricus SWI2/SNF2 ATPase core and its complex with DNA. Cell **121:**363-73.
22. **Eisen, J. A., K. S. Sweder, and P. C. Hanawalt.** 1995. Evolution of the SNF2 family of proteins: subfamilies with distinct sequences and functions. Nucleic Acids Res **23:**2715-23.
23. **Ezhkova, E., H. A. Pasolli, J. S. Parker, N. Stokes, I. h. Su, G. Hannon, A. Tarakhovsky, and E. Fuchs.** 2009. Ezh2 Orchestrates Gene Expression for the Stepwise Differentiation of Tissue-Specific Stem Cells. **136:**1122-1135.
24. **Flaus, A., D. M. Martin, G. J. Barton, and T. Owen-Hughes.** 2006. Identification of multiple distinct Snf2 subfamilies with conserved structural motifs. Nucleic Acids Res **34:**2887-905.
25. **Francis, N. J., R. E. Kingston, and C. L. Woodcock.** 2004. Chromatin compaction by a polycomb group protein complex. Science **306:**1574-7.
26. **Fyodorov, D. V., and J. T. Kadonaga.** 2002. Dynamics of ATP-dependent chromatin assembly by ACF. Nature **418:**897-900.
27. **Gil, J., and G. Peters.** 2006. Regulation of the INK4b-ARF-INK4a tumour suppressor locus: all for one or one for all. Nat Rev Mol Cell Biol **7:**667-677.
28. **Guidi, C. J., A. T. Sands, B. P. Zambrowicz, T. K. Turner, D. A. Demers, W. Webster, T. W. Smith, A. N. Imbalzano, and S. N. Jones.** 2001. Disruption of Ini1 leads to peri-implantation lethality and tumourigenesis in mice. Mol Cell Biol **21:**3598-603.
29. **Haas, J. E., N. F. Palmer, A. G. Weinberg, and J. B. Beckwith.** 1981. Ultrastructure of malignant rhabdoid tumour of the kidney. A distinctive renal tumour of children. Hum Pathol **12:**646-57.
30. **He, J., E. M. Kallin, Y.-i. Tsukada, and Y. Zhang.** 2008. The H3K36 demethylase Jhdm1b/Kdm2b regulates cell proliferation and senescence through p15Ink4b. Nat Struct Mol Biol **15:**1169-1175.
31. **Jacobs, J. J. L., K. Kieboom, S. Marino, R. A. DePinho, and M. van Lohuizen.** 1999. The oncogene and Polycomb-group gene bmi-1 regulates cell proliferation and senescence through the ink4a locus. Nature **397:**164-168.
32. **Johnson, C. N., N.L. Adkins, and P. Georgel.** 2005. Chromatin remodelling complexes: ATP-dependent machines in action. Biochem Cell Biol. **83:**405-17.
33. **Jones, P. A., and S. B. Baylin.** 2007. The Epigenomics of Cancer. Cell **128:**683-692.
34. **Judkins, A. R., J. Mauger, A. Ht, L. B. Rorke, and J. A. Biegel.** 2004. Immunohistochemical analysis of hSNF5/INI1 in pediatric CNS neoplasms. Am J Surg Pathol **28:**644-50.
35. **Kamijo, T., F. Zindy, M. F. Roussel, D. E. Quelle, J. R. Downing, R. A. Ashmun, G. Grosveld, and C. J. Sherr.** 1997. Tumour Suppression at the Mouse INK4a Locus Mediated by the Alternative Reading Frame Product p19 ARF. **91:**649-659.
36. **Katayama K, N. A., Sugimoto Y, Tsuruo T, Fujita N.** 2008. FOXO transcription factor-dependent p15(INK4b) and p19(INK4d) expression. Oncogene **27:**1677–1686.
37. **Kheradmand Kia S., M. Gorsky, S. Giannakopoulos, and C.P. Verrijzer.** 2008. SWI/SNF Mediates Polycomb Eviction and Epigenetic Reprogramming of the INK4b-ARF-INK4a Locus. MCB **28:**3457-3464.
38. **Kim, J. K., S. O. Huh, H. Choi, K. S. Lee, D. Shin, C. Lee, J. S. Nam, H. Kim, H. Chung, H. W. Lee, S. D. Park, and R. H. Seong.** 2001. Srg3, a mouse homolog of yeast SWI3, is essential for early embryogenesis and involved in brain development. Mol Cell Biol **21:**7787-95.
39. **Kim, S. H., J. Rowe, H. Fujii, R. Jones, B. Schmierer, B. W. Kong, K. Kuchler, D. Foster, D. Ish-Horowicz, and G. Peters.** 2006. Upregulation of chicken p15INK4b at senescence and in the developing brain, p. 2435-2443, vol. 119.
40. **Kim, W. Y., and N. E. Sharpless.** 2006. The Regulation of INK4/ARF in Cancer and Aging. **127:**265-275.
41. **Klochendler-Yeivin, A., L. Fiette, J. Barra, C. Muchardt, C. Babinet, and M. Yaniv.** 2000. The murine SNF5/INI1 chromatin remodelling factor is essential for embryonic development and tumour suppression. EMBO Rep **1:**500-6.
42. **Ko, M., D.H. Sohn. D., H. Chung, R.H. Seong.** Mutat Res. 2008 Dec 1;647(1-2):59-67. Epub 2008 Aug 20. Chromatin remodelling, development and disease. Mutat Res. **647:**59-67.

43. **Kotake, Y., R. Cao, P. Viatour, J. Sage, Y. Zhang, and Y. Xiong.** 2007. pRB family proteins are required for H3K27 trimethylation and Polycomb repression complexes binding to and silencing p16INK4a tumour suppressor gene. Genes Dev **21:**49-54.
44. **Krimpenfort, P., A. Ijpenberg, J.-Y. Song, M. van der Valk, M. Nawijn, J. Zevenhoven, and A. Berns.** 2007. p15Ink4b is a critical tumour suppressor in the absence of p16Ink4a. Nature **448:**943-946.
45. **Krishnamurthy J, T. C., Ramsey MR, Kovalev GI, Al-Regaiey K, Su L, Sharpless NE.** 2004. Ink4a/Arf expression is a biomarker of aging. J Clin Invest. **114:**1299-307.
46. **Kuzmichev A, N. K., Erdjument-Bromage H, Tempst P, Reinberg D.** 2002. Histone methyltransferase activity associated with a human multiprotein complex containing the Enhancer of Zeste protein. Genes Dev **16:**2893-905.
47. **Kwon, H., A. N. Imbalzano, P. A. Khavari, R. E. Kingston, and M. R. Green.** 1994. Nucleosome disruption and enhancement of activator binding by a human SW1/SNF complex. Nature **370:**477-81.
48. **Latres E, M. M., Sotillo R, Martín J, Ortega S, Martín-Caballero J, Flores JM, Cordón-Cardo C, Barbacid M.** 2000. Limited overlapping roles of P15(INK4b) and P18(INK4c) cell cycle inhibitors in proliferation and tumourigenesis. EMBO J. **19:**3496-506.
49. **Lee, T. I., R. G. Jenner, L. A. Boyer, M. G. Guenther, S. S. Levine, R. M. Kumar, B. Chevalier, S. E. Johnstone, M. F. Cole, K.-i. Isono, H. Koseki, T. Fuchikami, K. Abe, H. L. Murray, J. P. Zucker, B. Yuan, G. W. Bell, E. Herbolsheimer, N. M. Hannett, K. Sun, D. T. Odom, A. P. Otte, T. L. Volkert, D. P. Bartel, D. A. Melton, D. K. Gifford, R. Jaenisch, and R. A. Young.** 2006. Control of Developmental Regulators by Polycomb in Human Embryonic Stem Cells. **125:**301-313.
50. **Lia, G., E. Praly, H. Ferreira, C. Stockdale, Y. C. Tse-Dinh, D. Dunlap, V. Croquette, D. Bensimon, and T. Owen-Hughes.** 2006. Direct observation of DNA distortion by the RSC complex. Mol Cell **21:**417-25.
51. **Lowe, S. W., and C. J. Sherr.** 2003. Tumour suppression by Ink4a-Arf: progress and puzzles. Current Opinion in Genetics & Development **13:**77-83.
52. **Luger, K., A. W. Mader, R. K. Richmond, D. F. Sargent, and T. J. Richmond.** 1997. Crystal structure of the nucleosome core particle at 2.8 A resolution. Nature **389:**251-60.
53. **Lund AH, v. L. M.** 2004. Epigenetics and cancer. Genes Dev **1:**2315-35.
54. **MateosLangerak, J., G. Cavalli, and E. H. Veronica van Heyningen and Robert.** 2008. Chapter 2 Polycomb Group Proteins and Long[hyphen (true graphic)]Range Gene Regulation, p. 45-66, Advances in Genetics, vol. Volume 61. Academic Press.
55. **Mohd-Sarip, A., and C. P. Verrijzer.** 2004. Molecular biology. A higher order of silence. Science **306:**1484-5.
56. **Moshkin, Y. M., L. Mohrmann, W. F. van Ijcken, and C. P. Verrijzer.** 2007. Functional differentiation of SWI/SNF remodellers in transcription and cell cycle control. Mol Cell Biol **27:**651-61.
57. **Nie, Z., Y. Xue, D. Yang, S. Zhou, B. J. Deroo, T. K. Archer, and W. Wang.** 2000. A specificity and targeting subunit of a human SWI/SNF family-related chromatin-remodelling complex. Mol Cell Biol **20:**8879-88.
58. **Olave, I., W. Wang, Y. Xue, A. Kuo, and G. R. Crabtree.** 2002. Identification of a polymorphic, neuron-specific chromatin remodelling complex. Genes Dev **16:**2509-17.
59. **Ortega, S., M. Malumbres, and M. Barbacid.** 2002. Cyclin D-dependent kinases, INK4 inhibitors and cancer. Biochimica et Biophysica Acta (BBA) - Reviews on Cancer **1602:**73-87.
60. **Oruetxebarria, I., F. Venturini, T. Kekarainen, A. Houweling, L. M. Zuijderduijn, A. Mohd-Sarip, R. G. Vries, R. C. Hoeben, and C. P. Verrijzer.** 2004. P16INK4a is required for hSNF5 chromatin remodeller-induced cellular senescence in malignant rhabdoid tumour cells. J Biol Chem **279:**3807-16.
61. **Parry, D., D. Mahony, K. Wills, and E. Lees.** 1999. Cyclin D-CDK Subunit Arrangement Is Dependent on the Availability of Competing INK4 and p21 Class Inhibitors, p. 1775-1783, vol. 19.
62. **Pasini, D., A. P. Bracken, J. B. Hansen, M. Capillo, and K. Helin.** 2007. The Polycomb Group Protein Suz12 Is Required for Embryonic Stem Cell Differentiation, p. 3769-3779, vol. 27.
63. **Peterson, C. L., and I. Herskowitz.** 1992. Characterization of the yeast SWI1, SWI2, and SWI3 genes, which encode a global activator of transcription. Cell **68:**573-83.
64. **Pirrotta, V.** 2009. Polycomb Repression under the Skin. **136:**992-994.

65. **Pomerantz, J., N. Schreiber-Agus, N. J. Liégeois, A. Silverman, L. Alland, L. Chin, J. Potes, K. Chen, I. Orlow, H.-W. Lee, C. Cordon-Cardo, and R. A. DePinho.** 1998. The Ink4a Tumour Suppressor Gene Product, p19Arf, Interacts with MDM2 and Neutralizes MDM2's Inhibition of p53. **92:**713-723.
66. **Reisman, D. N., J. Sciarrotta, W. Wang, W. K. Funkhouser, and B. E. Weissman.** 2003. Loss of BRG1/BRM in human lung cancer cell lines and primary lung cancers: correlation with poor prognosis. Cancer Res **63:**560-6.
67. **Reyes, J. C., J. Barra, C. Muchardt, A. Camus, C. Babinet, and M. Yaniv.** 1998. Altered control of cellular proliferation in the absence of mammalian brahma (SNF2alpha). Embo J **17:**6979-91.
68. **Roberts, C. W., S. A. Galusha, M. E. McMenamin, C. D. Fletcher, and S. H. Orkin.** 2000. Haploinsufficiency of Snf5 (integrase interactor 1) predisposes to malignant rhabdoid tumours in mice. Proc Natl Acad Sci U S A **97:**13796-800.
69. **Roberts, C. W., M. M. Leroux, M. D. Fleming, and S. H. Orkin.** 2002. Highly penetrant, rapid tumourigenesis through conditional inversion of the tumour suppressor gene Snf5. Cancer Cell **2:**415-25.
70. **Roberts, C. W., and S. H. Orkin.** 2004. The SWI/SNF complex--chromatin and cancer. Nat Rev Cancer **4:**133-42.
71. **Rorke LB, P. R., Biegel J.** 1995. Central nervous system atypical teratoid/rhabdoid tumours of infancy and childhood. J Neurooncol. **24:**21-8.
72. **Saha, A., J. Wittmeyer, and B. R. Cairns.** 2002. Chromatin remodelling by RSC involves ATP-dependent DNA translocation. Genes Dev **16:**2120-34.
73. **Saha, A., J. Wittmeyer, and B. R. Cairns.** 2005. Chromatin remodelling through directional DNA translocation from an internal nucleosomal site. Nat Struct Mol Biol **12:**747-55.
74. **Schwartz YB, K. T., Nix DA, Li XY, Bourgon R, Biggin M, Pirrotta V.** 2006. Genome-wide analysis of Polycomb targets in Drosophila melanogaster. Nat Genet **38:**700-5.
75. **Schwartz, Y. B., and V. Pirrotta.** 2007. Polycomb silencing mechanisms and the management of genomic programmes. Nat Rev Genet **8:**9-22.
76. **Sevenet, N., A. Lellouch-Tubiana, D. Schofield, K. Hoang-Xuan, M. Gessler, D. Birnbaum, C. Jeanpierre, A. Jouvet, and O. Delattre.** 1999. Spectrum of hSNF5/INI1 somatic mutations in human cancer and genotype-phenotype correlations. Hum Mol Genet **8:**2359-68.
77. **Sevenet, N., E. Sheridan, D. Amram, P. Schneider, R. Handgretinger, and O. Delattre.** 1999. Constitutional mutations of the hSNF5/INI1 gene predispose to a variety of cancers. Am J Hum Genet **65:**1342-8.
78. **Sharpless, N. E.** 2005. INK4a/ARF: A multifunctional tumour suppressor locus. Mutation Research/Fundamental and Molecular Mechanisms of Mutagenesis **576:**22-38.
79. **Sharpless, N. E., M. R. Ramsey, P. Balasubramanian, D. H. Castrillon, and R. A. DePinho.** The differential impact of p16INK4a or p19ARF deficiency on cell growth and tumourigenesis. Oncogene **23:**379-385.
80. **Simon, J. A., and C. A. Lange.** 2008. Roles of the EZH2 histone methyltransferase in cancer epigenetics. Mutation Research/Fundamental and Molecular Mechanisms of Mutagenesis **647:**21-29.
81. **Sotillo, R., E. Hernando, E. Diaz-Rodriguez, J. Teruya-Feldstein, C. Cordon-Cardo, S. W. Lowe, and R. Benezra.** 2007. Mad2 overexpression promotes aneuploidy and tumourigenesis in mice. Cancer Cell **11:**9-23.
82. **Sparmann, A., and M. van Lohuizen.** 2006. Polycomb silencers control cell fate, development and cancer. Nat Rev Cancer **6:**846-856.
83. **Su, I.H., A. Basavaraj, A.N. Krutchinsky AN, O. Hobert, A. Ullrich, B.T. Chait, and A. Tarakhovsky.** 2003. Ezh2 controls B cell development through histone H3 methylation and Igh rearrangement. Nat Immunol **4:**124-31.
84. **Takayama, M. A., T. Taira, K. Tamai, S. M. Iguchi-Ariga, and H. Ariga.** 2000. ORC1 interacts with c-Myc to inhibit E-box-dependent transcription by abrogating c-Myc-SNF5/INI1 interaction. Genes Cells **5:**481-90.
85. **Tamkun, J. W., R. Deuring, M. P. Scott, M. Kissinger, A. M. Pattatucci, T. C. Kaufman, and J. A. Kennison.** 1992. brahma: a regulator of Drosophila homeotic genes structurally related to the yeast transcriptional activator SNF2/SWI2. Cell **68:**561-72.

86. **Thoma, N. H., B. K. Czyzewski, A. A. Alexeev, A. V. Mazin, S. C. Kowalczykowski, and N. P. Pavletich.** 2005. Structure of the SWI2/SNF2 chromatin-remodelling domain of eukaryotic Rad54. Nat Struct Mol Biol **12:**350-6.
87. **Tiwari VK, C. L., McGarvey KM, Ohm JE, Baylin SB.** 2008. A novel 6C assay uncovers Polycomb-mediated higher order chromatin conformations. Genome Res. **18**.
88. **Valk-Lingbeek, M. E., S. W. M. Bruggeman, and M. van Lohuizen.** 2004. Stem Cells and Cancer: The Polycomb Connection. **118:**409-418.
89. **van Deursen, J. M.** 2007. Rb loss causes cancer by driving mitosis mad. Cancer Cell **11:**1-3.
90. **Versteege, I., S. Medjkane, D. Rouillard, and O. Delattre.** 2002. A key role of the hSNF5/INI1 tumour suppressor in the control of the G1-S transition of the cell cycle. Oncogene **21:**6403-12.
91. **Versteege, I., N. Sevenet, J. Lange, M. F. Rousseau-Merck, P. Ambros, R. Handgretinger, A. Aurias, and O. Delattre.** 1998. Truncating mutations of hSNF5/INI1 in aggressive paediatric cancer. Nature **394:**203-6.
92. **Vire, E., C. Brenner, R. Deplus, L. Blanchon, M. Fraga, C. Didelot, L. Morey, A. Van Eynde, D. Bernard, J.-M. Vanderwinden, M. Bollen, M. Esteller, L. Di Croce, Y. de Launoit, and F. Fuks.** 2006. The Polycomb group protein EZH2 directly controls DNA methylation. Nature **439:**871-874.
93. **Vries, R. G., V. Bezrookove, L. M. Zuijderduijn, S. K. Kia, A. Houweling, I. Oruetxebarria, A. K. Raap, and C. P. Verrijzer.** 2005. Cancer-associated mutations in chromatin remodeller hSNF5 promote chromosomal instability by compromising the mitotic checkpoint. Genes Dev **19:**665-70.
94. **Wang, Z., W. Zhai, J. A. Richardson, E. N. Olson, J. J. Meneses, M. T. Firpo, C. Kang, W. C. Skarnes, and R. Tjian.** 2004. Polybromo protein BAF180 functions in mammalian cardiac chamber maturation. Genes Dev **18:**3106-16.
95. **Whitehouse, I., C. Stockdale, A. Flaus, M. D. Szczelkun, and T. Owen-Hughes.** 2003. Evidence for DNA translocation by the ISWI chromatin-remodelling enzyme. Mol Cell Biol **23:**1935-45.
96. **Wong, A. K., F. Shanahan, Y. Chen, L. Lian, P. Ha, K. Hendricks, S. Ghaffari, D. Iliev, B. Penn, A. M. Woodland, R. Smith, G. Salada, A. Carillo, K. Laity, J. Gupte, B. Swedlund, S. V. Tavtigian, D. H. Teng, and E. Lees.** 2000. BRG1, a component of the SWI-SNF complex, is mutated in multiple human tumour cell lines. Cancer Res **60:**6171-7.
97. **Xue, Y., J. C. Canman, C. S. Lee, Z. Nie, D. Yang, G. T. Moreno, M. K. Young, E. D. Salmon, and W. Wang.** 2000. The human SWI/SNF-B chromatin-remodelling complex is related to yeast rsc and localizes at kinetochores of mitotic chromosomes. Proc Natl Acad Sci U S A **97:**13015-20.
98. **Yan, Z., K. Cui, D. M. Murray, C. Ling, Y. Xue, A. Gerstein, R. Parsons, K. Zhao, and W. Wang.** 2005. PBAF chromatin-remodelling complex requires a novel specificity subunit, BAF200, to regulate expression of selective interferon-responsive genes. Genes Dev **19:**1662-7.
99. **Zhang, H. S., M. Gavin, A. Dahiya, A. A. Postigo, D. Ma, R. X. Luo, J. W. Harbour, and D. C. Dean.** 2000. Exit from G1 and S phase of the cell cycle is regulated by repressor complexes containing HDAC-Rb-hSWI/SNF and Rb-hSWI/SNF. Cell **101:**79-89.
100. **Zhang, Y., C. L. Smith, A. Saha, S. W. Grill, S. Mihardja, S. B. Smith, B. R. Cairns, C. L. Peterson, and C. Bustamante.** 2006. DNA translocation and loop formation mechanism of chromatin remodelling by SWI/SNF and RSC. Mol Cell **24:**559-68.
101. **Zhang, Z. K., K. P. Davies, J. Allen, L. Zhu, R. G. Pestell, D. Zagzag, and G. V. Kalpana.** 2002. Cell cycle arrest and repression of cyclin D1 transcription by INI1/hSNF5. Mol Cell Biol **22:**5975-88.
102. **Zofall, M., J. Persinger, S. R. Kassabov, and B. Bartholomew.** 2006. Chromatin remodelling by ISW2 and SWI/SNF requires DNA translocation inside the nucleosome. Nat Struct Mol Biol **13:**339-46.

Outline of the thesis

The mammalian SWI/SNF ATP-dependent chromatin remodeling complexes are highly conserved molecular motors that play crucial roles in a variety of cellular processes, including differentiation, proliferation. Human SNF5/INI1 is a subunit of SWI/SNF and tumour-suppressor lost in malignant rhabdoid tumors (MRTs), rare but highly aggressive paediatric cancers. Previously our group found that re-expression of hSNF5 in MRT cells caused an accumulation in G0/G1, cellular senescence and apoptosis. Cellular senescence is largely the result of direct transcriptional activation of the tumor-suppressor p16INK4a by hSNF5. We have developed MRT-derived G401 cell lines lacking genomic hSNF5 gene, which can express wild type or mutant hSNF5 (S284L) upon induction. We also transduced wild type hSNF5 to parental malignant rhabdoid MON cell lines lacking endogenous hSNF5.

To elucidate the pathways controlled by hSNF5 in rhabdoid tumor cells, in chapter2 we performed a cDNA microarray analysis to compare the temporal expression profile in MRT cells trasduced with GFP to those transduced with wild type hSNF5 or cancer related mutation (S284L) in different time course (24h, 48h and 5 days). To investigate direct targets of hSNF5 we performed chromatin immunoprecipitation on some of the genes which were up or down regulated by hSNF5. The aim of this chapter was to identify the downstream targets of the chromatin remodelling factor hSNF5 in two different MRT cells.

As uncontrolled cell proliferation and chromosomal instability is a hallmark of many cancers, we decided to investigate the role of hSNF5 in ploidy control. In chapter3, we report that loss of hSNF5 function in MRT-derived cells leads to polyploidization and chromosomal instability. We also examined the pathway through which hSNF5 controls cellular ploidy.

It is well known that both Polycomb repressive complex (PRC1 and PRC2) directly bind and silence the *INK4a-ARF* locus. In chapter4 we wondered whether this is also the case in MRT cells and, more interestingly, how SWI/SNF might overcome PcG silencing. We explored the molecular mechanism by which restoration of SWI/SNF functionality through hSNF5 re-expression overcomes epigenetic silencing and mediates *p16*^{INK4a} transcriptional activation in MRT cells. In chapter 5 we present evidence using human cells in which p15^{INK4b} and p16^{INK4a}, but not p14^{ARF}, are coordinately induced during cellular aging, multi-potent progenitor cell differentiation or induction of senescence. We showed that EZH2 depletion is sufficient for loss of PcG silencers from the INK4b and INK4a loci, and induction of the INK4a and INK4b expression. We showed that there is a physical and spatial interaction between p15^{INK4b} and p16^{INK4a} but not p14^{ARF}. This repressive chromatin loop disappears during aging, concomitant with EZH2 depletion and INK4a/b de-repression. Our results demonstrate that PcG proteins dynamically regulate higher order chromatin structure to balance proliferation and differentiation of human cells.

Chapter2

Global Gene Expression Regulation by hSNF5

Sima Kheradmand Kia[1] Rob G.J. Vries[1], Lobke M.P. Zuijderduijn[1], Sigrid Swagemakers[2], C. Peter Verrijzer[1]

1-Department of Biochemistry, Center for Biomedical Genetics, Center for Biomics, Erasmus University Medical Center, P.O. Box 1738, 3000 DR Rotterdam, The Netherlands
2-Erasmus center for Bioinformatics, Erasmus University Medical Center

Abstract

hSNF5/INI1 is a member of the ATP-dependent hSWI-SNF chromatin-remodeling complex. This gene is a tumor suppressor gene and frequently mutated in malignant rhabdoid tumours (MRT). We have developed MRT-derived G401 cell lines lacking genomic hSNF5 gene, which can express wild type or mutant hSNF5 (S284L) upon induction. We also transduced wild type hSNF5 to parental malignant rhabdoid MON cell lines lacking endoegenous hSNF5. We studied time course variation (24h, 48h and 5 days) of 22,500 genes/expressed sequence tags upon hSNF5/INI1 or mutant hSNF5 (S284L) induction or transfection. A total of 2404 responsive probe sets were identified after transduction of wild type hSNF5 in MON cell lines. After 5 days induction of wild type hSNF5 and mutant hSNF5 (S284L), 1705 and 444 responsive probe sets were significant, respectively. The expression levels of identified genes were evaluated by quantitative RT-PCR. The identified genes were functionally clustered into specific categories and probability of each category was determined using the computer program EASE. Our genome wide expression suggests that hSNF5 can function in both transcription activation and repression. Whole genome expression profiling of hSNF5 cells revealed expression change of many E2F targets, including mitotic control genes and pre-replication complex. This study identifies hSNF5/INI1 target genes and provides evidence that hSNF5/INI1 may modulate cell cycle control through the regulation of the p16 INK4A-cyclinD/CDK4-pRb-E2F pathway.

Introduction

ATP-dependent chromatin-remodelling factors (remodellers) are critical for the transmission, maintenance and expression of the eukaryotic genome. They function by mobilizing nucleosomes at the sites of DNA replication/repair and transcription activation/repression thus opening or closing chromatin for DNA-binding proteins. ATP-dependent chromatin remodeling complex can affect gene expression, cell cycle progression, and cell differentiation(3). The multi subunit SWI/SNF complex is evolutionary highly conserved and present in all eukaryotes(28). Human SNF5 (hSNF5, INI1 or SMARCB1) is a core component of the hSWI/SNF and it has been implicated in gene regulation, cell division and tumorogenesis(20). A significant majority of malignant rhabdoid tumors (MRTs) carry specific, biallelic, inactivating mutations in hSNF5. These tumors are extremely aggressive malignancies of early childhood. The most common sites of tumor are kidney and central nervous system (Atypical Teratoid/Rhabdoid Tumors (ATRT)(5, 37, 39, 44). Loss of SNF5/INI1 has been also detected in pediatric choroid plexus carcinoma, meningioma, medulloblastoma and primitive neuroectodermal tumours, which are histologically distinct from ATRT/MRTs(36). Inherited mutation of SNF5 leads to rhabdoid predisposition syndrom (5,39). As the majority of these extremely aggressive cancers have an entirely normal karyotype with only loss of SNF5, these tumors may be a result of extensive epigenetic changes caused by lack of SNF5(10, 38). Although most of the biallelic mutations in SNF5 are deletions, truncating nonsense or frameshift mutations and a number of point mutations resulting in single amino

acid substitutions (Figure 1A) have been identified in tumors (9, 39). These include proline 48 to serine (P48S), arginine 127 to glycine (R127G), serine 284 to leucine (S284L), and proline 116 to threonine (P116T). S284 is located within one of the most highly conserved regions of SNF5, which forms part of direct repeat 2 (RPT2) and it is conserved during evolution (Figure1B).

The ability of SNF5 to function as a tumor suppressor has been confirmed in studies utilizing SNF5-deficient mice. Homozygous deficiency of Snf5 results in early embryonic lethality prior to implantation, while heterozygous mice are predisposed to develop tumours in which there is loss of hetrozygocity for SNF5(13, 23, 35).

Re-expression of hSNF5 in MRT cells caused an accumulation in G0/G1, cellular senescence and apoptosis. Cellular senescence is largely the result of direct transcriptional activation of the tumour-suppressor $p16^{INK4a}$ by hSNF5(1, 4, 31, 43, 45, 48). Loss of hSNF5 function in MRT cells promotes chromosomal instability by compromised mitosis(45). hSNF5 activates the mitotic checkpoint through the $p16^{INK4a}$-cyclinD/CDK4-pRb-E2F pathway, revealing a convergence of tumour suppressor pathways.

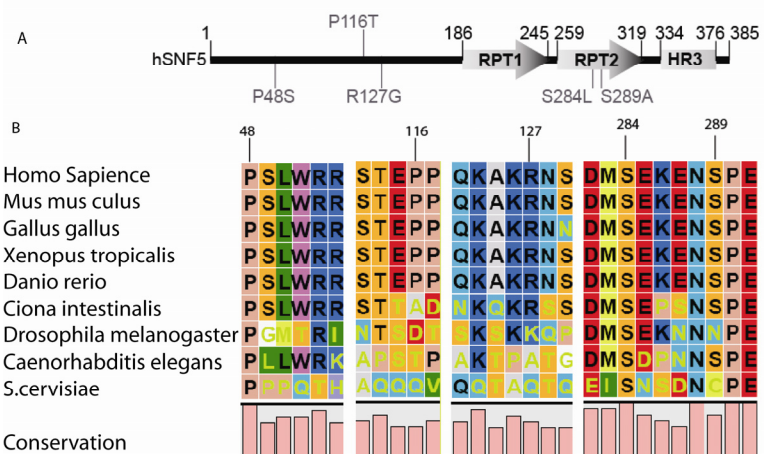

Figure1: Cancer associated amino acid substitution of hSNF5

A) Schematic representation of hSNF5 depicting the two repeats (RPT1 and RPT2) and cancer-associated amino acid substitution mutations. **B)** Conservation of cancer-associated amino acid substitution mutations from Human to Yeast

To identify the target genes of hSNF5 we carried out cDNA microarray analysis to determine the expression changes of genes in two hSNF5 deficient Rhabdoid cell lines (Mon and G401) upon re-introduction of hSNF5. We compared our data with other previously reported global gene expression profiles of hSNF5 in different human and mouse cell lines (7, 27, 29, 34, 35). Our genome wide expression suggests that hSNF5 can function in both transcription activation and repression.

Methods

Cell lines, Lentivirus production and Transduction.

All tissue cultures were according to standard protocols. Stable cell lines were generated using the LacSwitch™ II system (Stratagene). First pCMVLac1 followed by either pOPRSVI or pOPRSVI-hSNF5-FLAG, generated with a PCR-based strategy, encoding hSNF5 with a C-terminal FLAG epitope, were stably integrated in G401 MRT cells. FuGENE 6 (Roche Applied Science) was used for transfections. The resulting Lac-Empty or Lac-hSNF5 lines were isolated and most experiments were repeated using independent lines. Cells were maintained in Dulbecco's modified Eagle's medium supplemented with 10% fetal calf serum, 2 mM glutamine, 500 µg/ml G418, 100 µg/ml Hygromycin (Invitrogen). Mutants were generated using QuickChange mutagenesis (Stratagene).

The hSNF5 expressing lentiviral vector was generated by replacing the GFP encoding sequence of pRRLsin.sPPT.CMV.GFP.Wpre (12) with the hSNF5 cDNA (31). High titer vector stocks were produced in 293T cells by co-transfection of transfer vector constructs with the packaging constructs using standard transfection procedures (12). Mon cells were transduced with the appropriate vector.

RNA purification and Real- time RT-PCR analysis.

Total RNA was extracted from the MRT cells at 24 and 48 hours and 5 days post-stimulation using the SV Total RNA Isolation System (Promega) and cDNA synthesized from 1 µg of total RNA using random hexamers and SuperscriptTM II RNase H- Reverse Transcriptase (Invitrogen). Quantitative real-time PCR (MyIQ, Bio Rad) was performed using SYBR Green I. PCR primers were designed by Beacon designer (Premier Biosoft). The qPCR Core Kit (Invitrogen) was used with 400 nM of each primer under the following cycling conditions: 95°C for 3 min, 40 cycles of 10 s at 95°C, 45 s at 60°C. We used Usp14 as an endogenous normalization control. Enrichment of specific DNA sequences was calculated using the comparative C_T method (24). Primer sequences are provided in Table 1B.

Cell extracts and western blotting.

Cell extracts were prepared in RIPA buffer (10 mM Tris-HCl, pH 7.5, 150 mM NaCl, 1% Nonidet P-40, 1% NaDOC, 0.1% SDS), assayed for protein concentration, and 50 µg of extract was resolved by SDS-PAGE, and analyzed by immunoblotting. Primary antibodies: SNF5 (Abcam; ab12167) and Histone H3 (Abcam; ab1791). Western blots were developed with the ECL detection kit (PIERCE) according to the supplier's instructions.

Chromatin Immunoprecipitation (ChIP) assays.

ChIPs were performed as described by the Upstate protocol (http://www.upstate.com). Cross-linked chromatin was prepared from ~$2x10^7$ cells 48h following transduction with lentiviruses expressing either hSNF5 or GFP as a control. Cells were treated with 1% formaldehyde for 20 min at room temperature. Chromatin isolation, sonication yielding fragments of 300−600 bp and immunoprecipitations were performed according to protocol. The following antibodies were used: SNF5 (Abcam; ab12167), BRG1 (Abcam; ab4081), POL II (Santa Cruz; Sc-899), Histone H3 (Abcam; ab1791). The abundance of specific DNA sequences in the immunoprecipitates was determined by qPCR and corrected for the independently determined amplification curves of each primer set. ChIP using species and isotype-matched immunoglobins directed against an unrelated protein (GST) were used to determine background levels. Finally, DNA was purified by conventional phenol-chloroform extraction followed by ethanol precipitation and analyzed by qPCR. Enrichment of specific DNA sequences was calculated using the comparative C_T method (24). PCR primer sequences are provided in Table 1A. All data presented are the result of at least 3 independent ChIP experiments and triplicate qPCR reactions. Results were averaged and standard errors were determined using the R free software (http://www.r-project.org). ChIP levels for each region are presented as percentage of input chromatin.

Table 1. Primers used for (A) ChIP, (B) mRNA expression

A: Primers used for ChIP (q PCR)

	Forward Primer	Reverse Primer
ANGPT2	5′-GTTGGAGGGCAGGCATTC	5′-AGTTGATAAGAGCAGCCAGAC
ADAM19	5′-GGAGAGGGGTCCAGTTTAAC	5′-GGAGGAGGGATTTGTGGTG
ETS2	5′-GGGCTTCCTGGACTCCTTTC	5′-GCCTCCTGTCTGCTCTGG
INTGB5	5′-TAATCTCGGCTCGCCTAATAC	5′-CAGGTGGAAGTCGCTTGC
MAD2L1	5′-CGCAAAGGACCTGACGAC	5′-AACCACAGCGGCTCCAAC
P14	5′-CGCCGTGTCCAGATGTCG	5′-TGCTCTATCCGCCAATCAGG
TRIM22	5′-GTCCTGTTCTAAATCTCTGTAAAAG	5′-CAGTGCTGAGAATGTTGAAGG

B: Primers used for mRNA Expression (q PCR)

	Forward Primer	Reverse Primer
ANGPT2	5'-GCAGCTACACTTTCCTCCTG	5'-TTGTTTTCCATGATGTTCTCC
CASP4	5′-TCATGTCTCATGGCATCCTG	5′-TGACCTTGGGTTTGTCCTTC
CCNF	5′-CTCTCGCTTCTTCAGTCTCG	5′-CTCTGCAGCTGGCACTCTG
CDC25A	5′-AAGCTGTTTGACTCCCCTTC	5′-CAGACATGCTCTTCCTCCTC
CENPA	5′-CGAAAGCTTCAGAAGAGCAC	5′-CTTCTGCTGCCTCTTGTAGG
CENPE	5′-TTTTCCTGGGACCAGTTCAG	5′-AAACTTGGGCAGTTTCTCCA
CHAF1B	5′-GGACGGTTACTGCTCATTTG	5′-CCTCGATGTGTCTGACTCTTG
DR6	5′-CCAACGCGAAACTTGAGAAT	5′-GAGCCGCTGGATGTAGAGTC
ETS2	5′-ACTCCCAAAGACCACGACTCC	5′-GAAGCTCTCGAAGGAAGGAACC
E2F1	5′-ACTGAATCTGACCACCAAGC	5′-CAAGGACGTTGGTGATGTC
GAPDH	5′-GCCAAAAGGGTCATCATCTC	5′-GGTGCTAAGCAGTTGGTGGT
GAS6	5′-ATCAAGGTCAACAGGGATGC	5′-CTGCACGAGGTCCTTCTCAT
ITGB5	5′-GCAAACCTTGTCAAAAATGG	5′-CCTGTGGTGTCATCTGAATG
FAS	5′-GCCCAAGTGACTGACATCAA	5′-GACAGGGCTTATGGCAGAAT
MAD2L1	5′-ATACGGACTCACCTTGCTTG	5′-CCAGGACCTCACCACTTTC
MAP1B	5′-GAAGGGGACTGGAAGAACTC	5′-GATGGGACTTCCACTGATTC
MCM5	5′-TGCTGCCAACTCAGTGTTC	5′-ACATCCCTCTCCTCATTGTG
P16 ^{INK4a}	5′-CCCCTTGCCTGGAAAGATAC	5′-AGCCCCTCCTCTTTCTTCCT
POLD3	5′-CAAGTGAGACACAAGCCAAC	5′-TTCTTGGGTTTTAGCAGCAG
SERPINE2	5′-AGTCGAGGCCTCATGACAAC	5′-TACGCCGTATCTCATCACCA
TRIM22	5′-AGCAGAGAGAGCTGCAAAAG	5′-GCTGGAGATCTGAGATGAGC

Gene Expression profiling.

MRT cells were grown to optimal densities. RNA was isolated and tested on an Agilent BioAnalyzer (Agilent). Samples with RNA integrity numbers of >8 were selected. Labelling, hybridization, washes, and staining of AffymetrixU133A microarrays were performed according to Affymetrix geneChip manual. We have used the R and Bioconductor free software (http://www.bioconductor.org) to get the intensities and the calls. Intensity values for all genes were scaled using the quantile normalization and further normalized with Ominiviz software 3.6 (BIOwisdom, Maynard, MA). Intensity values<40were set to 40. Differential gene expression was based on log2 transformed distances to the geometric mean for each probe set. Unsupervised Pearson correlation were performed on <-2 and >2 and <-1.5 and >1.5 log2 geometric mean. Patterns of correction were revealed by applying a matrix-ordering method that sorts samples into correlated blocks, resulting in highly similar plots and identical grouping for LogGM<-2 and>2 or Log2GM<-1.5 and>1.5 probe subsets.

Biological Pathway analysis.

First the down stream genes of hSNF5 were evaluated for biological function and network interactions by using Ingenuity pathway analysis software (www.ingenuity.com). Genes were ranked by their ingenuity score, reflecting their involvements in biological networks are unique but not mutually exclusive. Ingenuity also identifies the most relevant biological processes among the signature genes by gene ontology analysis and calculates the significance of association of signature genes with canonical pathways and diseases. Second, the identified genes were functionally clustered into specific categories and probability of each category was determined using the computer program EASE.

Results

hSNF5 Can Function in Transcription Activation and Repression of the Genome

To study the function of hSNF5 in MRT cells, we established two distinct strategies to re-express hSNF5 in G401 and Mon, two different MRT cell lines. We reintroduced hSNF5 gene under Lac repressor-operator control in G401 cell line; in parallel hSNF5 was transduced to Mon cells using lentiviral transfection.

Samples were harvested 24 hours, 48 hours and 5 days after induction of wild-type hSNF5 expression in G401 MRT-derived cell line or 48 hours after transduction of either GFP or SNF5 in MON cells. hSNF5 is not essential for SWI/SNF complex integrity (10, 30, 31). Moreover, induced exogenous hSNF5 expression levels were comparable to the endogenous levels in a variety of cell lines (11, 31).

To elucidate pathways controlled by hSNF5 in rhabdoid tumor cells, we performed cDNA microarray analysis. Temporal gene expression profile in G401 cells lacking hSNF5 compared

to those induced by adding IPTG to express either wild type or mutant hSNF5, serine 284 to leucine (S284L). The same comparison was performed for Mon cells trasduced with GFP to those transduced with hSNF5. hSNF5 expression could be clearly detected 24 h after either induction or transduction. Three different time points, 24 h, 48 h and 5 days were harvested for microarray studies. RNA isolated at three time points from G401, and last time point from Mon cells, labeled, and used for cDNA microarray analysis. Differentially expressed genes above 1.5 fold threshold were selected. We found 26 consistently differentially expressed genes (24 up; 4 down) by *hSNF5* in all data points and different MRT cells. Further we focused on consistent differentially expressed genes upon wild type *hSNF5* induction after 5 days in both MRT cell lines. We found 179 and 177 genes were up and down-regulated, respectively, in G401 cells and Mon cells.

The majority of the up-regulated genes encode proteins involved in extracellular matrix remodelling, adhesion or cell migration (SERPINE2, ITGB5, MAP1B), apoptosis (DR6, FAS, CASP4, GAS6, ADAM19), and cancer related pathway or other specialized functions (CDKN2A, ETS2 and TRIM22). This group of genes did not change or were down-regulated upon mutant SNF5 induction. The majority of down-regulated genes by hSNF5 encode proteins playing a key role during the cell cycle (i.e. CENPE, POLD3, CENPA, CDC25A, CCNF and MAD2) and remain unchanged upon mutant hSNF5 induction. These results suggested misexpression of mitotic checkpoint components might cause abnormal ploidy of MRT cells. For example, over-expression of Mad2 and its regulator E2F1 was implicated in mitotic defects leading to aneuploidy (16). In our microarray experiments both genes were down-regulated following hSNF5 induction. We used qRT-PCR to corroborate our microarray results (Figure. 2). We found that Mad2, E2F1and E2F1 target genes are highly expressed in MRT cells, but are strongly down-regulated following hSNF5 induction.

Further we transduced GFP or SNF5 in MRT (G401 and MON), Hela and U2OS cells using lentiviral transduction. Western immunoblot analysis of extracts from cells transduced by lentiviruses expressing GFP (lanes 1,3,5 and 7, Figure. 3A) or SNF5 (lanes 2,4,6 and 8) revealed normal hSNF5 expression in G401 and Mon cells (lane 2,4) and over-expression in Hela and U2OS cells compare to endogenous levels (lane 6 and 8). Antibodies directed against histone H3 were used as loading control. qRT-PCR revealed up-regulation of FAS, ETS2, TRIM22, GAS6, ADAM19 and SERPINE2 in MRT cells upon SNF5 induction while they remain unchanged or down-regulated in either Hela or U2OS cells (Figure. 3B-G).

To investigate direct targets of hSNF5, we performed chromatin immunoprecipitation on some of up or down regulated genes by hSNF5. MRT cells transduced with lentivirus (or induced with IPTG). hSNF5 was expressed to detectable levels at 48 hours post stimulation (data not shown). Chromatin was prepared from cells at 48 hours post-stimulation and subjected to chromatin immunoprecipitation with an antibody specific for hSNF5. Quantitative PCR analysis performed on immunoprecipitated material using primers specific for promoters for genes of interest as indicated in Table1B. As shown in Figure.4A our results indicate while hSNF5 is initially absent from TRIM22, ETS2, ANGPT2 and MAD2L genes, it is specifically

recruited to these promoters in response to SNF5 expression induction. hSNF5 expression does not result in recruitment of SNF5 to the adjacent P14, ADAM19 and INTGB5 promoters. Taken together these results demonstrate that re-expression of hSNF5 in MRT cells results in specific recruitment of hSNF5 to TRIM22, ETS2, ANGPT2 promoters, up-regulated genes by hSNF5, and MAD2L promoters, down regulated gene by hSNF5, but not P14, ADAM19 and INTGB5 promoters, no significant change and up-regulate genes by hSNF5, respectively. Our data therefore supports the notion that hSNF5, an essential subunit of SWI/SNF complexes directly mediates both activation and repression of its target genes most likely in collaboration with gene-specific transcription factors and other chromatin modifying complexes, such as histone acetylases and deacetylases (22, 32).

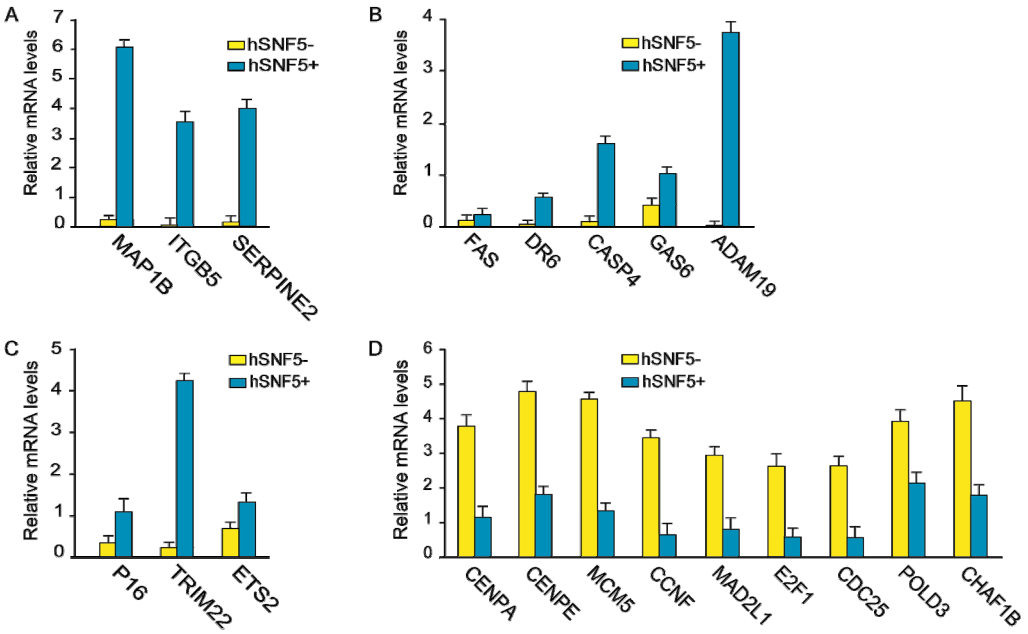

Figure2. QRT-PCR analysis of gene regulated by hSNF5 identified by whole-genome expression profiling.
RT-qPCR analysis of gene expression in MRT cells reveals hSNF5-dependent induction of genes involved in **A)** apoptosis pathway **B)** Cell migration and invasion **C)** Other pathway and **D)** depletion of E2F and E2F target genes affected. Cells were collected 48 hours following transduction with lentiviruses expressing either GFP (yellow bars) or hSNF5 (blue bars). mRNA levels were plotted as percentage of GAPDH mRNA. The bar graphs represent the mean of three independent biological replicates, each analyzed by three separate qPCR reactions. Standard deviations are indicated.

hSNF5 Mediates BRG1 (SWI/SNF) Recruitment

Previously we showed that hSNF5 is required for BRG1 recruitment to the $p16^{INK4a}$ and $P15^{ink4b}$ promoters(21, 31). We now examined whether hSNF5 also mediates the recruitment of BRG1 to the TRIM22, ETS2, ANGPT2 and MAD2L Promoters. We used chromatin

immunoprecipitation (ChIP) to study the occupancy of TRIM22, ETS2, ANGPT2, P14, ADAM19, INTGB5 and MAD2L promoters in MRT cells either lacking or induced to express SNF5. Chromatin isolated from MRT cells, 48 hours post-stimulation, immunoprecipitated using antibodies specific for BRG1 and species- isotype-matched immunoglobulins. Immunoprecipitated chromatin was analyzed by real time PCR using primer sets specific for promoter regions of genes of interest indicated in table1. While initially absent from these target genes. Following hSNF5 induction, BRG1 specifically bound to the TRIM22, ETS2, ANGPT2 and MAD2L promoters. Neither hSNF5 nor BRG1 were detected at the P14, ADAM19 and INTGB5 promoters prior or after induction.

These results suggest that hSNF5 mediates recruitment of BRG1, the catalytic subunit of SWI/SNF to TRIM22, ETS2, ANGPT2 and MAD2L promoters to either stimulate or repress transcription.

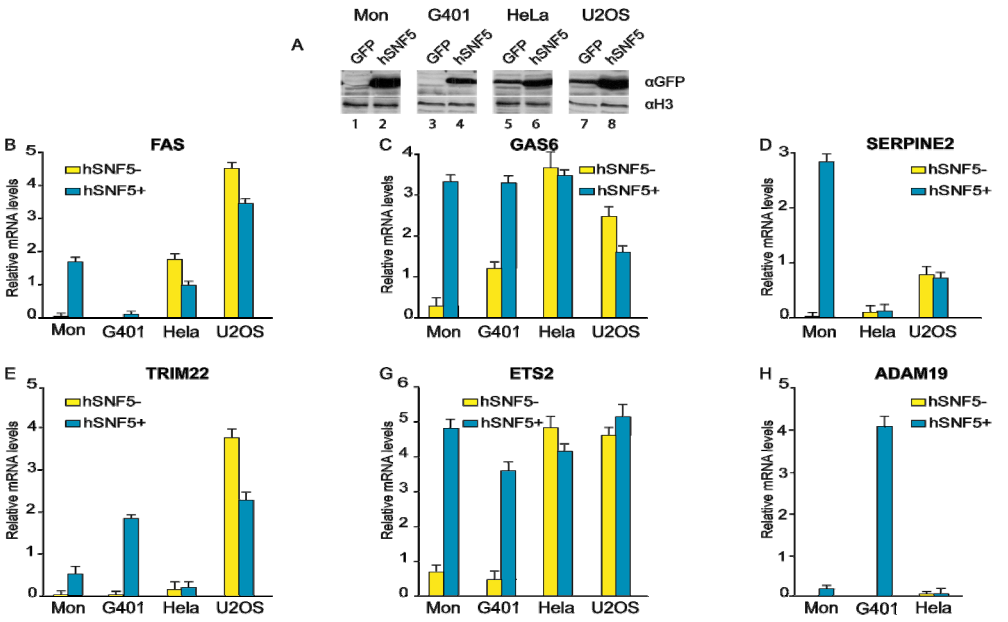

Figure3. RTQ-PCR analysis of gene regulated by hSNF5 in different cells
(A) Western immunoblotting analysis of hSNF5 expression in MON. G401, Hela and U2OS cells transduced with lentiviruses expressing either GFP (lanes 1, 3, 5,7) or hSNF5 (lanes 2,4,6,8). Cell lysates were resolved by SDS-PAGE and analyzed by Western immunoblotting using antibodies directed against hSNF5. Histone H3 serves as a loading control. (B-E) RTQ-PCR analysis of genes upon induction or over expression of hSNF5 in two MRT cells (Mon, G401) Hela and U2OS cells. PCR revealed induction of **(B)** FAS, **(C)** GAS6, **(D)** SERPINE2, **(E)** TRIM22, **(F)** ETS2 and **(G)** ADAM19 in MRT cells upon induction of SNF5 while they remain unchanged or down-regulated in either Hela or U2OS cells. Procedures were as described in the legend to Figure. 2.

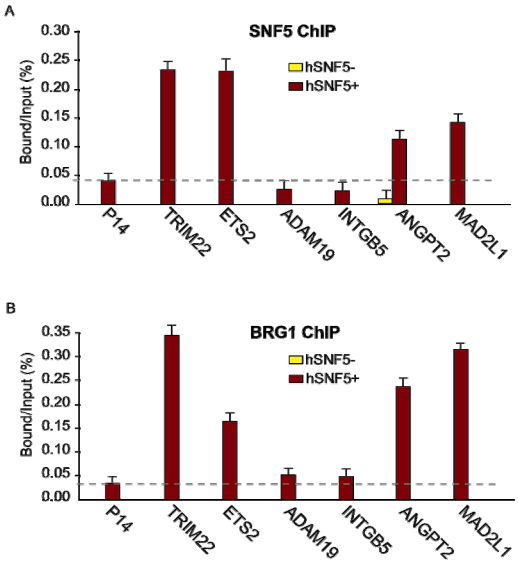

Figure4. hSNF5 Mediates BRG1 Recruitment to the MAD2, TRIM22, ETS2 and ANGPT2 promoters
(A)ChIP-qPCR analysis of hSNF5 binding to the *MAD2, TRIM22, ETS2 and ANGPT2* ,$p14^{Arf}$, INTGB5 and ADAM19 revealed that hSNF5 binds directly to the *MAD2, TRIM22, ETS2* and *ANGPT2* promoters, but not to $p14^{Arf}$. Cross-linked chromatin was isolated from MRT cells that either lack- (light bars) or express hSNF5 (dark bars). (B) BRG-1 binding to the *MAD2, TRIM22, ETS2* and *ANGPT2* promoters is hSNF5-dependent, as revealed by ChIP-qPCR using antibodies directed against BRG-1.

Discussion

The aim of this study was to identify the downstream targets of the chromatin remodeling factor hSNF5 in two different MRT cells. Our genome wide expression suggests that hSNF5 can function in both transcription activation and repression of genome. ySWI/SNF subunits is required for the activation of a number of specific genes which are involved in mating-type switch, sucrose and galactose fermenting(33). Genome-wide expression profiling indicates that the ySWI/SNF complex regulates about 6% of the genes, both positively and negatively(17, 42). This suggests that the ySWI/SNF complex can function in both transcription activation and repression. Indeed, other studies have shown that ySWI/SNF complex cooperates with the SAGA histone-acetyltransferase complex to displace nucleosomes from the promoters of target genes upon transcription activation allowing binding of transcription factors to promoter DNA(8, 14). Systematic RNAi knockdown survey of the BAP and PBAP subunits has been recently performed in Drosophila embryonic cells(28, 30). Genome-wide expression profiling and comprehensive statistical analysis showed that both complexes function as holoenzymes to activate or repress expression of multiple target genes either cooperatively, antagonistically or separately. Strikingly, RNAi knockdown of the BAP subunits results in accumulation of the cells in G2/M phase of the cell cycle, whereas depletion of the PBAP specific subunits has no significant effect on growth and cell cycle progression(30). However, it is already clear that besides regulation of G2/M phase, SWI/SNF complexes could be involved in the control of G1/S phase via cyclin E-E2F/Rb pathway(6, 41).

Other study have analyzed hSNF5-induced gene expression changes at early time points in rhabdoid cells (27). They studied 7 time course variations of 22,000 genes/expressed sequence tags upon hSNF5/INI1 induction in Mon cells. We found 78% and 80% of up-regulated or down-regulated genes reported in these studies that were up-regulated or down-regulated respectively in our study after reintroduce of hSNF5 in Mon cells (Table2). Recently it has been shown that inhibition of migration induced by hSNF5 correlates with depletion of RhoA activity(7). Another group showed that hSNF5 induces Interferon signalling and spindle checkpoint in rhabdoid tumours (29) as we showed previously(45). Others have explored the hSNF5-dependent expression profile changes in the nonrhabdoid mouse embryo fibroblasts(19). Cell cycle genes that were up-regulated in that study are down-regulated in our microarray data (Table3). Table 4 shows the comparison of our data with the outcome of array data of central nervous system embryonal tumor (34).

Notably these findings suggest that hSNF5 acts as a transcriptional co-activator or co-repressor, which is required for the recruitment of the BRG1 containing SWI/SNF chromatin remodeling complex to the TRIM22, ETS2, ANGPT2 and MAD2L but not $p14^{ARF}$, ADAM19 and INTGB5 genes. The mechanisms by which the SWI/SNF complexes can influence both gene activation and repression in vivo are not fully understood(32). The hSNF5 containing SWI/SNF complex activates its targets by actively disrupting chromatin structure at promoters to allow increased access of the general transcription machinery or sequence specific activators to DNA. For example hSWI/SNF fractions were shown to increase binding of TFIIA and TBP to the TATA sequence on nucleosomal DNA(18). Several models explain gene-specific SWI/SNF-mediated repression. First, distinct sub-complexes like Sin3 repressor complex may mediate activation and repression functions of SWI/SNF differential subunit (40). A second model involves recruitment of the SWI/SNF complex to promoters as components of larger co-repressor complexes. In mammals, the hBRM/BRG-1 complexes form co-repressors with retinoblastoma (pRB) and HDACs to block cell cycle progression at the G1-S boundary(15, 25, 47). hSNF5 represses *cyclinD1* expression in G1 through collaborations with HDAC complexes(48). Also, the tumor suppressor gene *prohibitin* represses *E2F*-mediated transcription by recruitment of BRG1 to *E2F* promoters(46). Ets-2 and components of mammalian SWI/SNF (hSNF5 and BAF57/p50 and BRG1) form a repressor complex that negatively regulates the *BRCA1(2)*; again suggesting that SWI/SNF coordinates with repressor proteins to actively repress gene expression. A third model is that the SWI/SNF complex mediates gene repression by directly altering nucleosome structure in an ATP-dependent (SWI2/SNF2) manner to form a repressive chromatin environment (26). In all of these models, SWI/SNF actively represses gene expression, either directly through the ATP-dependent chromatin remodeling functions of the complex itself, or as part of large repressor complexes. Thus, because of its direct involvement in both transcriptional activation as well as repression, hSNF5 can be thought of as transcriptionally inert but capable of mediating both activation and repression in a context dependent manner.

Table2: Genes are up and down regulated in our Mon WTSNF5+/- microarray data and Medjkani et al. data (Ref27)

Cancer Research 2004		Our Microarray data				
Gene Symbol	UniGene ID	G401 WTSNF5+/- 24h	G401 WTSNF5+/- 48h	G401 WTSNF5+/- 5d	G401 S284L+/-	Mon WTSNF5+/-
Prereplication complex/DNA Repair						
MCM2	Hs.57101	1,02	1,30	-1,80	1,04	-1,68
MCM4	Hs.460184	1,23	1,95	-2,59	-1,02	-2,18
MCM5	Hs.77171	1,02	1,37	-2,12	-1,02	-2,62
MCM10	Hs.198363	-1,02	1,36	-1,69	1,10	-1,64
RFC3	Hs.115474	-1,01	1,62	-1,49	1,20	-2,33
CDT1	Hs.122908	1,37	1,74	-1,52	1,07	-1,58
PIR51	Hs.24596	1,44	1,71	-1,25	1,11	-2,23
G1-S						
CDC6	Hs.405958	1,23	1,30	-1,43	1,03	-1,94
CDC7	Hs.28853	-1,03	1,03	-1,48	1,25	-1,68
DHFR	Hs.464813	-1,26	4,18	-1,89	1,54	-1,65
CCNA2	Hs.85137	1,12	2,52	-1,30	1,14	-1,95
Mitosis						
CDC2	Hs.334562	-1,05	1,31	-1,61	1,41	-1,48
CENPE	Hs.75573	1,05	2,25	-2,02	-1,02	-1,50
KIF11	Hs.8878	1,21	2,37	-1,55	1,00	-1,89
KIF23	Hs.270845	1,10	2,11	-1,06	1,18	-1,49
PLK4	Hs.172052	1,58	2,64	-1,27	1,11	-1,41
SMC4L1	Hs.50758	-1,02	1,72	-1,38	1,02	-1,41
Cytoskeleton						
EMS1	Hs.301348	1,00	-1,22	3,01	1,61	1,43
BICD1	Hs.412020	-1,71	-1,90	1,33	-1,12	2,27
KLHL4	Hs.49075	1,00	1,00	1,00	1,00	4,82
TMOD1	Hs.374849	-1,03	1,02	1,00	1,28	2,14
WASF3	Hs.82318	1,19	1,00	1,17	1,14	6,00
ADD3	Hs.324470	1,93	4,15	-1,16	1,26	1,42
AMPH	Hs.173034	1,00	1,00	1,00	1,00	1,66
ARHGAP4	Hs.3109	1,26	-1,07	-1,13	1,13	1,62
Cell Matrix-interaction/adhesion/cell-cell interaction						
COL1A1	Hs.172928	1,43	1,10	1,56	-1,12	2,39
SPARC	Hs.111779	1,13	1,00	-1,02	-1,15	24,37
JUP	Hs.2340	1,81	3,19	-1,78	1,06	5,68
POSTN	Hs.136348	1,00	1,00	1,00	1,50	4,27
PLXNB2	Hs.3989	-1,02	1,18	1,26	-1,03	2,74
DOCK4	Hs.118140	1,00	1,00	1,00	1,00	1,77
NEO1	Hs.388613	-1,08	-1,08	1,00	1,00	4,67
Signal Transduction, Cytokines, Reseptors						
DTR	Hs.799	1,21	-1,07	2,18	1,67	8,00
FZD7	Hs.173859	1,67	1,99	2,91	1,34	2,44
IGF1R	Hs.239176	-1,23	1,19	-1,26	1,35	1,51
IGF2R	Hs.76473	1,04	1,16	1,21	-1,05	2,44
TNFRSF6	Hs.82359	1,00	1,00	3,01	1,00	1,93
IL15RA	Hs.12503	1,31	-1,27	1,45	1,36	2,55
Intracellular Transduction signal						
PLCL1	Hs.153322	1,00	1,00	1,00	1,00	3,28
RAB3B	Hs.123072	1,11	1,39	1,69	1,13	2,23
RAB5C	Hs.479	1,20	1,13	-1,42	-1,31	1,82
Others						
IFI16	Hs.370873	1,00	1,00	1,00	1,19	5,58
ATP1B1	Hs.78629	-1,26	-1,22	1,04	-1,08	15,60

Down Regulated genes (Cancer Rsearch64,3406-13,2004)
Up Regulated genes in (Cancer Rsearch64,3406-13,2004)

Table3: Intersection between our data and cell cycle genes in MEFs (without SNF5) (Roberts et al Ref35)

PNAS 2000 data		Our Microarray data		
Gene Symbol	Gene Title	G401 WTSNF5+/-	G401 S284L+/-	Mon WTSNF5+/-
E2F1 target gene set				
MCM7	MCM7 minichromosome maintenance deficient 7	-1,55	-1,09	-2,07
MCM5	MCM5 minichromosome maintenance deficient 5	-2,34	1,04	-2,15
MKI67	antigen identified by monoclonal antibody Ki-67	-1,09	-1,04	-1,64
CCNA2	cyclin A2	-1,30	1,14	-1,95
MCM2	MCM2 minichromosome maintenance deficient 2	-1,80	1,04	-1,68
TK1	thymidine kinase 1, soluble	-1,45	1,32	-1,28
TMPO	thymopoietin	-1,95	-1,03	-1,68
FEN1	flap structure-specific endonuclease 1	-1,53	1,04	-1,74
HMMR	hyaluronan-mediated motility receptor (RHAMM)	-1,64	-1,09	-1,44
TYMS	thymidylate synthetase	-1,06	1,06	-1,23
MCM6	MCM6 minichromosome maintenance deficient 6	-1,64	1,03	-1,61
CDC25C	cell division cycle 25C	-1,45	1,01	-2,32
RRM1	ribonucleotide reductase M1 polypeptide	-1,39	1,09	-1,80
MCM3	MCM3 minichromosome maintenance deficient 3	-1,54	1,02	-1,27
RFC3	replication factor C (activator 1) 3, 38kDa	-1,49	1,20	-2,33
RRM2	ribonucleotide reductase M2 polypeptide	-1,28	1,01	-1,57
DCK	deoxycytidine kinase	-1,04	1,12	-1,72
CDK2	cyclin-dependent kinase 2	-1,14	1,02	-1,06
TRA1	tumor rejection antigen (gp96) 1	-1,47	1,09	-1,20
CDC6	CDC6 cell division cycle 6 homolog	-1,43	1,03	-1,94
MCM4	MCM4 minichromosome maintenance deficient 4	-2,59	-1,02	-2,18
DHFR	dihydrofolate reductase	-1,89	1,54	-1,65
SLBP	stem-loop (histone) binding protein	1,06	1,02	-1,61
Cyclin & CDK gene Set				
CCNB2	cyclin B2	-1,20	1,16	-1,51
CCNB1	cyclin B1	-1,60	-1,10	-1,71
CCNA2	cyclin A2	-1,30	1,14	-1,95
CDKN2C	cyclin-dependent kinase inhibitor 2C	-1,24	1,13	-1,23
CCND2	cyclin D2	2,97	1	1
CCND3	cyclin D3	1,13	1,10	-1,26
CDK2	cyclin-dependent kinase 2	-1,14	1,02	-1,06
CCNF	cyclin F	-2,30	-1,19	-1,60
CIZ1	CDKN1A interacting zinc finger protein 1	1,68	-1,17	-1,21
CDKN1B	cyclin-dependent kinase inhibitor 1B (p27, Kip1)	-1,66	1,17	-1,01
CDK5RAP1	CDK5 regulatory subunit associated protein 1	-1,05	1,05	-1,64
CDKN1A	cyclin-dependent kinase inhibitor 1A (p21, Cip1)	1,95	1,28	1,66
CDK9	cyclin-dependent kinase 9 (CDC2-related kinase)	-1,42	-1,16	1,76
CDKN2A	cyclin-dependent kinase inhibitor 2A	1,96	1,18	1,54
CDK5RAP3	CDK5 regulatory subunit associated protein 3	-1,39	1,14	1,82
CCND1	cyclin D1	1,56	-1,03	1,41

Down Regulated genes in Roberts data
Up Regulated genes in Roberts data

Table4: comparison of our data with outcome of array data of central nervous system embryonal tumour (Pomeroy 2002, Ref34)

Nature 2002 data			Our Microarray data				
	Gene Symbol	UniGene ID	G401 WTSNF5+/- 24h	G401 WTSNF5+/- 48h	G401 WTSNF5+/- 5d	G401 S284L+/-	Mon WTSNF5+/-
Apoptosis							
	PEA15	Hs.194673	1,20	-1,05	2,60	1,60	1,7
Cell adhesion							
	ARVCF	Hs.326730	1,81	1,32	1,40	2,13	1,39
	CELSR2	Hs.57652	-1,32	1,10	1,14	-1,06	1,76
	TYRO3	Hs.381282	1,28	1,60	1,03	1,28	1,63
	BYSL	Hs.106880	-1,11	-1,50	1,04	1,11	-1,60
	C5R1	Hs.2161	-1,27	-2,06	-2,42	-1,33	1
Cell cycle							
	CCNI	Hs.369110	1,19	1,54	-1,05	-1,05	1,17
	MCC	Hs.409515	-1,13	1,17	1,15	1,06	1,81
	ERF	Hs.440332	1,05	1,15	-3,62	1,00	1,31
Cell Metabolism							
	CALM3	Hs.334330	1,03	2,20	1,26	-1,33	1,58
	ENO2	Hs.511915	1,32	1,16	2,95	1,05	1,54
	FKBP4	Hs.848	1,00	-1,22	1,57	1,01	-1,63
	QDPR	Hs.75438	1,06	1,22	1,92	1,22	-1,22
	RIMS3	Hs.78748	1,25	1,28	1,13	1,08	1,57
	SMPD1	Hs.77813	1	1	1,08	-1,25	5,01
	WASF3	Hs.82318	1,19	1	1,17	1,14	6,00
Cell Motility							
	ACTC	Hs.118127	-1,77	-1,46	1,56	1,52	-1,00
Cell Signaling							
	D4S234E	Hs.79404	1,08	1,31	1,15	1,49	2,73
Development							
	MAP1A	Hs.194301	1,34	1,33	1,93	1,16	-3,04
Signal Transduction							
	ADORA2B	Hs.45743	1,10	-1,05	1,59	1,13	-1,28
	PPP2R5B	Hs.75199	1,14	-1,08	1,27	1,07	1,57
	SQSTM1	Hs.182248	1,57	-1,15	1,40	1,16	1,77
	TIAM1	Hs.115176	1	1	1	1	2,75
Transcription							
	HIVEP2	Hs.75063	1,12	-1,59	1,53	-1,08	1
	HNF4A	Hs.54424	-1,18	-1,03	1,05	1	1,68
	NCOA1	Hs.386092	1,64	2,26	1,08	1,23	2,64
	NR1D1	Hs.276916	-1,08	-1,61	1,39	-1,10	1,04
	PIPPIN	Hs.106635	1,33	1,70	1,27	1,67	1
	PRRX1	Hs.443452	1,35	1,19	1,35	1,20	1,73
Translation							
	EEF1A2	Hs.433839	1	1	1	-1,14	2,08
Transport							
	ATP1B1	Hs.78629	-1,26	-1,22	1,04	-1,08	15,60
	DNM1	Hs.436132	1,19	1,76	1,10	-1,10	1,11
	SLC9A1	Hs.170222	1,44	-1,12	1,19	1,28	1,80
	SORL1	Hs.438159	1	1	1	1	1,82
	STXBP1	Hs.325862	-1,14	1,09	-1,59	-1,26	1,37

Down Regulated genes in Pomeroy data

Up Regulated genes in Pomeroy data

References

1. **Ae, K., N. Kobayashi, R. Sakuma, T. Ogata, H. Kuroda, N. Kawaguchi, K. Shinomiya, and Y. Kitamura.** 2002. Chromatin remodeling factor encoded by ini1 induces G1 arrest and apoptosis in ini1-deficient cells. Oncogene **21:**3112-20.
2. **Baker, K. M., G. Wei, A. E. Schaffner, and M. C. Ostrowski.** 2003. Ets-2 and Components of Mammalian SWI/SNF Form a Repressor Complex That Negatively Regulates the BRCA1 Promoter, p. 17876-17884, vol. 278.
3. **Becker, P. B., and W. Horz.** 2002. ATP-dependent nucleosome remodeling. Annu Rev Biochem **71:**247-73.
4. **Betz, B. L., M. W. Strobeck, D. N. Reisman, E. S. Knudsen, and B. E. Weissman.** 2002. Re-expression of hSNF5/INI1/BAF47 in pediatric tumour cells leads to G1 arrest associated with induction of p16ink4a and activation of RB. Oncogene **21:**5193-203.
5. **Biegel, J. A., J. Y. Zhou, L. B. Rorke, C. Stenstrom, L. M. Wainwright, and B. Fogelgren.** 1999. Germ-line and acquired mutations of INI1 in atypical teratoid and rhabdoid tumours. Cancer Res **59:**74-9.
6. **Brumby, A. M., C. B. Zraly, J. A. Horsfield, J. Secombe, R. Saint, A. K. Dingwall, and H. Richardson.** 2002. Drosophila cyclin E interacts with components of the Brahma complex. Embo J **21:**3377-89.
7. **Caramel, J., F. Quignon , and O. Delattre.** 2008. RhoA-Dependent Regulation of Cell Migration by the Tumour Suppressor hSNF5/INI1. Cancer Research **68:**6154-6161.
8. **Chandy, M., J. L. Gutierrez, P. Prochasson, and J. L. Workman.** 2006. SWI/SNF displaces SAGA-acetylated nucleosomes. Eukaryot Cell **5:**1738-47.
9. **Cho, Y. M., J. Choi, O.J. Lee, H.I. Lee, D. J. Han, and J. Y. Ro.** 2006. SMARCB1/INI1 missense mutation in mucinous carcinoma with rhabdoid features. Pathology International **56:**702-706.
10. **Doan, and V. T. DN, Yan Z, Wang W, Jones SN, Imbalzano AN.** 2004. Loss of the INI1 tumour suppressor does not impair the expression of multiple BRG1-dependent genes or the assembly of SWI/SNF enzymes. Oncogene **23:**3462-73.
11. **Douglass EC, R. S., Valentine M, Parham D, Meyer WH, Thompson EI. .** 1990. A second nonrandom translocation, der(16)t(1;16)(q21;q13), in Ewing sarcoma and peripheral neuroectodermal tumour. Cytogenet Cell Genet **53:**87-90.
12. **Follenzi, A., G. Sabatino, A. Lombardo, C. Boccaccio, and L. Naldini.** 2002. Efficient Gene Delivery and Targeted Expression to Hepatocytes In Vivo by Improved Lentiviral Vectors. Hum Gene Ther **13:**243-260.
13. **Guidi, C. J., A. T. Sands, B. P. Zambrowicz, T. K. Turner, D. A. Demers, W. Webster, T. W. Smith, A. N. Imbalzano, and S. N. Jones.** 2001. Disruption of Ini1 leads to peri-implantation lethality and tumourigenesis in mice. Mol Cell Biol **21:**3598-603.
14. **Gutierrez, J. L., M. Chandy, M. J. Carrozza, and J. L. Workman.** 2007. Activation domains drive nucleosome eviction by SWI/SNF. Embo J.
15. **Harbour, J. W., and D. C. Dean.** 2000. Chromatin remodeling and Rb activity. Current Opinion in Cell Biology **12:**685-689.
16. **Hernando E, N. Z., Juan G, Diaz-Rodriguez E, Alaminos M, Hemann M, Michel L, Mittal V, Gerald W, Benezra R, Lowe SW, Cordon-Cardo C.** 2004. Rb inactivation promotes genomic instability by uncoupling cell cycle progression from mitotic control. Nature **430:**797-802.
17. **Holstege, F. C., E. G. Jennings, J. J. Wyrick, T. I. Lee, C. J. Hengartner, M. R. Green, T. R. Golub, E. S. Lander, and R. A. Young.** 1998. Dissecting the regulatory circuitry of a eukaryotic genome. Cell **95:**717-28.
18. **Imbalzano, A. N., Kwon, H., Green, M.R., Kingston, R.E.** 1994 Facilitated binding of TATA-binding protein to nucleosomal DNA. Nature **11:**481-5.
19. **Isakoff MS, and T. P. Sansam CG, Subramanian A, Evans JA, Fillmore CM, Wang X, Biegel JA, Pomeroy SL, Mesirov JP, Roberts CW.** 2005. Inactivation of the Snf5 tumour suppressor stimulates cell cycle progression and cooperates with p53 loss in oncogenic transformation. Proc Natl Acad Sci U S A **102:**17745–17750.

20. **Johnson.** 2005. Chromatin remodeling complexes: ATP-dependent machines in action. Biochem Cell Biol. **83:**405-17.
21. **Kheradmand Kia S., M.M. Gorski, S. Giannakopoulos, and C. P. Verrijzer.** 2008. SWI/SNF Mediates Polycomb Eviction and Epigenetic Reprogramming of the INK4b-ARF-INK4a Locus. MCB **28:**3457-3464.
22. **Kingston, R. E., Bunker, C.A and Imbalzano, A.N.** 1996. Repression and activation by multiprotein complexes that alter chromatin structure, Genes Dev. 10 (1996), pp. 905–920. Genes Dev **10:**905-920.
23. **Klochendler-Yeivin, A., L. Fiette, J. Barra, C. Muchardt, C. Babinet, and M. Yaniv.** 2000. The murine SNF5/INI1 chromatin remodeling factor is essential for embryonic development and tumour suppression. EMBO Rep **1:**500-6.
24. **Livak, K. J., and T. D. Schmittgen.** 2001. Analysis of Relative Gene Expression Data Using Real-Time Quantitative PCR and the 2-[Delta][Delta]CT Method. Methods **25:**402-408.
25. **Luo, R. X., A. A. Postigo, and D. C. Dean.** 1998. Rb Interacts with Histone Deacetylase to Repress Transcription. Cell **92:**463-473.
26. **Martens, J. A., and F. Winston.** 2003. Recent advances in understanding chromatin remodeling by Swi/Snf complexes. Current Opinion in Genetics & Development **13:**136-142.
27. **Medjkane S, N. E., Versteege I, Delattre O.** 2004. The tumour suppressor hSNF5/INI1 modulates cell growth and actin cytoskeleton organization. cancer Research **64:**3406-13.
28. **Mohrmann, L., and C. P. Verrijzer.** 2005. Composition and functional specificity of SWI2/SNF2 class chromatin remodeling complexes. Biochim Biophys Acta **1681:**59-73.
29. **Morozov A, S.J. Lee, Z.K. Zhang, V. Cimica, D. Zagzag, and G. V. Kalpana.** 2007. INI1 Induces Interferon Signaling and Spindle Checkpoint in Rhabdoid Tumours. Clinical Cancer Research **13:**4721-4730.
30. **Moshkin, Y. M., L. Mohrmann, W. F. van Ijcken, and C. P. Verrijzer.** 2007. Functional differentiation of SWI/SNF remodellers in transcription and cell cycle control. Mol Cell Biol **27:**651-61.
31. **Oruetxebarria, I., F. Venturini, T. Kekarainen, A. Houweling, L. M. Zuijderduijn, A. Mohd-Sarip, R. G. Vries, R. C. Hoeben, and C. P. Verrijzer.** 2004. P16INK4a is required for hSNF5 chromatin remodeller-induced cellular senescence in malignant rhabdoid tumour cells. J Biol Chem **279:**3807-16.
32. **Peterson, C. L.** 2002. Chromatin remodeling enzymes: taming the machines Embo Reports **3:**319-322.
33. **Peterson, C. L., and I. Herskowitz.** 1992. Characterization of the yeast SWI1, SWI2, and SWI3 genes, which encode a global activator of transcription. Cell **68:**573-83.
34. **Pomeroy S.L., P. Tamayo, M. Gaasenbeek , L.M. Sturla , M. Angelo , M.E. McLaughlin , J.Y. Kim , L.C. Goumnerova , C. L. P.M. Black, J.C. Allen , J. D. Zagzag, .M. Olson , T. Curran, C. Wetmore, J.A. Biegel, T. Poggio, S. Mukherjee , R. Rifkin , A. Califano , G. Stolovitzky , D.N. Louis , J.P. Mesirov , E.S. Lander , and T. R. Golub.** 2002. Prediction of central nervous system embryonal tumour outcome based on gene expression. Nature **415:**436-442.
35. **Roberts, C. W., S. A. Galusha, M. E. McMenamin, C. D. Fletcher, and S. H. Orkin.** 2000. Haploinsufficiency of Snf5 (integrase interactor 1) predisposes to malignant rhabdoid tumours in mice. Proc Natl Acad Sci U S A **97:**13796-800.
36. **Roberts, C. W., and S. H. Orkin.** 2004. The SWI/SNF complex--chromatin and cancer. Nat Rev Cancer **4:**133-42.
37. **Rorke LB, P. R., Biegel J.** 1995. Central nervous system atypical teratoid/rhabdoid tumours of infancy and childhood. J Neurooncol. **24:**21-8.
38. **Sansam CG, R. C.** 2006. Epigenetics and Cancer: Altered Chromatin Remodeling via Snf5 Loss Leads to Aberrant Cell Cycle Regulation. CELL CYCLE **5:**621-4.
39. **Sevenet, N., E. Sheridan, D. Amram, P. Schneider, R. Handgretinger, and O. Delattre.** 1999. Constitutional mutations of the hSNF5/INI1 gene predispose to a variety of cancers. Am J Hum Genet **65:**1342-8.
40. **Sif, S., Saurin, A.J, Imbalzano,A.N and Kingston,R.E** 2001. Purification and characterization of mSin3A-containing Brg1 and hBrm chromatin remodeling complexes. Genes Dev **15:**603-618.
41. **Staehling-Hampton, K., P. J. Ciampa, A. Brook, and N. Dyson.** 1999. A genetic screen for modifiers of E2F in Drosophila melanogaster. Genetics **153:**275-87.
42. **Sudarsanam, P., V. R. Iyer, P. O. Brown, and F. Winston.** 2000. Whole-genome expression analysis of snf/swi mutants of Saccharomyces cerevisiae. Proc Natl Acad Sci U S A **97:**3364-9.

43. **Versteege, I., S. Medjkane, D. Rouillard, and O. Delattre.** 2002. A key role of the hSNF5/INI1 tumour suppressor in the control of the G1-S transition of the cell cycle. Oncogene **21:**6403-12.
44. **Versteege, I., N. Sevenet, J. Lange, M. F. Rousseau-Merck, P. Ambros, R. Handgretinger, A. Aurias, and O. Delattre.** 1998. Truncating mutations of hSNF5/INI1 in aggressive paediatric cancer. Nature **394:**203-6.
45. **Vries, R. G., V. Bezrookove, L. M. Zuijderduijn, S. K. Kia, A. Houweling, I. Oruetxebarria, A. K. Raap, and C. P. Verrijzer.** 2005. Cancer-associated mutations in chromatin remodeller hSNF5 promote chromosomal instability by compromising the mitotic checkpoint. Genes Dev **19:**665-70.
46. **Wang, S., Zhang, B. and Faller, D.V.** 2002. Prohibitin requires Brg-1 and Brm for the repression of E2F and cell growth. EMBO J. **21:**3019–3028.
47. **Zhang, Z. K., K. P. Davies, J. Allen, L. Zhu, R. G. Pestell, D. Zagzag, and G. V. Kalpana.** 2002. Cell cycle arrest and repression of cyclin D1 transcription by INI1/hSNF5. Mol Cell Biol **22:**5975-88.

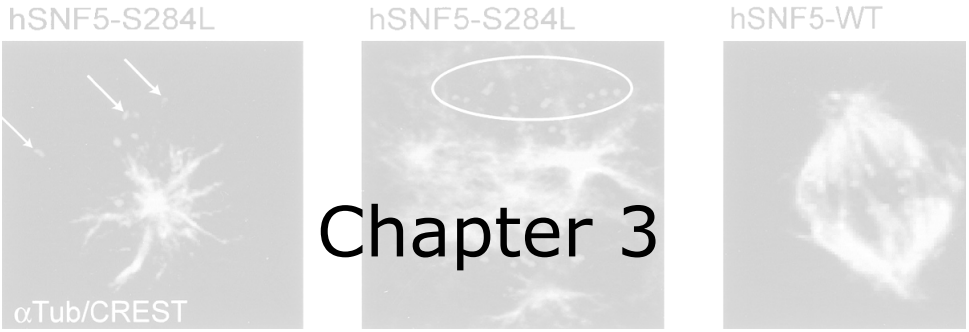

Chapter 3

Cancer-associated mutations in chromatin remodeler hSNF5 promote chromosomal instability by compromising the mitotic checkpoint

Rob G.J. Vries[1,2], Vladimir Bezrokove[1,] Lobke M.P. Zuijderduijn[1,2],**Sima Kheradmand Kia**[2] Ada Houweling[1], Igor Oruetxebarrial[1], Anton K.Raap and C. Peter Verrijzer[1]

1- Molecular and Cell Biology, Leiden University Medical Center, 2300 RA Leiden, The Netherlands
2- Department of Biochemistry, Center for Biomedical Genetics, Center for Biomics, Erasmus University Medical Center, P.O. Box 1738, 3000 DR Rotterdam, The Netherlands

Genes and Development, 2005 19(6):665-70

RESEARCH COMMUNICATION

Cancer-associated mutations in chromatin remodeler hSNF5 promote chromosomal instability by compromising the mitotic checkpoint

Robert G.J. Vries,[1,3,4] Vladimir Bezrookove,[1,3] Lobke M.P. Zuijderduijn,[1,2] Sima Kheradmand Kia,[2] Ada Houweling,[1] Igor Oruetxebarria,[1] Anton K. Raap,[1] and C. Peter Verrijzer[1,2,5]

[1]Department of Molecular and Cell Biology, Leiden University Medical Centre, 2300 RA Leiden, The Netherlands; [2]Department of Biochemistry and Centre for Biomedical Genetics, Erasmus University Medical Centre, 3015 GE Rotterdam, The Netherlands

The hSNF5 subunit of human SWI/SNF ATP-dependent chromatin remodeling complexes is a tumor suppressor that is inactivated in malignant rhabdoid tumors (MRTs). Here, we report that loss of hSNF5 function in MRT-derived cells leads to polyploidization and chromosomal instability. Re-expression of hSNF5 restored the coupling between cell cycle progression and ploidy checkpoints. In contrast, cancer-associated hSNF5 mutants harboring specific single amino acid substitutions exacerbated poly- and aneuploidization, due to abrogated chromosome segregation. We found that hSNF5 activates the mitotic checkpoint through the $p16^{INK4a}$–cyclinD/CDK4–pRb–E2F pathway. These results establish that poly- and aneuploidy of tumor cells can result from mutations in a chromatin remodeler.

Received January 12, 2005; revised version accepted January 27, 2005.

ATP-dependent chromatin remodeling factors are critical components of the elaborate machinery that controls gene expression in eukaryotic cells (Becker and Horz 2002). The multisubunit SWI/SNF complex is the prototypical chromatin remodeling factor, present in all eukaryotes (Mohrmann and Verrijzer 2005). Human *SNF5* (*hSNF5*, also known as *Ini1*, *Baf47*, or *SmarcB1*) encodes for a universal SWI/SNF subunit and tumor suppressor that is mutated in malignant rhabdoid tumors (MRTs) (Versteege et al. 1998; Klochendler-Yeivin et al. 2002; Roberts and Orkin 2004). MRTs are rare but highly aggressive pediatric cancers with a high mortality rate. Carriers of germline mutations are predisposed to various cancers and, consistent with a classic tumor suppressor phenotype, the wild-type allele is either lost or deleted in a large proportion of tumors (Biegel et al. 1999; Sevenet et al. 1999a,b; Taylor et al. 2000). *hSNF5* mutations are also associated with a number of neoplasms other than MRTs (Grand et al. 1999; Sevenet et al. 1999a,b; Roberts and Orkin 2004). SNF5 inactivation studies in mice established its requirement during early embryogenesis and its role as a tumor suppressor (Klochendler-Yeivin et al. 2000; Roberts et al. 2000; Guidi et al. 2001; Roberts et al. 2002).

Several studies found that re-expression of hSNF5 in MRT-derived cell lines caused an accumulation in G0/G1, cellular senescence, and apoptosis (Ae et al. 2002; Betz et al. 2002; Versteege et al. 2002; Zhang et al. 2002; Oruetxebarria et al. 2004). These effects are largely the result of direct transcriptional activation of the tumor suppressor $p16^{INK4a}$ by hSNF5, which appears to be both necessary and sufficient for reduced cell proliferation and induction of cellular senescence and apoptosis (Oruetxebarria et al. 2004). $p16^{INK4a}$ controls the activity of pRb via inhibition of the cyclin D1–CDK4 kinase, which phosphorylates pRb (Lowe and Sherr 2003). Tumor suppressor pRb is a corepressor that is tethered to a broad range of genes by the E2F transcription factors. Hyperphosphorylation of pRb causes its dissociation from E2F, and relieves its antiproliferative activities. In addition to genes required for cell cycle progression from G1 to S phase, E2Fs also regulate genes involved in mitosis, spindle checkpoints, G2/M control, apoptosis, and differentiation (Stevaux and Dyson 2002).

Besides uncontrolled cell proliferation, chromosomal instability, which is characterized by changes in chromosome number or structure, is a hallmark of cancer cells (Rajagopalan and Lengauer 2004). Although still debated, there has been increasing support for the idea that polyploidy can lead to aneuploidy and contribute to the development of cancer (Rajagopalan and Lengauer 2004; Storchova and Pellman 2004). Although gross aneuploidy appears to be rare, chromosomal imbalances are commonly detected in MRTs and other hSNF5-related cancers (Berrak et al. 2002; Mitelman et al. 2003; Rickert and Paulus 2003; Kusafuka et al. 2004). Therefore, we decided to investigate the role of hSNF5 in ploidy control. Our results define a critical function for this chromatin remodeler in the maintenance of numerical chromosome stability.

Results and Discussion

hSNF5 deficiency in MRT cells leads to polyploidization

In the majority of MRTs, hSNF5 is inactivated due to deletions, truncating nonsense mutations, or frameshift mutations. However, a number of point mutations, resulting in single amino acid substitutions (Fig. 1A), have been identified in tumors (Sevenet et al. 1999a,b). These include proline 48 to serine (P48S), arginine 127 to glycine (R127G), and serine 284 to leucine (S284L). In addition, we also changed serine 289 to alanine (S289A). S284 and S289 are located within one of the most highly con-

[*Keywords*: Chromosomal instability; chromatin; tumor suppressor; hSNF5/INI1/Baf47/SmarcB1]
[3]These authors contributed equally to this work.
[4]Present address: Department of Developmental Biology, Howard Hughes Medical Institute, Stanford University, Stanford, CA 94305, USA.
[5]Corresponding author.
E-MAIL c.verrijzer@erasmusmc.nl; FAX 31-10-40879472.
Article and publication are at http://www.genesdev.org/cgi/doi/10.1101/gad.335805.

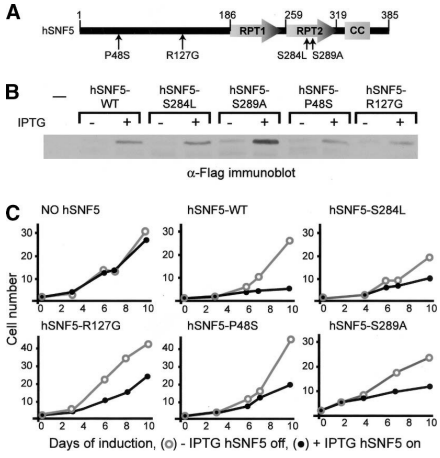

Figure 1. Effect of wild-type or mutant hSNF5 expression in MRT cells. (*A*) Schematic representation of hSNF5 depicting the two repeats (RPT1 and RPT2) and cancer-associated amino acid substitution mutations. (*B*) Constructs expressing wild-type or mutant hSNF5-Flag were introduced in the MRT-derived cell line G401 under control of the Lac repressor-operator system. Protein expression following induction with IPTG was determined by Western blotting with anti-Flag antibodies. (*C*) Cell accumulation in the presence (filled circles) or absence (open circles) of hSNF5, induced by IPTG.

served regions of SNF5, which forms part of direct repeat 2 (RPT2).

Wild-type or mutant hSNF5 was reintroduced in MRT-derived G401 cells lacking the hSNF5 gene. Expression of hSNF5 was under control of the Lac repressor-operator system and could be induced by the addition of IPTG (Fig. 1B). Previously, we used these "Lac-hSNF5" cells to establish that re-expression of hSNF5 in MRT cells induces a $p16^{INK4a}$-dependent G0/G1 arrest, cellular senescence, and apoptosis (Oruetxebarria et al. 2004). It should be noted that the induced levels of hSNF5 fall within the normal physiological range (Oruetxebarria et al. 2004) and that hSNF5 is not required for the assembly of a SWI/SNF complex (Doan et al. 2004; Oruetxebarria et al. 2004). Induction of tumor-derived hSNF5 mutants still caused a reduced cell accumulation, albeit not as pronounced as when wild-type hSNF5 was expressed (Fig. 1C). As expected, addition of IPTG to "Lac-empty" control cells, lacking the hSNF5 gene, did not affect cell accumulation. These results indicated that a failed growth arrest might not fully explain the cancer association of these single amino acid substitutions in hSNF5.

Examination of the nuclear morphology of cells expressing mutant hSNF5-S284L provided a clue towards other processes relevant to tumor suppression by hSNF5 (Fig. 2A,B). Four days after induction of hSNF5-S284L, the majority of cells contained multilobed nuclei or sometimes multiple nuclei. We never observed multilobed nuclei after expression of wild-type hSNF5, whereas they occurred regularly in cells lacking hSNF5. Next, we tested the effect of hSNF5-S284L on unrelated cells, expressing endogenous wild-type hSNF5. In both MRC-5V1 (Fig. 2C) and Ad5HER cells (data not shown), expression of hSNF5-S284L induced multilobed nuclei, whereas overexpression of wild-type hSNF5 had no effect. Thus, the S284L substitution mutation can have a dominant effect, which is not restricted to MRT cells.

Because multilobed nuclei are a feature of cells that have undergone endoreplication, we tested whether hSNF5-S284L might promote polyploidization. The full karyotypes of G401 MRT-derived cells that either lack hSNF5 or express wild-type hSNF5 or hSNF5-S284L were determined by multicolor pq-COBRA-FISH analysis (Fig. 2D; Wiegant et al. 2000). About 90 of Lac-empty cells or Lac-hSNF5 cells before induction were in the diploid range of chromosome content, but displayed frequent numerical chromosome aberrations. The remaining 10 was near tetraploid. Strikingly, after expression of wild-type hSNF5 for 96 h, the cell population became almost perfectly diploid. The disappearance of aneuploid cells from the cycling population suggested a role for hSNF5 in mitotic checkpoint control. In contrast, hSNF5-S284L expression exacerbated poly- and aneuploidization, resulting in ~25 of cells in the tetraploid range and almost 10 of cells that were near octaploid. We note that, because mitotic cells were obtained by a colcemid block, the karyotypes were derived from cycling cells. Moreover, the presence of octaploid cells demonstrated that a significant portion of tetraploid cells did not arrest due to the tetraploidy checkpoint but re-entered mitosis.

Concomitant with polyploidization we observed centrosome- and spindle amplification, as revealed by γ-tubulin and α-tubulin staining, respectively (Fig. 2E,F). Following hSNF5-S284L induction, the percentage of mitotic cells containing more than one spindle increased from ~5 to, respectively, 22 of cells with two spindles and 11 with more than two spindles. However, mitotic cells expressing wild-type hSNF5 virtually always contain one spindle. In summary, these results revealed that loss of hSNF5 in MRT cells promotes poly- and aneuploidization, whereas the cancer-associated S284L substitution acts as a gain-of-function mutation, exacerbating chromosomal instability. Collectively, these observations suggest a critical function for hSNF5 during mitosis.

Mutations in hSNF5 abrogate chromosome segregation

We utilized time-lapse microscopy to determine the cell cycle stage at which the hSNF5-S284L-induced defect occurs (Fig. 3A). Cells expressing hSNF5-S284L enter mitosis normally, as judged by rounding up of the cells and chromosomal condensation (indicated with an arrow). However, a significant proportion of these cells subsequently exited mitosis, as judged by cell flattening and chromatin decondensation, but abstained from karyokinesis and cytokinesis. Most cells that do not express hSNF5-S284L progress normally through mitosis and cell division. uantification of distinct stages of mitosis revealed a defective anaphase in hSNF5-S284L-expressing cells (data not shown). The aborted anaphase appeared to be caused by a failure of the mitotic spindle to connect to the kinetochores, as revealed by confocal microscopy using CREST and α-tubulin antibodies to visualize kinetochores and spindles, respectively (Fig. 3B). In cells expressing wild-type hSNF5, however, the spindles

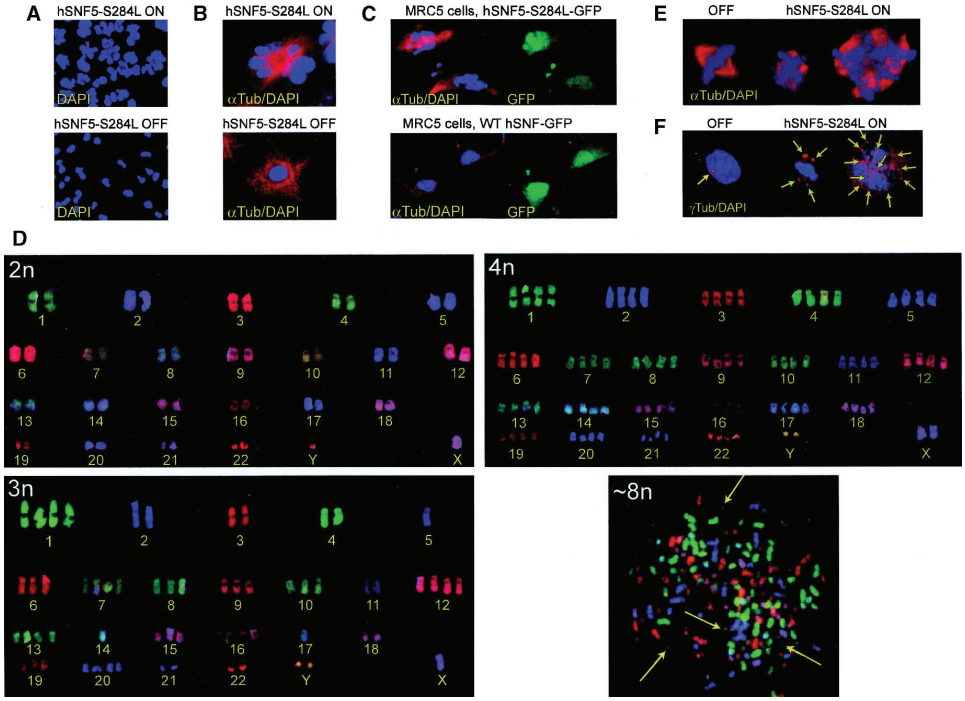

Figure 2. hSNF5-S284L expression exacerbates polyploidization. (*A*) DNA staining with DAPI revealed an increased number of multilobed nuclei after hSNF5-S284L expression. (*B*) Costaining of DNA (blue) and α-tubulin (red). (*C*) GFP-hSNF5-S284L but not GFP-hSNF5 induces multilobed nuclei in MRC5 cells. The GFP signal (green) identifies the transfected cells. (*D*) Representative examples of pq-COBRA-FISH analysis of Lac-hSNF5-S284L cells. Di-, tri, tetra-, and near octaploid metaphases are shown. Four Y-chromosomes, indicative of octaploidy, are indicated by arrows. (*E*) Representative examples of Lac-hSNF5-S284L cells with one, two, or more mitotic spindles. (*F*) Visualization of centrosomes (arrows) by γ-tubulin staining.

provided an orderly connection between metaphase chromosomes and centrosomes. Expression of hSNF5-S289A had similar effects on mitosis as hSNF5-S284L. It will be of interest to investigate whether S284 and S289 might be targets for phosphorylation, regulating the mitotic functions of hSNF5.

hSNF5 is critical for precise ploidy control

We used pq-COBRA-FISH to determine the effects of cancer-associated mutations in hSNF5 on ploidy distribution (Fig. 4A) and on numerical chromosome variation, as determined by the gain or loss of individual chromosomes (Fig. 4B). Examination of cells prior to induction of hSNF5 revealed that more than half displayed general numerical chromosomal aberrations and that ~10 were near tetraploid. Strikingly, after hSNF5 induction virtually all poly- and aneuploid cells were purged and the cell population became almost perfectly diploid. This dramatic effect of hSNF5 expression on numerical chromosome instability was highly significant ($p \quad 2.0 \times 10^{-6}$), as determined by the Mann-Whitney U-test. Thus, restoration of hSNF5 expression in MRT-derived cells, which lost the hSNF5 gene in the original cancerous lesion, suffices to revert chromosomal instability. In contrast, two different cancer-associated hSNF5 substitution mutants, hSNF5-P48S and hSNF5-

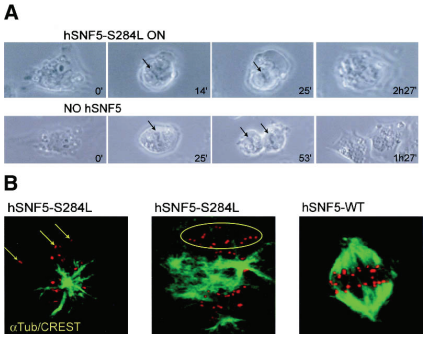

Figure 3. hSNF5-S284L induction causes an abortive cell cycle. (*A*) Time-lapse microscopy of hSNF5-S284L-expressing cells, which en ter mitosis but exit prior to cell division. Arrows indicate condensed chromatin. (*B*) Failure of microtubule–kinetochore association in cells expressing hSNF5-S284L. Kinetochores were identified with CREST (red) antibodies and mitotic spindles with α-tubulin (green) antibodies.

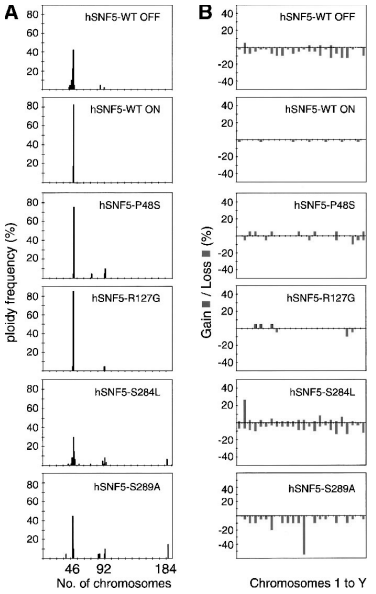

Figure 4. Restoration of wild-type hSNF5 expression, but not of cancer-associated mutants, reverts chromosomal instability. (*A*) Histogram depicting the frequency of cells with a given chromosome number as determined by metaphase analysis using pq-COBRA-FISH. The total number of chromosomes per cell was determined either before or after the induction of hSNF5. (*B*) Individual chromosome gains or losses.

R127G, failed to generate a diploid cell population. Expression of either hSNF5-S284L ($p \quad 3.6 \times 10^{-5}$) or hSNF5-S289A ($p \quad 2 \times 10^{-6}$) strongly promoted polyploidization and aneuploidy. In conclusion, our analysis of both loss-of-function and gain-of-function mutations revealed the critical role of hSNF5 in ploidy control.

hSNF5 activates the mitotic checkpoint through the p16^{INK4a}–cyclinD/CDK4–pRb–E2F pathway

Our results suggested that re-expression of hSNF5 tightens the mitotic checkpoint such that cell cycle progression of cells with an abnormal ploidy is blocked. To karyotype these noncycling cells, we used the drug calyculin A to induce premature chromosome condensation of interphase cells (Bezrookove et al. 2003). Indeed, we found that the karyotypes of noncycling hSNF5-expressing cells displayed a significantly higher degree of chromosome gains and losses than those of mitotic cells ($p \quad 10^{-2}$) (Fig. 5A,B). These results suggest that the reduced accumulation of hSNF5-expressing cells is caused by selective arrest and senescence of aneuploid cells. After hSNF5 induction, only diploid cells remain cycling.

Next, we considered the pathway through which hSNF5 controls cellular ploidy. Whole-genome expression profiling of Lac-hSNF5 cells prior to and after hSNF5 induction revealed, among other findings, changed expression of many E2F targets, including mitotic control genes. This is illustrated by the representative selection in Figure 5C. Interestingly, recent studies established that the pRb–E2F pathway couples cell cycle progression to the mitotic checkpoint (Hernando et al. 2004). Our earlier work had already shown that the ability of p16^{INK4a} to inhibit CDK4 kinase activity was critical for hSNF5-induced senescence (Oruetxebarria et al. 2004). To test whether ploidy control by hSNF5 is exerted via the p16^{INK4a}–cyclinD/CDK4–pRb–E2F pathway, we debilitated this route by expression of the p16^{INK4a}-insensitive CDK4^{R24C} mutant (Rane et al. 2002). Karyotypic analysis revealed that the high level of poly- and aneuploidy of these cells could not be reversed by hSNF5 expression (Fig. 5D–F). Thus, derailment of the pRb pathway blocks ploidy control by hSNF5.

Our gene expression profiling results suggested that misexpression of mitotic checkpoint components might cause the abnormal ploidy of MRT cells. For example, overexpression of Mad2 and its regulator E2F1 was recently implicated in mitotic defects leading to aneuploidy (Hernando et al. 2004). Interestingly, in our microarray experiments, both genes were down-regulated following hSNF5 induction. We used RT–PCR to corroborate our microarray results (Fig. 5G). We found that both Mad2 and E2F1 are highly expressed in MRT cells, but are strongly down-regulated following hSNF5 induction. CDK4^{R24C} expression abrogated attenuation of these genes by hSNF5. Collectively, these results suggest that in MRT cells, loss of hSNF5 function causes elevated levels of Mad2 due to unregulated E2F1 activity. This in turn can be sufficient to cause a defective spindle checkpoint driving aneuploidization, as shown by Hernando et al. (2004).

We conclude that transcriptional regulation of the p16^{INK4a}–cyclinD/CDK4–pRb–E2F pathway plays a critical role in ploidy control by hSNF5. However, this does not exclude additional functions for hSNF5 in ploidy control or other cellular processes relevant for tumorigenesis. Moreover, a more structural role in the establishment of centromeric chromatin or in sister chromatid cohesion and segregation remains possible, as has been suggested for the SWI/SNF-related yeast RSC complex (Baetz et al. 2004; Huang et al. 2004; Mohrmann and Verrijzer 2005). Using a conditional siRNA approach, we recently observed polyploidization of non-MRT cells due to the loss of hSNF5 (R.G.J. Vries and C.P. Verrijzer, unpubl.), suggesting that the mitotic functions of hSNF5 might be general and not cell-type-specific.

Inactivation of ATP-dependent chromatin remodeling factors has been implicated in the development of distinct types of tumors (Klochendler-Yeivin et al. 2002; Roberts and Orkin 2004). Here, we report that restoration of hSNF5 expression in MRT-derived cells, which lost the hSNF5 gene in the original cancerous lesion, leads to the purging of poly- and aneuploid cells. We propose that inactivation of chromatin remodeler hSNF5 causes both the selective growth advantage and the genetic instability necessary for tumor initiation and progression. Our finding that hSNF5 activates the mitotic checkpoint through the p16^{INK4a}–cyclinD/CDK4–pRb–E2F pathway reveals a convergence of tumor suppressor pathways.

Materials and methods

Cell culture, plasmids, and mRNA expression

Generation and culture of the G401 cell lines has been described (Oruetxebarria et al. 2004). CDK4^{R24C} was stably expressed in Lac-

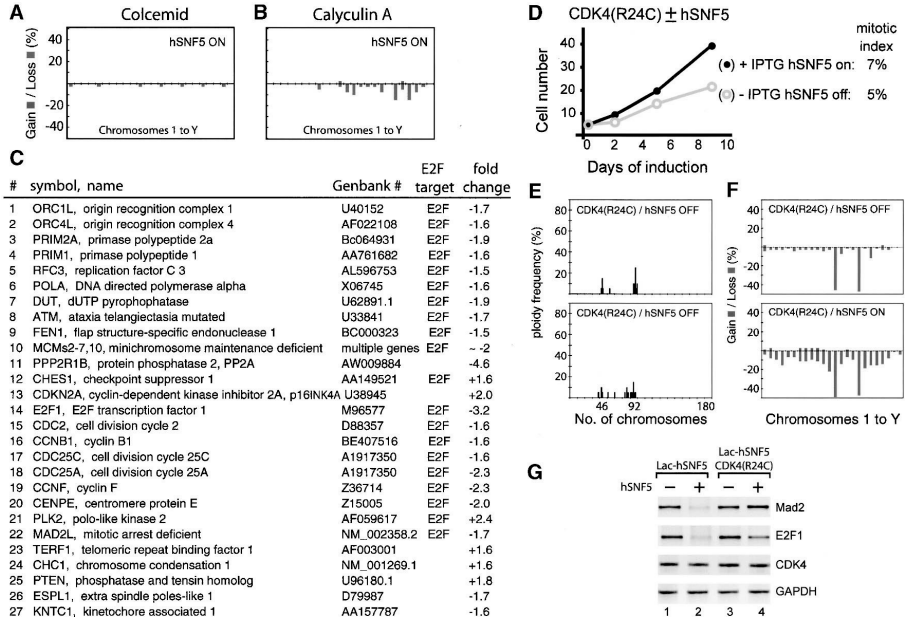

C

#	symbol, name	Genbank #	E2F target	fold change
1	ORC1L, origin recognition complex 1	U40152	E2F	-1.7
2	ORC4L, origin recognition complex 4	AF022108	E2F	-1.6
3	PRIM2A, primase polypeptide 2a	Bc064931	E2F	-1.9
4	PRIM1, primase polypeptide 1	AA761682	E2F	-1.6
5	RFC3, replication factor C 3	AL596753	E2F	-1.5
6	POLA, DNA directed polymerase alpha	X06745	E2F	-1.6
7	DUT, dUTP pyrophophatase	U62891.1	E2F	-1.9
8	ATM, ataxia telangiectasia mutated	U33841	E2F	-1.7
9	FEN1, flap structure-specific endonuclease 1	BC000323	E2F	-1.5
10	MCMs2-7,10, minichromosome maintenance deficient	multiple genes	E2F	~ -2
11	PPP2R1B, protein phosphatase 2, PP2A	AW009884		-4.6
12	CHES1, checkpoint suppressor 1	AA149521	E2F	+1.6
13	CDKN2A, cyclin-dependent kinase inhibitor 2A, p16INK4A	U38945		+2.0
14	E2F1, E2F transcription factor 1	M96577	E2F	-3.2
15	CDC2, cell division cycle 2	D88357	E2F	-1.6
16	CCNB1, cyclin B1	BE407516	E2F	-1.6
17	CDC25C, cell division cycle 25C	A1917350	E2F	-1.6
18	CDC25A, cell division cycle 25A	A1917350	E2F	-2.3
19	CCNF, cyclin F	Z36714	E2F	-2.3
20	CENPE, centromere protein E	Z15005	E2F	-2.0
21	PLK2, polo-like kinase 2	AF059617	E2F	+2.4
22	MAD2L, mitotic arrest deficient	NM_002358.2	E2F	-1.7
23	TERF1, telomeric repeat binding factor 1	AF003001		+1.6
24	CHC1, chromosome condensation 1	NM_001269.1		+1.6
25	PTEN, phosphatase and tensin homolog	U96180.1		+1.8
26	ESPL1, extra spindle poles-like 1	D79987		-1.7
27	KNTC1, kinetochore associated 1	AA157787		-1.6

Figure 5. Expression of $p16^{INK4a}$-insensitive $CDK4^{R24C}$ blocks hSNF5-induced mitotic checkpoint activation. Individual chromosome gains or losses as determined by karyotyping after a colcemid block (*A*) or calyculin A-induced premature chromosome condensation (*B*) of interphase cells. (*C*) Selection of E2F targets and mitotic controllers, regulated by hSNF5 identified by whole-genome expression profiling. Gene symbols according to unigene convention, known E2F targets, and fold changes in expression following hSNF5 are indicated. (*D*) Cell accumulation of Lac-hSNF5 cells stably expressing $CDK4^{R24C}$ in the presence (filled circles) or absence (open circles) of hSNF5. (*E*) Histogram depicting the frequency of cells with a given chromosome number. (*F*) Individual chromosome gains or losses. ( ) RT–PCR analysis of gene expression. The same mRNA isolates were used to detect expression of the indicated genes.

hSNF5 cells (Lac-hSNF5/$CDK4^{R24C}$) from a pREP4-derived vector (Rane et al. 2002). Mutants were generated using uickChange mutagenesis (Stratagene). mRNA expression analysis was performed as described (Oruetxebarria et al. 2004). All primer sequences will be provided upon request. Gene expression profiling was performed using Affymetrix U133A GeneChips, and data analyses were performed using Omniviz software and the Ease program. An extensive description of these experiments will be reported elsewhere.

Immunofluorescence and time lapse microscopy

Cells were grown on cover slips, fixed with 4 paraformaldehyde, and permeabilized in PBS with 0.1 Triton -100, followed by standard indirect immunofluorescence. Nuclei were visualized by DAPI staining. Antibodies used: anti-Flag, F3165 (Sigma); anti-α-tubulin, T5168 (Sigma); anti-γ-tubulin, T6557 (Sigma); anti-CREST was a gift from H. Clevers (Hubrecht Laboratory, Utrecht, The Netherlands) (Fodde et al. 2001). To quantify centrosome- and spindle amplification, ~1000 mitotic cells for each condition were analyzed. Cells for time-lapse microscopy were grown on glass-bottom culture dishes (MatTek). Two hours before transfer to the 37°C microscope, medium was changed to HEPES-buffered DMEM without Phenol red (21063-029, Life Technology).

pq-COBRA-FISH and cytogenetic analysis

Detailed cytogenetic analysis using pq-COBRA-FISH was performed essentially as described (Wiegant et al. 2000). ULS reagent was provided by Kreatech Biotechnology. Interphase cells were karyotyped following Calyculin A-induced chromosome condensation (Bezrookoove et al. 2003). For each condition, between 20 and 60 cells were analyzed. Chromosome copy number is depicted as histograms, and the numerical abnormalities are presented as percentage of gain and loss for each chromosome, for which the nearest ploidy of each cell was considered. The significance of differences in total gain or loss of chromosomes was determined by the Mann-Whitney U-test.

Acknowledgments

We thank N. Nagelkerke for help with the statistical analysis; S. Swagemarkers, C. Gaspar, and R. Fodde for help with the microarray analysis; H. Clevers for anti-CREST serum; M.J. van der Burg for help with COBRA-FISH analysis; R. Dirks for advice on microscopy; R. Fodde for discussions; and J. Svejstrup, R. Fodde, M. Gorski, and T. Mahmoudi for comments on the manuscript. This work was supported by a grant from the Dutch Cancer Society (KWF) to C.P.V.

References

Ae, K., Kobayashi, N., Sakuma, R., Ogata, T., Kuroda, H., Kawaguchi, N., Shinomiya, K., and Kitamura, Y. 2002. Chromatin remodeling factor encoded by ini1 induces G1 arrest and apoptosis in ini1-deficient cells. *ncogene* **21:** 3112–3120.

Baetz, K.K., Krogan, N.J., Emili, A., Greenblatt, J., and Hieter, P. 2004. The ctf13-30/CTF13 genomic haploinsufficiency modifier screen identifies the yeast chromatin remodeling complex RSC, which is required for the establishment of sister chromatid cohesion. *Mol Cell Biol* **24:** 1232–1244.

Becker, P.B. and Horz, W. 2002. ATP-dependent nucleosome remodeling. *Annu Rev Biochem* **71:** 247–273.

Berrak, S.G., Ozek, M.M., Canpolat, C., Dagcunar, A., Sav, A., El-Naggar, A., and Langford, L.A. 2002. Association between DNA content and tumor suppressor gene expression and agressiveness of atypical tera-

toid/rhabdoid tumors. *Child's Nerv Syst* **18:** 485–491.
Betz, B.L., Strobeck, M.W., Reisman, D.N., Knudsen, E.S., and Weissman, B.E. 2002. Re-expression of hSNF5/INI1/BAF47 in pediatric tumor cells leads to G1 arrest associated with induction of p16ink4a and activation of RB. *ncogene* **21:** 5193–5203.
Bezrookove, V., Smits, R., Moeslein, G., Fodde, R., Tanke, H.J., Raap, A.K., and Darroudi, F. 2003. Premature chromosome condensation revisited: A novel chemical approach permits efficient cytogenetic analysis of cancers. *enes Chrom Cancer* **38:** 177–186.
Biegel, J.A., Zhou, J.Y., Rorke, L.B., Stenstrom, C., Wainwright, L.M., and Fogelgren, B. 1999. Germ-line and acquired mutations of INI1 in atypical teratoid and rhabdoid tumors. *Cancer Res* **59:** 74–79.
Doan, D.D., Veal, T.M., Yan, Z., Wang, W., Jones, S.N., and Imbalzano, A.N. 2004. Loss of the INI1 tumor suppressor does not impair the expression of multiple BRG1-dependnet genes or the assembly of SWI/SNF enzymes. *ncogene* **23:** 3462–3473.
Fodde, R., Kuipers, J., Rosenberg, C., Smits, R., Kielman, M., Gaspar, C., van Es, J.H., Breukel, C., Wiegant, J., Giles, R.H., et al. 2001. Mutations in the APC tumour suppressor gene cause chromosomal instability. *Nat Cell Biol* **3:** 433–438.
Grand, F., Kulkarni, S., Chase, A., Goldman, J.M., Gordon, M., and Cross, N.C. 1999. Frequent deletion of hSNF5/INI1, a component of the SWI/SNF complex, in chronic myeloid leukemia. *Cancer Res* **59:** 3870–3874.
Guidi, C.J., Sands, A.T., Zambrowicz, B.P., Turner, T.K., Demers, D.A., Webster, W., Smith, T.W., Imbalzano, A.N., and Jones, S.N. 2001. Disruption of Ini1 leads to peri-implantation lethality and tumorigenesis in mice. *Mol Cell Biol* **21:** 3598–3603.
Hernando, E., Nahle, Z., Juan, G., Diaz-Rodriguez, E., Alaminos, M., Hemann, M., Michel, L., Mittal, V., Gerald, W., Benezra, R., et al. 2004. Rb inactivation promotes genomic instability by uncoupling cell cycle progression from mitotic control. *Nature* **430:** 797–802.
Huang, J., Hsu, J.M., and Laurent, B.C. 2004. The RSC nucleosome-remodeling complex is required for Cohesin's association with chromosome arms. *Mol Cell* **13:** 739–750.
Klochendler-Yeivin, A., Fiette, L., Barra, J., Muchardt, C., Babinet, C., and Yaniv, M. 2000. The murine SNF5/INI1 chromatin remodeling factor is essential for embryonic development and tumor suppression. *EMB Rep* **1:** 500–506.
Klochendler-Yeivin, A., Muchardt, C., and Yaniv, M. 2002. SWI/SNF chromatin remodeling and cancer. *Curr pin enet Dev* **12:** 73–79.
Kusafuka, T., Miao, J., Yoneda, A., Kuroda, S., and Fukuzawa, M. 2004. Novel germ-line deletion of SNF5/INI1/SMARCB1 gene in neonate presenting with congenital malignant rhabdoid tumor of kidney and brain primitive neuroectodermal tumor. *enes Chromosomes Can cer* **40:** 133–139.
Lowe, S.W. and Sherr, C.J. 2003. Tumor suppression by Ink4a–Arf: Progress and puzzles.*Curr pin enet Dev* **13:** 77–83.
Mitelman, F., Johansson, B., and Mertens, F. 2003. Mitelman database of chromosome aberrations in cancer. http://cgap.nci.nih.gov/Chromosomes/Mitelman
Mohrmann, L. and Verrijzer, C.P. 2005. Composition and functional specificity of SWI2/SNF2 class chromatin remodeling complexes. *Biochim Biophys Acta* **1681:** 59–73.
Oruetxebarria, I., Venturini, F., Kekarainen, T., Houweling, A., Zuijderduijn, L.M., Mohd-Sarip, A., Vries, R.G., Hoeben, R.C., and Verrijzer, C.P. 2004. P16INK4a is required for hSNF5 chromatin remodeler-induced cellular senescence in malignant rhabdoid tumor cells. *Biol Chem* **279:** 3807–3816.
Rajagopalan, H., and Lengauer, C. 2004. Aneuploidy and cancer. *Nature* **432:** 338–341.
Rane, S.G., Cosenza, S.C., Mettus, R.V., and Reddy, E.P. 2002. Germ line transmission of the Cdk4(R24C) mutation facilitates tumorigenesis and escape from cellular senescence. *Mol Cell Biol* **22:** 644–656.
Rickert, C.H., and Paulus, W. 2004. Chromosomal imbalances detected by comparative genomic hybridisation in atypical teratoid/rhabdoid tumours. *Childs Nerv Syst* **20:** 221–224.
Roberts, C.W. and Orkin, S.H. 2004. The SWI/SNF complex—Chromatin and cancer. *Nat Rev Cancer* **4:** 133–142.
Roberts, C.W., Galusha, S.A., McMenamin, M.E., Fletcher, C.D., and Orkin, S.H. 2000. Haploinsufficiency of Snf5 (integrase interactor 1) predisposes to malignant rhabdoid tumors in mice. *roc Natl Acad Sci* **97:** 13796–13800.
Roberts, C.W., Leroux, M.M., Fleming, M.D., and Orkin, S.H. 2002. Highly penetrant, rapid tumorigenesis through conditional inversion of the tumor suppressor gene Snf5. Cancer Cell **2:** 415–425.
Sevenet, N., Lellouch-Tubiana, A., Schofield, D., Hoang- uan, K., Gessler, M., Birnbaum, D., Jeanpierre, C., Jouvet, A., and Delattre, O. 1999a. Spectrum of hSNF5/INI1 somatic mutations in human cancer and genotype-phenotype correlations. *um Mol enet* **8:** 2359–2368.
Sevenet, N., Sheridan, E., Amram, D., Schneider, P., Handgretinger, R., and Delattre, O. 1999b. Constitutional mutations of the hSNF5/INI1 gene predispose to a variety of cancers. *Am um enet* **65:** 1342–1348.
Stevaux, O. and Dyson, N.J. 2002. A revised picture of the E2F transcriptional network and RB function. *Curr p Cell Biol* **14:** 684–691.
Storchova, Z. and Pellman, D. 2004. From polyploidy to aneuploidy, genome instability and cancer. *Nat Rev Mol Cell Biol* **5:** 45–54.
Taylor, M.D., Gokgoz, N., Andrulis, I.L., Mainprize, T.G., Drake, J.M., and Rutka, J.T. 2000. Familial posterior fossa brain tumors of infancy secondary to germline mutation of the hSNF5 gene. *Am um enet* **66:** 1403–1406.
Versteege, I., Sevenet, N., Lange, J., Rousseau-Merck, M.F., Ambros, P., Handgretinger, R., Aurias, A., and Delattre, O. 1998. Truncating mutations of hSNF5/INI1 in aggressive paediatric cancer. *Nature* **394:** 203–206.
Versteege, I., Medjkane, S., Rouillard, D., and Delattre, O. 2002. A key role of the hSNF5/INI1 tumour suppressor in the control of the G1–S transition of the cell cycle. *ncogene* **21:** 6403–6412.
Wiegant, J., Bezrookove, V., Rosenberg, C., Tanke, H.J., Raap, A.K., Zhang, H., Bittner, M., Trent, J.M., and Meltzer, P. 2000. Differentially painting human chromosome arms with combined binary ratio-labeling fluorescence in situ hybridization. Genome Res. **10:** 861–865.
Zhang, Z.K., Davies, K.P., Allen, J., Zhu, L., Pestell, R.G., Zagzag, D., and Kalpana, G.V. 2002. Cell cycle arrest and repression of cyclin D1 transcription by INI1/hSNF5. *Mol Cell Biol* **22:** 5975–5988.

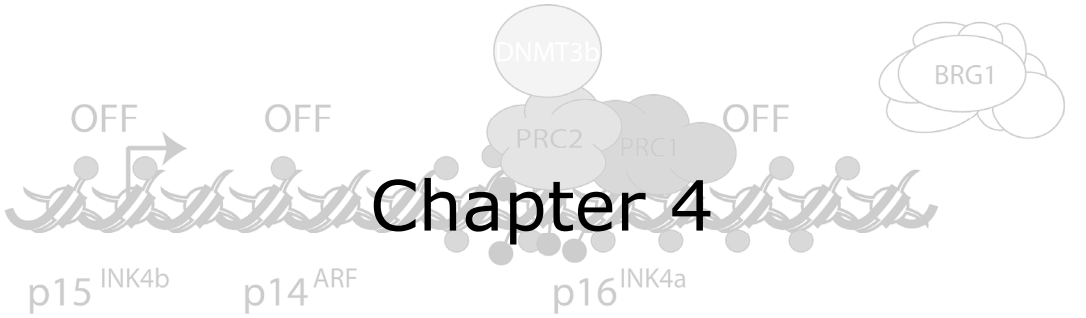

Chapter 4

SWI/SNF Mediates Polycomb Eviction and Epigenetic Reprogramming of the *INK4b-ARF-INK4a* Locus

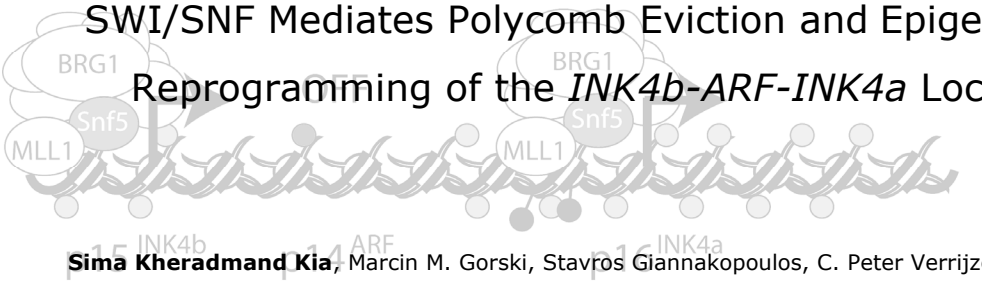

Sima Kheradmand Kia, Marcin M. Gorski, Stavros Giannakopoulos, C. Peter Verrijzer[#]

Department of Biochemistry, Center for Biomedical Genetics, Erasmus University Medical Center, P.O. Box 1738, 3000 DR Rotterdam, The Netherlands

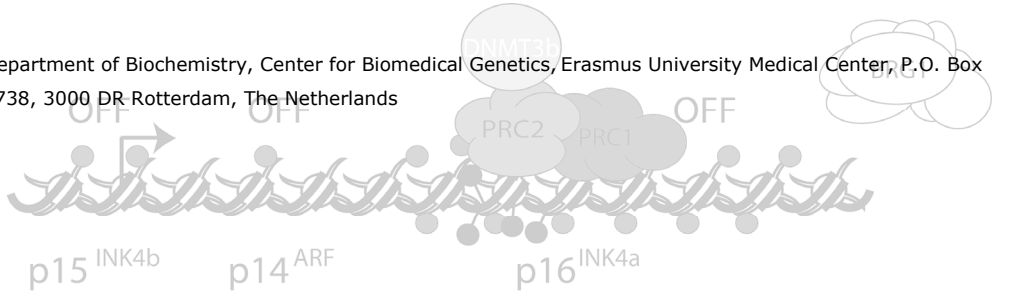

Molecular and Cellular Biology 2008 **28:**3457-3464

SWI/SNF Mediates Polycomb Eviction and Epigenetic Reprogramming of the *INK4b-ARF-INK4a* Locus[▽]

Sima Kheradmand Kia, Marcin M. Gorski, Stavros Giannakopoulos, and C. Peter Verrijzer*

Department of Biochemistry, Center for Biomedical Genetics, Erasmus University Medical Center, P.O. Box 1738, 3000 DR Rotterdam, The Netherlands

Received 9 November 2007/Returned for modification 29 November 2007/Accepted 14 February 2008

Stable silencing of the *INK4b-ARF-INK4a* tumor suppressor locus occurs in a variety of human cancers, including malignant rhabdoid tumors (MRTs). MRTs are extremely aggressive cancers caused by the loss of the hSNF5 subunit of the SWI/SNF chromatin-remodeling complex. We found previously that, in MRT cells, hSNF5 is required for $p16^{INK4a}$ induction, mitotic checkpoint activation, and cellular senescence. Here, we investigated how the balance between Polycomb group (PcG) silencing and SWI/SNF activation affects epigenetic control of the *INK4b-ARF-INK4a* locus in MRT cells. hSNF5 reexpression in MRT cells caused SWI/SNF recruitment and activation of $p15^{INK4b}$ and $p16^{INK4a}$, but not of $p14^{ARF}$. Gene activation by hSNF5 is strictly dependent on the SWI/SNF motor subunit BRG1. SWI/SNF mediates eviction of the PRC1 and PRC2 PcG silencers and extensive chromatin reprogramming. Concomitant with PcG complex removal, the mixed lineage leukemia 1 (MLL1) protein is recruited and active histone marks supplant repressive ones. Strikingly, loss of PcG complexes is accompanied by DNA methyltransferase DNMT3B dissociation and reduced DNA methylation. Thus, various chromatin states can be modulated by SWI/SNF action. Collectively, these findings emphasize the close interconnectivity and dynamics of diverse chromatin modifications in cancer and gene control.

Epigenetic mechanisms confer inherited states of gene expression that involve neither alterations in the DNA sequence nor the continuous presence of the initiating signal (16, 28). The memory of gene expression status through cell divisions plays an important role in development and disease (8, 11, 17, 29, 32). For example, the stable silencing of tumor suppressor genes, such as $p16^{INK4a}$, is believed to contribute to the development of human cancers. In a variety of tumors, $p16^{INK4a}$ is inactivated through epigenetic silencing, involving Polycomb group (PcG) proteins and DNA methylation (10, 17, 36). The principal function of $p16^{INK4a}$ is the induction of cellular senescence, a physiologically relevant state of permanent cell cycle arrest in response to aberrant proliferative signals (10, 25). $p16^{INK4a}$ acts mainly through inhibition of the Cyclin D1-CDK4 kinase, which phosphorylates and inactivates the retinoblastoma tumor suppressor protein (pRb). The $p16^{INK4a}$ gene is part of the *INK4b-ARF-INK4a* locus that encodes two other tumor suppressor proteins, $p15^{INK4b}$ and $p14^{ARF}$ (Fig. 1A) (10). $p15^{INK4b}$ is related to $p16^{INK4a}$ and also encodes a cyclin-dependent kinase inhibitor that activates pRb. Although the $p14^{ARF}$ transcription unit overlaps with the $p16^{INK4a}$ gene, it encodes a structurally unrelated protein that acts through activation of the p53 pathway.

Malignant rhabdoid tumors (MRTs) are extremely aggressive cancers of early childhood that are associated with loss of the hSNF5 subunit of the SWI/SNF chromatin-remodeling complex (4, 19, 30, 34, 38). hSNF5 reexpression in MRT cells induces $p16^{INK4a}$, but not $p14^{ARF}$ (3, 26). Accumulated evidence indicates that the failure to activate $p16^{INK4a}$ transcription due to the loss of hSNF5 (also known as *INI1*, *BAF47*, or *SMARCB1*) is an important oncogenic step in MRTs. First, in MRT cells induction of the epigenetically silenced $p16^{INK4a}$ gene is both necessary and sufficient for hSNF5-mediated mitotic checkpoint activation and cellular senescence (26, 40). Second, studies in mice have suggested that hSNF5 tumor suppression acts in parallel to p53 (14) but interacts functionally with the pRb pathway (13). In conclusion, MRT cells provide a physiologically relevant cell system to study the antagonistic effects of silencing and SWI/SNF action on the chromatin status of the multigene *INK4b-ARF-INK4a* tumor suppressor locus.

Genetic studies in *Drosophila* identified SWI/SNF as a trithorax group (trxG) activator, which counteracts PcG-mediated silencing (29, 32, 37). Significantly, the PcG protein BMI1 promotes oncogenesis in mice through silencing of the *INK4a-ARF* locus (15). Both the PRC1 and the PRC2 PcG complexes directly bind and silence the *INK4a-ARF* locus (5, 20). We therefore wondered whether this is also the case in MRT cells and, more interestingly, how SWI/SNF might overcome PcG silencing. Current models of PcG function favor the notion that binding of PcG silencing complexes create a chromatin structure that is refractory to remodeling by SWI/SNF (24, 29, 32, 33). This hypothesis is mainly based on results from in vitro experiments suggesting that PRC1-coated chromatin cannot be remodeled by SWI/SNF (35). However, this model raises a conundrum for genes that need to be reactivated after PcG silencing.

Here, we explored the molecular mechanism by which restoration of SWI/SNF functionality through hSNF5 reexpression overcomes epigenetic silencing and mediates $p16^{INK4a}$

* Corresponding author. Mailing address: Department of Biochemistry, Center for Biomedical Genetics, Erasmus University Medical Center, P.O. Box 1738, 3000 DR Rotterdam, The Netherlands. Phone: (31) 10-408-7326. Fax: (31) 10-7044747. E-mail: c.verrijzer@erasmusmc.nl.

▽ Published ahead of print on 10 March 2008.

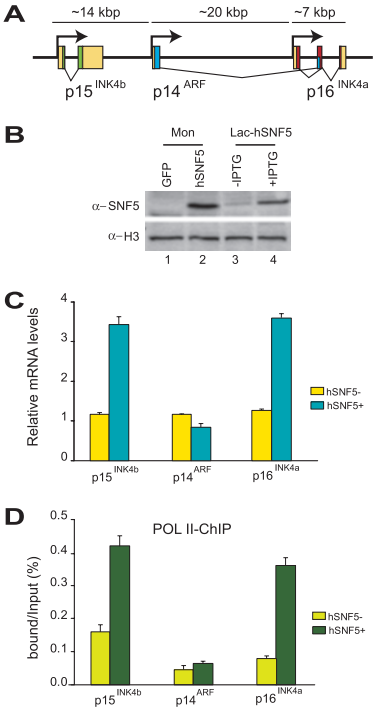

FIG. 1. Reexpression of hSNF5 in MRT cells induces $p15^{INK4b}$ and $p16^{INK4a}$ but not $p14^{ARF}$. (A) Organization of the human INK4b-ARF-INK4a locus (not drawn to scale). The genomic locus spans approximately 40 kbp of human chromosome 9 and encodes three distinct proteins: $p15^{INK4b}$, $p14^{ARF}$, and $p16^{INK4a}$. The 5′ and 3′ untranslated regions (yellow boxes), the coding sequences of $p15^{INK4b}$ (green), $p14^{ARF}$ (blue), and $p16^{INK4a}$ (red) are indicated. (B) Western immunoblotting analysis of hSNF5 expression in MON cells transduced with lentiviruses expressing either GFP (lane1) or hSNF5 (lane2) and either noninduced (lane 3) or induced (lane 4) G401-derived Lac-hSNF5 cells. Cell lysates were resolved by SDS-PAGE and analyzed by Western immunoblotting with antibodies directed against hSNF5. Histone H3 serves as a loading control. (C) RT-qPCR analysis of gene expression in MRT cells reveals hSNF5-dependent induction of $p15^{INK4b}$ and $p16^{INK4a}$, whereas $p14^{ARF}$ transcription remains unaffected. Cells were collected 48 h after transduction with lentiviruses expressing either GFP (yellow bars) or hSNF5 (blue bars). RT-qPCR analysis of isolated mRNA was used to determine the relative expression levels of $p15^{INK4b}$, $p16^{INK4a}$, $p14^{ARF}$, and *USP14* (a control gene that is independent of hSNF5). mRNA levels were plotted as percentage of *USP14* mRNA × 0.006. The bar graphs represent the mean of three independent biological replicates, each analyzed by three separate qPCR reactions. The standard deviations are indicated. (D) RNA Pol II promoter binding was analyzed by ChIP-qPCR. Cross-linked chromatin was prepared from MRT cells lacking hSNF5 but expressing GFP (light green bars) or from cells expressing hSNF5 (dark green bars). All ChIP data presented here are the result of at least three independent experiments. The abundance of specific DNA sequences in the immunoprecipitates was determined by qPCR and corrected for the independently determined amplification curves for each primer set. Background levels were determined by ChIP using species and isotype-matched immunoglobulins directed against an unrelated protein (GST). ChIPs with antibodies directed against RNA Pol II were analyzed by qPCR using primer sets corresponding to the $p15^{INK4b}$, $p14^{ARF}$, and $p16^{INK4a}$ promoters. ChIP signal levels for each region are presented as a percentage of input chromatin.

transcriptional activation in MRT cells. Our results reveal that in vivo SWI/SNF activity can effectively overrule PcG complex-induced chromatin silencing. We suggest that the antagonistic interactions between SWI/SNF and PcG silencers involve a dynamic equilibrium rather than a static chromatin state.

MATERIALS AND METHODS

Cell culture and lentiviral procedures. All tissue culture was performed according to standard protocols. The hSNF5-inducible MRT-derived cell lines have been described (26). The hSNF5 expressing lentiviral vector was generated by replacing the green fluorescent protein (GFP) encoding sequence of pRRLsin .sPPT.CMV.GFP.Wpre (9) with the hSNF5 cDNA (26). High-titer vector stocks were produced in 293T cells by cotransfection of transfer vector constructs with the packaging constructs by using standard transfection procedures (9). MON cells were transduced with the appropriate vector. To knock down BRG1, the cells were transduced with lentiviruses expressing short hairpin RNA (shRNA) directed against *BRG1* (clone 15549; Expression Arrest-RNAi Consortium human shRNA library purchased from Open Biosystems) for 4 days. In a control experiment, the cells were transduced with *GFP*-expressing lentiviruses as described previously. Approximately 24 h after initial viral transduction, the lentivirus-mediated expression of *hSNF5* or *GFP* controls was induced for additional 72 h. For 5-aza-2′-deoxycytidine (5-azadC) treatment, MON cells were incubated with 50 μmol of 5-azadC/liter, and the medium was refreshed every 24 h. After approximately 48 h, *hSNF5* or *GFP* expression was induced for an additional 48 h, and then the cells were harvested. Protein, RNA extraction and reverse transcription-quantitative PCR (RT-qPCR) were performed as described below.

RNA purification and real-time RT-PCR analysis. Total RNA was extracted from MRT cells by using the SV total RNA isolation system (Promega) 48 h after hSNF5 expression was induced. cDNA was synthesized from 1 μg of total RNA by using random hexamers and Superscript II RNase H-reverse transcriptase (Invitrogen). Quantitative real-time PCR (MyIQ; Bio-Rad) was performed with Sybr green I. PCR primers were designed by using Beacon designer (Premier Biosoft). A Q-PCR core kit (Invitrogen) was used with a 400 nM concentration of each primer under the following cycling conditions: 3 min at 95°C, followed by 40 cycles of 10 s at 95°C and 45 s at 60°C. The *Usp14* gene, whose expression is hSNF5 independent, was used as an endogenous reference for normalization. Enrichment of specific DNA sequences was calculated by using the comparative threshold cycle (C_T) method (22). PCR primer sequences are provided in Table 1.

Cell extracts and Western blotting. Cell extracts were prepared in radioimmunoprecipitation assay buffer (10 mM Tris-HCl [pH 7.5], 150 mM NaCl, 1% Nonidet P-40, 1% sodium deoxycholate, 0.1% sodium dodecyl sulfate [SDS]) and assayed for protein concentration, and 50 μg of extract was resolved by SDS-polyacrylamide gel electrophoresis (PAGE) and then analyzed by immunoblotting. Primary antibodies included SNF5 (ab12167 [Abcam]), BRG1 (ab4081 [Abcam]), SUZ12 (ab12073 [Abcam]), BMI1 (ab14389 [Abcam]), EZH2 (Sc-25383 [Santa Cruz]), DNMT3B (IMG-184A [IMGENEX]), and histone H3 (ab1791 [Abcam]). Western blots were developed by using an ECL detection kit (Pierce) according to the supplier's instructions.

ChIP and MeDIP assays. Chromatin immunoprecipitations (ChIPs) were performed as described by the Upstate protocol. Cross-linked chromatin was prepared from ~2×10^7 cells 48 h after transduction with lentiviruses expressing either hSNF5 or GFP as a control. Cells were treated with 1% formaldehyde for 20 min at room temperature. Chromatin isolation, sonication yielding fragments of 300 to 600 bp, and immunoprecipitations were performed according to previously established protocols. The following antibodies were used: SNF5 (ab12167 [Abcam]), BRG1 (ab4081 [Abcam]), SUZ12 (ab12073 [Abcam]), BMI1 (ab14389 [Abcam]), EZH2 (Sc-25383 [Santa Cruz]), DNMT3B (IMG-184A [IMGENEX]), POL II (Sc-899 [Santa Cruz]), mixed lineage leukemia 1 (MLL1; A300-086A [Bethyl Laboratories]), Histone H3 (ab1791 [Abcam]), H3-K4me3 (ab12209 [Abcam]), and H3-K27me3 (catalog no. 07-449 [Upstate]). The abundance of specific DNA sequences in the immunoprecipitates was determined by qPCR and corrected for the independently determined amplification curves of each primer set. ChIP using species- and isotype-matched immunoglobulins directed against an unrelated protein (glutathione *S*-transferase [GST]) were used to determine background levels. For methylated DNA immunoprecipitate (MeDIP) assays, genomic DNA was prepared by overnight proteinase K treatment, phenol-chloroform extraction, and ethanol precipitation. Genomic DNA was digested with MboI, and 4 μg of fragmented DNA was used for a standard MeDIP assay. After denaturation at 95°C for 10 min, the reaction was quenched on ice, and 500 μl of MeIP buffer (phosphate-buffered saline–0.05% Triton

TABLE 1. Q-PCR primers used for ChIP, mRNA expression, or DIP assay along the *INK4-ARF* locus

Technique and primer (location)	Primer set	Sequence (5′–3′)
ChIP		
$p15^{INK4b}$-Pm	A	GGCAGTGGTGAACATTCC
		GCCCAAAGATGCTAGGAC
$p14^{ARF}$-Pm	B	CGCCGTGTCCAGATGTCG
		TGCTCTATCCGCCAATCAGG
$p16^{INK4a}$ (−8.7 kb)	C	ACTAGGCTTGTCCCACTTGC
		TCAGTTCCTCTCTCCATT CTCC
$p16^{INK4a}$ (−0.6 kb)	D	CCCGTCCGTATTAAATA AACC
		GACTGCTCTCTCCTTCCC
$p16^{INK4a}$ (−0.3 kb)	E	GGGCTCTCACAACTAGG AAAG
		GGGTGTTTGGTGTCAT AGGG
$p16^{INK4a}$ (+85 bp)	F	CCCCTTGCCTGGAAAGATAC
		AGCCCCTCCTCTTTCTTCCT
$p16^{INK4a}$ (+0.5 kb)	G	CTGGAGGACGAAGTTTGC
		AGGAGGAGGTCTGTGA TTAC
$p16^{INK4a}$ (+1.5 kb)	H	GTGTTTCTCCTCTCCCTA CTCC
		CCGGGTTCAAGCTGTTGGC
$p16^{INK4a}$ (+5.6 kb)	I	ACCAAGACTTCGCTGACC
		CAAGGAGGACCATAATTC TACC
mRNA expression		
$p15^{INK4b}$		TAGTGGAGAAGGTGCG ACAG
		GCGCTGCCCATCATCATG
$p14^{ARF}$		GGTTTTCGTGGTTCACATCC
		CCTAGACGCTGGCTCCTC
$p16^{INK4a}$		CCCCTTGCCTGGAAAGATAC
		AGCCCCTCCTCTTTCTTCCT
USP14		AACGCTAAAGGATGATGAT TGGG
		TTTGGCTGAGGGTTCTT CTGG
DIP assay		
$p15^{INK4b}$		AGCAGCGTGGGAAAGA AGGG
		CTTGTTCTCCTCGCGCA TTCC
$p14^{ARF}$		CGCCGTGTCCAGATGTCG
		TGCTCTATCCGCCAATCAGG
$p16^{INK4a}$		GGGCTCTCACAACTAGG AAAG
		GGGTGTTTGGTGTCAT AGGG
H19		GCGAGCCGTAAGCACAGC
		GCCGATTCCCATCCAGT TGAC

X-100), 50 μl of salmon sperm DNA–protein G-agarose beads (Upstate), and 10 μg of anti-5-methylcytosine monoclonal antibody (Eurogentec) was added. As a negative control, DNA fragments were incubated with nonspecific mouse immunoglobulin G. After an overnight incubation on a rotating wheel at 4°C, beads were washed with 700 μl of MeIP buffer and resuspended in 100 μl and treated with proteinase K for 3 h at 50°C. Finally, DNA was purified by conventional phenol-chloroform extraction, followed by ethanol precipitation and analysis by qPCR. The enrichment of specific DNA sequences was calculated by using the comparative C_T method (22). PCR primer sequences are provided in Table 1. All data presented are the result of at least three independent ChIP or MeDIP experiments and triplicate qPCR reactions. The results were averaged, and standard errors were determined by using the R free software (http://www.r-project.org). The ChIP and MeDIP levels for each region are presented as the percentage of input chromatin. ChIPs using antibodies directed against H3-K27me3 or H3-K4me3 were normalized against histone H3 density.

RESULTS

hSNF5 is required for selective recruitment of BRG1 to the *$p15^{INK4b}$* and *$p16^{INK4a}$* promoters. We utilized two distinct strategies to reexpress hSNF5 in MRT cells: the previously described Lac repressor-operator system (26) and transduction with hSNF5-expressing lentiviruses. Samples were taken 48 h after induction of hSNF5 expression in two different MRT-derived cell lines: MON and G401. We note that hSNF5 is not essential for SWI/SNF complex integrity (7, 23, 26). Lentiviral transduction resulted in expression levels that were comparable to that obtained using the Lac repressor operator system (Fig. 1B). Moreover, we previously showed that the levels of induced exogenous hSNF5 expression were comparable to the endogenous levels in a variety of cell lines (7, 23, 26). Below, we present results obtained for MON cells transduced with lentiviruses expressing either hSNF5 or GFP as a control. However, all results presented here were consistently observed for both cell lines and either delivery system.

To investigate the effect of hSNF5 on expression of the *INK4b-ARF-INK4a* locus, we quantified mRNA levels by RT-qPCR (Fig. 1C). In full agreement with our previous Western blotting results (26), we observed a clear induction of *$p16^{INK4a}$*, but not *$p14^{ARF}$* mRNA levels. In addition, we found that *$p15^{INK4b}$* was upregulated. ChIP experiments revealed that hSNF5 expression triggers RNA polymerase II (RNA Pol II) recruitment to the *$p15^{INK4b}$* and *$p16^{INK4a}$* promoters, but not to *$p14^{ARF}$* (Fig. 1D). We conclude that in the context of hSNF5 reexpression in MRT cells, *$p14^{ARF}$* is not induced coordinately with *$p15^{INK4b}$* and *$p16^{INK4a}$*. Thus, the coregulation of the *INK4b-ARF-INK4a* locus observed in selective cell lines (12) is not a general phenomenon.

To gain insight into the mechanism of *$p15^{INK4b}$* and *$p16^{INK4a}$* activation by hSNF5, we analyzed the chromatin status at the *INK4b-ARF-INK4a* locus. For qPCR we used primer sets corresponding to the promoter areas of *$p15^{INK4b}$* (primer set A) and *$p14^{ARF}$* (primer set B), an intergenic control (primer set C), whereas we probed the *$p16^{INK4a}$* locus at a higher resolution (primer sets D to I [Fig. 2, bottom]). ChIPs directed against hSNF5 revealed strong binding to the *$p15^{INK4b}$* and *$p16^{INK4a}$* promoters when hSNF5 is expressed (green bars; Fig. 2A). The *$p14^{ARF}$* promoter was not bound by hSNF5, as reflected by the low background signal, also present in cells devoid of hSNF5 (yellow bars). Importantly, hSNF5 was strictly required to bring BRG1, the central SWI/SNF motor subunit, to the *$p15^{INK4b}$* and *$p16^{INK4a}$* promoters (Fig. 2B). We note that hSNF5 expression does not influence BRG1 levels in the cell (Fig. 3A) (26). Finally, these ChIPs demonstrated that SWI/SNF recruitment is limited to the *$p15^{INK4b}$* and *$p16^{INK4a}$* promoter areas and does not spread across the locus.

Does hSNF5 mediate gene activation by itself, or does its function depend on the chromatin remodeling activity of SWI/SNF? To investigate this question, we used lentiviral expressed shRNAs to deplete MON cells for BRG1, the central ATPase that is critical for chromatin remodeling (Fig. 3A). Western

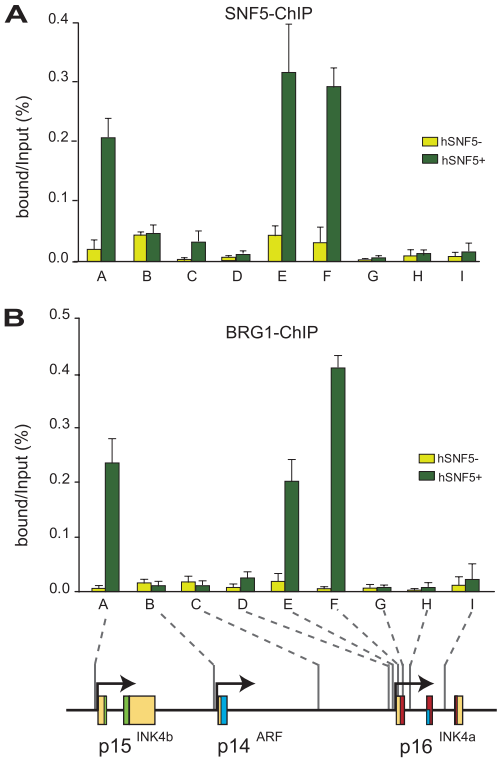

FIG. 2. hSNF5 mediates BRG1 recruitment to the *p15*^{INK4b} and *p16*^{INK4a} promoters. (A) ChIP-qPCR analysis of hSNF5 binding to the INK4b-ARF-INK4a locus revealed that hSNF5 binds directly to the *p15*^{INK4b} and *p16*^{INKa} promoters, but not to *p14*^{ARF}. Cross-linked chromatin was isolated from MRT cells that either lack (light green bars) or express (dark green bars) hSNF5. qPCR primer sets correspond to the *p15*^{INK4b} promoter (A), the *p14*^{ARF} promoter (B), an intergenic control region (C), and various regions of the *p16*^{INK4a} locus (sets D to I). Primer sets E and F cover the *p16*^{INK4a} promoter. The positions of the amplified regions on the *INK4b-ARF-INK4a* locus are indicated at the bottom. (B) BRG-1 binding to the *p15*^{INK4b} and *p16*^{INK4a} promoters is hSNF5 dependent, as revealed by ChIP-qPCR with antibodies directed against BRG-1. The procedures were as described in the legend to Fig. 1.

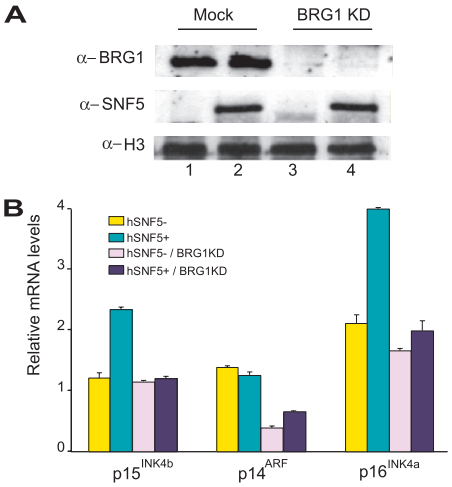

FIG. 3. BRG1 is required for hSNF5-mediated induction of *p15*^{INK4b} and *p16*^{INK4a}. (A) Western blot analysis of the BRG1 protein levels in MON cell extracts prepared 4 days after BRG1 knockdown using lentiviral transduction with viruses expressing shRNA targeting *BRG1* mRNA (clone 15549; Open Biosystems; top panel, lanes 3 and 4). As a control, cells were transduced with lentiviruses expressing GFP. One day after transduction with either GFP- or shRNA-expressing lentiviruses, cells were transduced again with viruses expressing either GFP (middle panel, lanes 1 and 3) or hSNF5 (lanes 2 and 3). Cell extracts were prepared 72 h after hSNF5 expression. Histone H3 serves as a loading control. (B) Loss of BRG1 abrogates transcriptional activation of *p15*^{INK4b} and *p16*^{INK4a} by hSNF5. Relative expression levels of *p15*^{INK4b}, *p14*^{ARF}, and *p16*^{INK4a} in these cells were determined by RT-qPCR of isolated mRNA, 72 h after hSNF5 expression. The bar graphs represent the mean of three independent experiments, each analyzed in triplicate by RT-qPCR.

immunoblot analysis of extracts from mock-treated cells (lanes 1 and 2) or cells transduced with lentiviruses expressing shRNAs directed against BRG1 (lanes 3 and 4) revealed a dramatic shRNA-mediated loss of BRG1. Next, we used lentiviral transduction of viruses expressing either GFP (lanes 1 and 3) or hSNF5 (lanes 2 and 4) to test the effect of hSNF5 reexpression in cells depleted of BRG1. Western immunoblotting confirmed our earlier observation (26) that hSNF5 reexpression did not influence BRG1 levels (Fig. 3A, compare lanes 1 and 2). Antibodies directed against histone H3 were used as a loading control. In agreement with our earlier results, hSNF5 expression in mock-treated cells led to a robust induction of both *15*^{INK4b} and *p16*^{INK4a}, but not of *p14*^{ARF}, as revealed by RT-qPCR (Fig. 3B). However, in BRG1-depleted cells hSNF5 could no longer activate *15*^{INK4b} and *p16*^{INK4a} expression. Surprisingly, the low level of *p14*^{ARF} expression was reduced further due to the loss of BRG1, indicating a potential role for BRG1, but not hSNF5. We conclude that hSNF5-mediated induction of *15*^{INK4b} and *p16*^{INK4a} is critically dependent on BRG1, the key catalytic subunit of SWI/SNF.

SWI/SNF displaces PcG silencing complexes. Overexpression of the PcG protein BMI1 promotes oncogenesis in mice through silencing of the INK4a-ARF locus (15). Growth of normal and cancerous prostate cells is controlled by PcG protein CBX7-dependent repression of INK4a-ARF (2). Recently, it was observed that both PcG complexes PRC1 and PRC2 can directly bind and silence the *INK4a-ARF* locus (5, 20). Because hSNF5 expression in MRT cells leads to SWI/SNF recruitment to the *p15*^{INK4b} and *p16*^{INK4a} promoters, we tested its effect on PcG complex binding. First, we established whether in MRT cells PcG silencers occupy the *INK4b-ARF-INK4a* locus by ChIPs directed against the PRC1 subunit BMI1 and the PRC2 subunits EZH2 and Suz12 (Fig. 4A to C). We observed strong binding of PcG silencers to the *p16*^{INK4a} promoter region (primer sets E and F) in the absence of

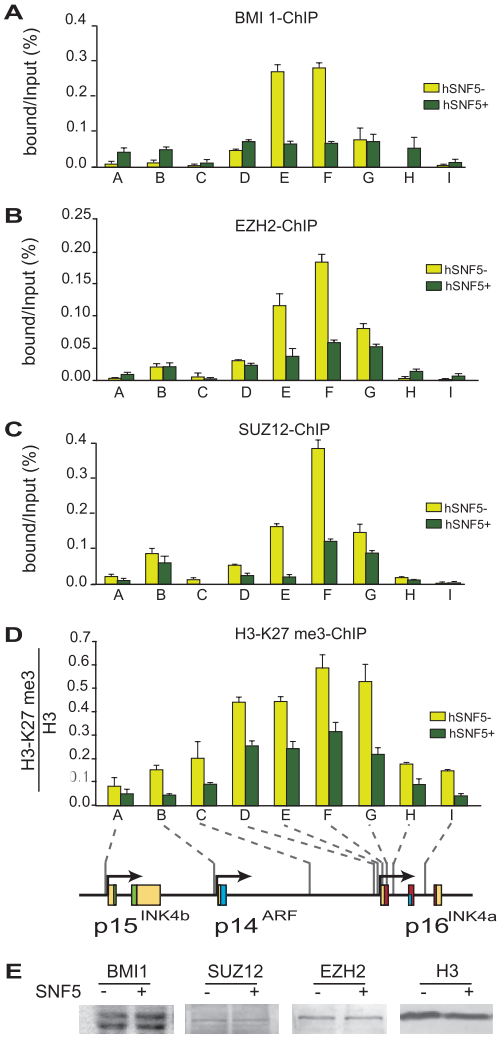

FIG. 4. Restoration of SWI/SNF causes eviction of PcG silencers and loss of H3-K27 methylation. ChIPs using antibodies directed against BMI1 (A), EZH2 (B), SUZ12 (C), and H3-K27me3 (D) were performed. Cross-linked chromatin was isolated from MRT cells that either lack (yellow bars) or express (dark green bars) hSNF5. ChIPs were analyzed by qPCR using primer sets specific for the regions indicated by A to I along the *INK4b-ARF-INK4a* locus, revealing that PcG silencer binding peaks at the $p16^{INK4a}$ promoter. After hSNF5 induction both PRC1 (BMI1) and PRC2 (EZH2 and SUZ12) were removed, and H3-K27me3 was strongly reduced. H3-K27me3 ChIPs were normalized to H3 ChIP. Procedures were as described in the legend to Fig. 1. (E) hSNF5 expression does not affect BMI1, SUZ12, and EZH2 levels. Western immunoblotting analysis of BMI1, SUZ12, and EZH2 expression in MON cells transduced by either GFP- or SNF5-expressing lentiviruses. Cell lysates were resolved by SDS-PAGE and analyzed by Western immunoblotting with antibodies to BMI1, SUZ12, and EZH2, respectively. Histone H3 serves as a loading control.

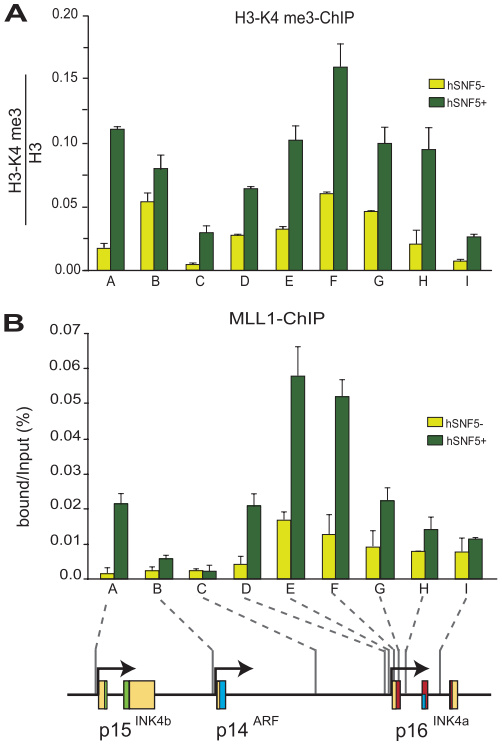

FIG. 5. hSNF5 induced recruitment of H3-K4 methylase MLL1. ChIPs with antibodies directed against H3-K4me3 (A) and MLL1 (B) reveal increased H3-K4me3 and MLL1 binding at $p15^{INK4b}$ and $p16^{INK4a}$ after hSNF5 expression. Cross-linked chromatin was isolated from MRT cells that either lack (yellow bars) or express (dark green bars) hSNF5. ChIPs were analyzed by qPCR using the primer sets specific for the regions indicated by A to I along the *INK4b-ARF-INK4a* locus. Histone H3-K4me3 ChIPs were normalized to histone H3 ChIP. The procedures were as described in the legend to Fig. 1.

hSNF5. Outside this domain of ~0.8 kb, PcG protein binding tapers off across the locus. Relatively low amounts of PcG proteins were detected at the $p14^{ARF}$ and $p15^{INK4b}$ promoters. Strikingly, hSNF5 expression strongly reduces the binding of both PRC1 and PRC2. We conclude that during $p16^{INK4a}$ activation, SWI/SNF mediates the eviction of PcG silencing complexes. The PRC2 subunit EZH2 catalyzes histone H3 lysine 27 trimethylation (H3-K27me3), a chromatin mark associated with gene repression (29, 32). Although this could be due to ChIP efficiency, the H3-K27me3 histone mark appears to spread more broadly than PRC2 (Fig. 4D). Clearly, H3-K27me3 is not a stable mark but is reduced upon hSNF5 expression and removal of PRC2. This is likely to be the result of the action of the recently identified H3-K27me3 demethylases (1, 21). Finally, we note that the loss of PcG protein binding was not due to a change in their expression, as revealed by Western blotting (Fig. 4E). In conclusion, our results dem-

at the $p15^{INK4b}$ promoter were comparably low, again we observed a clear reduction. These effects were gene selective, because CpG methylation at $p14^{ARF}$ or the imprinted *H19* locus remained unchanged. Next, we examined the distribution of the DNA methyltransferase DNMT3B, which has previously been associated with PcG silencing (31, 39). ChIPs revealed that, similar to the PcG silencers, DNMT3B binding peaks at the $p16^{INK4a}$ promoter region and tapers off to a low level across the locus. However, concomitant with the drop in CpG methylation, DNMT3B is evicted from the locus after SWI/SNF binding (Fig. 6B). Western immunoblotting demonstrated that the loss of DNMT3B binding is not caused by a reduced expression (Fig. 6C). We conclude that, similar to the chromatin association of PcG silencers, DNA methylation can be highly dynamic and modulated by SWI/SNF recruitment.

Next, we tested the effect of the DNA methylation inhibitor 5-azadC on the expression of the *INK4b-ARF-INK4a* locus in MRT cells. We incubated MON MRT cells with 5-azadC, followed by transduction with either GFP- or hSNF5-expressing lentiviruses. Expression analysis by RT-qPCR revealed that the addition of 5-azadC resulted in a robust induction of $p15^{INK4b}$ and $p16^{INK4a}$, but not of $p14^{ARF}$. Thus, treatment with a DNA methylation inhibitor leads to transcriptional derepression, supporting the functional importance of CpG methylation in $p15^{INK4b}$ and $p16^{INK4a}$ silencing. When 5-azadC treatment was combined with hSNF5 reexpression, we observed modestly additive stimulation of $p15^{INK4b}$ and $p16^{INK4a}$ transcription, whereas $p14^{ARF}$ remained unaffected. The absence of synergism could be interpreted as a suggestion that removal of CpG methylation and SWI/SNF action ultimately have similar consequences for the local chromatin structure. Again, these findings emphasize the close interconnectivity of various chromatin structure modulating activities.

DISCUSSION

The loss of hSNF5 in MRT cells precludes SWI/SNF binding to the $p15^{INK4b}$ and $p16^{INK4a}$ promoters, which are both stably silenced in these cells. By reexpressing hSNF5 in MRT cells, we created a switch allowing us to study the effect of SWI/SNF recruitment to a silenced locus bound by PcG silencers. Reexpression of hSNF5 in MRT cells overcomes epigenetic silencing and mediates transcriptional activation of $p15^{INK4b}$ and $p16^{INK4a}$. In contrast, $p14^{ARF}$ is not induced, demonstrating that the *INK4b-ARF-INK4a* locus is not coordinately regulated in MRT cells. Because SWI/SNF itself lacks sequence-specific DNA-binding activity, an important future goal is the identification of promoter binding recruiters. An issue that has remained unresolved for a considerable time is whether hSNF5 functions as part of the SWI/SNF complex or if it acts independently. shRNA-mediated depletion of BRG1 revealed that hSNF5 was completely dependent on the motor subunit of the SWI/SNF complex to activate either $p15^{INK4b}$ or $p16^{INK4a}$. Thus, it appears that gene activation by hSNF5 is dependent on BRG1-mediated chromatin remodeling. These results dovetail well with our functional dissection of *Drosophila* SWI/SNF remodelers in genome wide expression control (7, 23, 26). Both studies suggest that SWI/SNF subunits do not function outside the remodeling complexes.

Although the whole *INK4b-ARF-INK4a* locus is inactive, it is not evenly coated by PcG silencing complexes. Instead, we found that PRC1 and PRC2 binding peaks at the repressed $p16^{INK4a}$ promoter. These results indicate that the ~0.8-kb $p16^{INK4a}$ promoter area might function as a nucleation site for PcG complex recruitment. The H3-K27me3 mark appears to spread more broadly than the PcG proteins, indicative of a "kiss-and-go" mechanism of histone methylation by PRC2. A similar difference in the pattern of distribution of H3-K27me3 and PRC2 has been observed for *Drosophila* PREs and associated genes (18, 27). In contrast to the purported primacy of PRC1 prebinding over SWI/SNF action (35), we found that in MRT cells PRC1 could be effectively displaced by SWI/SNF. In fact, SWI/SNF binding initiates a cascade of chromatin reprogramming, which completely resets the epigenetic status of $p15^{INK4b}$ and $p16^{INK4a}$ but leaves $p14^{ARF}$ largely unaffected. The trxG activators SWI/SNF and MLL1 supplant their antagonists PRC1, PRC2, and the DNA methyltransferase DNMT3B. Concomitant with RNA Pol II recruitment and gene transcription, active histone marks replace repressive ones, and DNA methylation at the $p16^{INK4a}$ promoter is strongly reduced. We speculate that during stem cell differentiation, SWI/SNF remodelers might play a comparable role in removal of PcG silencers from genes that need to be expressed.

Previous studies have suggested a functional association between PcG silencing and CpG methylation by DNA methyltransferases such as DNMT3B (31, 39). Here, we observed that DNMT3B was displaced by SWI/SNF action concomitantly with the PcG silencing complexes. Moreover, we found that addition of the DNA methylation inhibitor 5-azadC leads to the transcriptional derepression of $p15^{INK4b}$ and $p16^{INK4a}$, whereas $p14^{ARF}$ remained unaffected. These results support the functional importance of CpG methylation for the silencing of these genes in MRT cells and might have therapeutic implications. Combining the 5-azadC treatment with hSNF5 expression in MRT cells resulted in modestly additive stimulation of $p15^{INK4b}$ and $p16^{INK4a}$ transcription. We interpret this absence of synergistic activation as an indication that the removal of CpG methylation and SWI/SNF action start a cascade that results in similar changes in chromatin structure. Collectively, these findings emphasize the intertwined dynamics of diverse chromatin marks and SWI/SNF function during transcriptional regulation.

ACKNOWLEDGMENTS

We thank D. Trono for the gift of lentiviral vectors; T. van Dijk for advice on lentiviral procedures; Parham Solaimani for the Brg1 knockdown experiment, and J. Svejstrup, R. Vries, S. Philipsen, and A. Bracken for valuable comments on the manuscript.

This study was supported by grants from the Dutch Cancer Society KWF (EMCR2006-3583) and NWO Chemical Sciences (TOP700.52.312) to C.P.V.

REFERENCES

1. **Agger, K., P. A. C. Cloos, J. Christensen, D. Pasini, S. Rose, J. Rappsilber, I. Issaeva, E. Canaani, A. E. Salcini, and K. Helin.** 2007. UTX and JMJD3 are histone H3K27 demethylases involved in HOX gene regulation and development. Nature **449:**731–734.
2. **Bernard, D., J. F. Martinez-Leal, S. Rizzo, D. Martinez, D. Hudson, T. Visakorpi, G. Peters, A. Carnero, D. Beach, and J. Gil.** 2005. CBX7 controls the growth of normal and tumor-derived prostate cells by repressing the Ink4a/Arf locus. Oncogene **24:**5543–5551.
3. **Betz, B. L., M. W. Strobeck, D. N. Reisman, E. S. Knudsen, and B. E. Weissman.** 2002. Re-expression of hSNF5/INI1/BAF47 in pediatric tumor cells leads to G_1 arrest associated with induction of p16ink4a and activation of RB. Oncogene **21:**5193–5203.

4. **Biegel, J. A., J. Y. Zhou, L. B. Rorke, C. Stenstrom, L. M. Wainwright, and B. Fogelgren.** 1999. Germ-line and acquired mutations of INI1 in atypical teratoid and rhabdoid tumors. Cancer Res. **59:**74–79.
5. **Bracken, A. P., D. Kleine-Kohlbrecher, N. Dietrich, D. Pasini, G. Gargiulo, C. Beekman, K. Theilgaard-Monch, S. Minucci, B. T. Porse, J.-C. Marine, K. H. Hansen, and K. Helin.** 2007. The Polycomb group proteins bind throughout the INK4A-ARF locus and are disassociated in senescent cells. Genes Dev. **21:**525–530.
6. **Canaani, E., T. Nakamura, T. Rozovskaia, S. T. Smith, T. Mori, C. M. Croce, and A. Mazo.** 2004. ALL-1/MLL1, a homologue of *Drosophila* TRITHORAX, modifies chromatin and is directly involved in infant acute leukaemia. Br. J. Cancer 90:Br J. Cancer 2004 Feb 23;. **90:**756–760.
7. **Doan, D., T. M. Veal, Z. Yan, W. Wang, S. N. Jones, and A. N. Imbalzano.** 2004. Loss of the INI1 tumor suppressor does not impair the expression of multiple BRG1-dependent genes or the assembly of SWI/SNF enzymes. Oncogene **23:**3462–3473.
8. **Feinberg, A. P., R. Ohlsson, and S. Henikoff.** 2006. The epigenetic progenitor origin of human cancer. Nat. Rev. Genet. **7:**21–33.
9. **Follenzi, A., G. Sabatino, A. Lombardo, C. Boccaccio, and L. Naldini.** 2002. Efficient gene delivery and targeted expression to hepatocytes in vivo by improved lentiviral vectors. Hum. Gene Ther. **13:**243–260.
10. **Gil, J., and G. Peters.** 2006. Regulation of the INK4b-ARF-INK4a tumour suppressor locus: all for one or one for all. Nat. Rev. Mol. Cell. Biol. **7:**667–677.
11. **Goldberg, A. D., C. D. Allis, and E. Bernstein.** 2007. Epigenetics: a landscape takes shape. Cell **128:**635–638.
12. **Gonzalez, S., P. Klatt, S. Delgado, E. Conde, F. Lopez-Rios, M. Sanchez-Cespedes, J. Mendez, F. Antequera, and M. Serrano.** 2006. Oncogenic activity of Cdc6 through repression of the INK4/ARF locus. Nature **440:**702–706.
13. **Guidi, C. J., R. Mudhasani, K. Hoover, A. Koff, I. Leav, A. N. Imbalzano, and S. N. Jones.** 2006. Functional interaction of the retinoblastoma and Ini1/Snf5 tumor suppressors in cell growth and pituitary tumorigenesis. Cancer Res. **66:**8076–8082.
14. **Isakoff, M. S., C. G. Sansam, P. Tamayo, A. Subramanian, J. A. Evans, C. M. Fillmore, X. Wang, J. A. Biegel, S. L. Pomeroy, J. P. Mesirov, and C. W. Roberts.** 2005. Inactivation of the Snf5 tumor suppressor stimulates cell cycle progression and cooperates with p53 loss in oncogenic transformation. Proc. Natl. Acad. Sci. USA **102:**17745–17750.
15. **Jacobs, J. J. L., K. Kieboom, S. Marino, R. A. DePinho, and M. van Lohuizen.** 1999. The oncogene and Polycomb-group gene *bmi-1* regulates cell proliferation and senescence through the *ink4a* locus. Nature **397:**164–168.
16. **Jenuwein, T., and C. D. Allis.** 2001. Translating the histone code. Science **293:**1074–1080.
17. **Jones, P. A., and S. B. Baylin.** 2007. The epigenomics of cancer. Cell **128:** 683–692.
18. **Kahn, T. G., Y. B. Schwartz, G. I. Dellino, and V. Pirrotta.** 2006. Polycomb complexes and the propagation of the methylation mark at the *Drosophila ubx* gene. J. Biol. Chem. **281:**29064–29075.
19. **Klochendler-Yeivin, A., C. Muchardt, and M. Yaniv.** 2002. SWI/SNF chromatin remodeling and cancer. Curr. Opin. Genet. Dev. **12:**73–79.
20. **Kotake, Y., R. Cao, P. Viatour, J. Sage, Y. Zhang, and Y. Xiong.** 2007. pRB family proteins are required for H3K27 trimethylation and Polycomb repression complexes binding to and silencing $p16^{INK4a}$ tumor suppressor gene. Genes Dev. **21:**49–54.
21. **Lee, M. G., R. Villa, P. Trojer, J. Norman, K.-P. Yan, D. Reinberg, L. Di Croce, and R. Shiekhattar.** 2007. Demethylation of H3K27 regulates Polycomb recruitment and H2A ubiquitination. Science **318:**447–450.
22. **Livak, K. J., and T. D. Schmittgen.** 2001. Analysis of relative gene expression data using real-time quantitative PCR and the 2-ΔΔCT method. Methods **25:**402–408.
23. **Moshkin, Y. M., L. Mohrmann, W. F. J. van Ijcken, and C. P. Verrijzer.** 2007. Functional differentiation of SWI/SNF remodelers in transcription and cell cycle control. Mol. Cell. Biol. **27:**651–661.
24. **Muller, J., and J. A. Kassis.** 2006. Polycomb response elements and targeting of Polycomb group proteins in *Drosophila*. Curr. Opin. Genet. Dev. **16:**476–484.
25. **Narita, M., and S. W. Lowe.** 2005. Senescence comes of age. Nat. Med. **11:**920–922.
26. **Oruetxebarria, I., F. Venturini, T. Kekarainen, A. Houweling, L. M. Zuijderduijn, A. Mohd-Sarip, R. G. Vries, R. C. Hoeben, and C. P. Verrijzer.** 2004. $p16^{INK4a}$ is required for hSNF5 chromatin remodeler-induced cellular senescence in malignant rhabdoid tumor cells. J. Biol. Chem. **279:**3807–3816.
27. **Papp, B., and J. Muller.** 2006. Histone trimethylation and the maintenance of transcriptional ON and OFF states by TrxG and PcG proteins. Genes Dev. **20:**2041–2054.
28. **Ptashne, M.** 2007. On the use of the word "epigenetic". Curr. Biol. **17:**R233–R236.
29. **Ringrose, L., and R. Paro.** 2007. Polycomb/Trithorax response elements and epigenetic memory of cell identity. Development **134:**223–232.
30. **Roberts, C. W., and S. H. Orkin.** 2004. The SWI/SNF complex: chromatin and cancer. Nat. Rev. Cancer **4:**133–142.
31. **Schlesinger, Y., R. Straussman, I. Keshet, S. Farkash, M. Hecht, J. Zimmerman, E. Eden, Z. Yakhini, E. Ben-Shushan, B. E. Reubinoff, Y. Bergman, I. Simon, and H. Cedar.** 2007. Polycomb-mediated methylation on Lys27 of histone H3 pre-marks genes for de novo methylation in cancer. Nat. Genet. **39:**232–236.
32. **Schuettengruber, B., D. Chourrout, M. Vervoort, B. Leblanc, and G. Cavalli.** 2007. Genome regulation by Polycomb and Trithorax proteins. Cell **128:**735–745.
33. **Schwartz, Y. B., and V. Pirrotta.** 2007. Polycomb silencing mechanisms and the management of genomic programmes. Nat. Rev. Genet. **8:**9–22.
34. **Sevenet, N., E. Sheridan, D. Amram, P. Schneider, R. Handgretinger, and O. Delattre.** 1999. Constitutional mutations of the hSNF5/INI1 gene predispose to a variety of cancers. Am. J. Hum. Genet. **65:**1342–1348.
35. **Shao, Z., F. Raible, R. Mollaaghababa, J. R. Guyon, C.-t. Wu, W. Bender, and R. E. Kingston.** 1999. Stabilization of chromatin structure by PRC1, a Polycomb complex. Cell **98:**37–46.
36. **Sparmann, A., and M. van Lohuizen.** 2006. Polycomb silencers control cell fate, development and cancer. Nat. Rev. Cancer **6:**846–856.
37. **Tamkun, J. W., R. Deuring, M. P. Scott, M. Kissinger, A. M. Pattatucci, T. C. Kaufman, and J. A. Kennison.** 1992. brahma: a regulator of *Drosophila* homeotic genes structurally related to the yeast transcriptional activator SNF2/SWI2. Cell **68:**561–572.
38. **Versteege, I., N. Sevenet, J. Lange, M. F. Rousseau-Merck, P. Ambros, R. Handgretinger, A. Aurias, and O. Delattre.** 1998. Truncating mutations of hSNF5/INI1 in aggressive paediatric cancer. Nature **394:**203–206.
39. **Vire, E., C. Brenner, R. Deplus, L. Blanchon, M. Fraga, C. Didelot, L. Morey, A. Van Eynde, D. Bernard, J.-M. Vanderwinden, M. Bollen, M. Esteller, L. Di Croce, Y. de Launoit, and F. Fuks.** 2006. The Polycomb group protein EZH2 directly controls DNA methylation. Nature **439:8**71–874.
40. **Vries, R. G., V. Bezrookove, L. M. Zuijderduijn, S. K. Kia, A. Houweling, I. Oruetxebarria, A. K. Raap, and C. P. Verrijzer.** 2005. Cancer-associated mutations in chromatin remodeler hSNF5 promote chromosomal instability by compromising the mitotic checkpoint. Genes Dev. **19:**665–670.

Chapter 5

An EZH2-Dependent Repressive Chromatin Loop Controls *INK4a* and *INK4b* Expression during Human Cell Differentiation, Aging and Senescence

Sima Kheradmand Kia[1], Parham Solaimani Kartalaei[1], Elnaz Farahbakhshian[2], Farzin Pourfarzad[3], Marieke von Lindern[2] and C. Peter Verrijzer[1*]

[1]Department of Biochemistry, Center for Biomedical Genetics, [2]Department of Hematology, [3]Department of Cell Biology, Erasmus University Medical Center, P.O. Box 1738, 3000 DR Rotterdam, The Netherlands.

Submitted for publication

SUMMARY

The *INK4b-ARF-INK4a* tumor suppressor locus controls the balance between progenitor cell renewal and cancer. Here, we investigated how chromatin structure modulates differential expression of the human *INK4b-ARF-INK4a* locus during cellular differentiation, aging and senescence. $p15^{INK4b}$ and $p16^{INK4a}$, but not $p14^{ARF}$, are coordinately up-regulated following differentiation of hematopoietic progenitor cells, in aging fibroblasts and senescent malignant rhabdoid tumor cells. Following progenitor cell differentiation and aging, Polycomb group (PcG) silencer EZH2 is down-regulated, causing reduced locus occupancy and induction of $p15^{INK4b}$ and $p16^{INK4a}$. EZH2 controls the formation of a ~40 kb repressive chromatin loop linking *INK4b* and *INK4a*, but excluding *ARF*. Attenuated EZH2 expression causes loop opening and de-repression of $p15^{INK4b}$ and $p16^{INK4a}$. Our results support a looping mechanism of long-range locus control rather than continuous spreading of PcG silencing. We conclude that PcG proteins regulate higher order chromatin structure dynamically to balance differentiation and proliferation of human cells.

INTRODUCTION

Development and homeostasis require the coordinate regulation of cell proliferation and differentiation. The *INK4b-ARF-INK4a* tumor suppressor locus plays a central role in controlling the balance between progenitor cell renewal and cancer (13, 15, 17, 25). This locus encodes three cell cycle inhibitory proteins: $p15^{INK4b}$, $p14^{ARF}$ and $p16^{INK4a}$. $p15^{INK4b}$ and $p16^{INK4a}$ are closely related proteins and both act through inhibition of the cyclin-dependent kinases CDK4 and CDK6, which promote proliferation (9, 22). $p14^{ARF}$ is structurally and functionally unrelated to $p15^{INK4b}$ or $p16^{INK4a}$, and works primarily through activation of the p53 pathway. A multitude of studies have suggested a role for the *INK4b-ARF-INK4a* locus in cancer suppression and promotion of aging (9). In particular $p16^{INK4a}$, has been proposed to control the equilibrium between proliferation of progenitor cells and tissue renewal on the one hand and the risk of tumorigenesis on the other. Perhaps not surprising, the regulation of the *INK4b-ARF-INK4a* locus is highly complex. Coordinate regulation of the whole locus, as well as individual patterns of gene expression, have been described (1, 9, 14). Thus, the *INK4b-ARF-INK4a* locus appears to be expressed differentially, depending on the circumstances.

The polycomb group (PcG) silencers form an important class of transcriptional corepressors that regulate expression of the *INK4b-ARF-INK4a* locus . This was first suggested by the finding that the PcG protein BMI1 promotes oncogenesis in mice through silencing of *INK4a* (12). Since then, other PcG silencers have also been implicated in silencing of the *INK4b-ARF-INK4a* locus, including the histone H3 lysine 27 (H3K27) methyltransferase EZH2 (1). PcG proteins function as part of larger multi-protein assemblages, referred to as Polycomb repressive complexes (PRCs). PRC1-like complexes, which include assemblages with BMI1 as a subunit, form one major class. Recent research in flies uncovered that PSC, the fly BMI1 homolog, is also part of an alternate complex named dRAF (18). PRC2-like complexes

that harbor histone H3K27 methylases, such as EZH2, form the second major class. However, it is important to stress that there is likely to be a greater variety of PRCs and possible enzymatic activities (26). Both PRC1 and PRC2 complexes directly bind and silence the *INK4a-ARF* locus (1, 6, 14, 16). Although the developmental roles of many PcG proteins await further analysis, recent research has emphasized their importance in dynamic gene control during differentiation of precursor cells, cancer and senescence (2, 7, 28-31,1, 6, 14, 29)). In particular, several studies have shown the importance of EZH2 for dynamic regulation of gene silencing orchestrating the differentiation of progenitor cells.

Here, we have addressed the role of PcG silencers in the regulation of the human *INK4b-ARF-INK4a* locus during cellular aging, differentiation of progenitor cells and cellular senescence of human cancer cells. During these physiological processes we noted a remarkable pattern of *INK4b-ARF-INK4a* expression: $p15^{INK4b}$ and $p16^{INK4a}$ were coordinately induced, whereas $p14^{ARF}$ remained unaltered. We found that EZH2 controlled the selective de-repression of $p15^{INK4b}$ and $p16^{INK4a}$. Our results support a looping mechanism of long-range control rather than "blanket" spreading across the *INK4b-ARF-INK4a* locus. We conclude that higher order chromatin conformation of the *INK4b-ARF-INK4a* locus underlies the coupling of cell differentiation to proliferation control.

RESULTS

Differential induction of the human *INK4b-ARF-INK4a* locus during aging, differentiation and senescence

To investigate the effects of cellular aging on expression of the human *INK4b-ARF-INK4a* locus, we compared $p15^{INK4b}$, $p14^{ARF}$ and $p16^{INK4a}$ expression in neonatal versus adult human diploid fibroblasts (HDFs). We also compared human embryonic fibroblasts (HEFs) with a low passage number with older cells. We noted that in aging cells the proliferative capacity diminished. The proliferation rate of adult HDFs is 2-3 fold slower than that of neonatal HDFs. Likewise during culturing of HEFs, we observed a gradual up to 2-3-fold increase in doubling time as the passage number becomes higher. To monitor *INK4b-ARF-INK4a* expression, we extracted RNA and used reverse transcription followed by real-time quantitative PCR (RT-qPCR) with gene-selective primers (Figure 1B and C). In HDFs and in HEFs, we detected a strong up-regulation of $p15^{INK4b}$ and $p16^{INK4a}$, but not of $p14^{ARF}$, in old (blue) versus young cells (yellow).

To study the expression of the *INK4b-ARF-INK4a* locus in cells with a broad versus restricted potential for differentiation, we compared $CD34^+$ with $CD34^-$ cells isolated from human umbilical cord blood (Figure 1D). $CD34^+$ cells comprise immature committed hematopoietic progenitor cells, including short term- hematopoietic stem cells, multipotent progenitors and common myeloid progenitors. The pool of mature $CD34^-$ cells is formed to a large extend by a variety of more highly differentiated cells, including lymphoblasts, late hematopoietic progenitors, and mature cells such as late erythroblasts and granulocytes. A

direct comparison of immature CD34^{+} cells (yellow) with mature CD34^{-} cells (green), revealed up-regulation of p15^{INK4b} and p16^{INK4a}, but not of p14^{ARF}, following differentiation. When the isolated CD34^{+} cells were cultured for 6 weeks, the majority (~80%) matured and became CD34^{-}, as revealed by FACS analysis and cell staining (see Figure D, bottom panels).

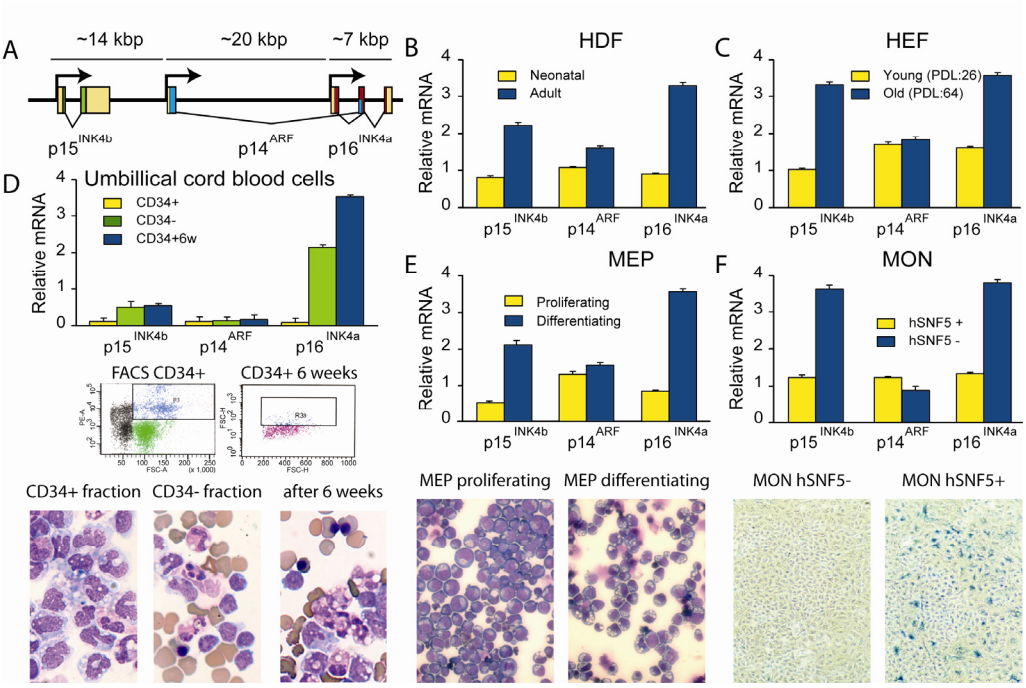

Figure 1. Gene regulation of INK4-ARF during aging, differentiation and senescence
(A) Organization of the human INK4b-ARF-INK4a locus (not drawn to scale). The genomic locus spans approximately 40 Kbp of human chromosome 9, and encodes three distinct proteins, *p15^{INK4b}*, *p14^{ARF}* and *p16^{INK4a}*. The 5' and 3' untranslated regions (yellow boxes), the coding sequences of *p15^{INK4b}* (green), *p14^{ARF}* (blue) and *p16^{INK4a}* (red) are indicated. (B) RT-qPCR analysis of gene expression in Human Diploid Fibroblast reveals induction of *p15^{INK4b}* and *p16^{INK4a}*, in adult cells (blue bar) compared to neonatal cells (yellow bar) whereas *p14^{ARF}* transcription remains unaffected. (C) RT-qPCR analysis of gene expression in Human Embryonic Fibroblast (TIG3) reveals the induction of *p15^{INK4b}* and *p16^{INK4a}*, in the old cells (at passage Doubling: PDL: 64, blue bar) compared to the young cells (PDL: 26, yellow bar), whereas *p14^{ARF}* transcription remains unaffected. (D) RT-qPCR analysis of gene expression in Committed progenitor cells, derived from umbilical cord blood after cell sorting with CD34 marker, reveals induction of *p15^{INK4b}* and *p16^{INK4a}*, in matured cells (CD34-, green bar) and immature cells were kept 6 weeks in culture, blue bar) compared to immature cells (CD34+, yellow bar) whereas *p14^{ARF}* transcription remains unaffected (upper part), fluorescence activated cell sorter (FACS) graphs (Middle part). In the lower panels, cells were cytocentrifuged onto glass slides and stained with cytologic dyes. (E) RT-qPCR analysis of gene expression in Megakaryocyte Erythrocyte progenitor (MEP) cells derived from human fetal liver reveals induction of *p15^{INK4b}* and *p16^{INK4a}* in differentiated cells toward the Erythrocyte (blue bar) compared to proliferative cells (yellow bar), whereas *p14^{ARF}* transcription remains unaffected. RT-qPCR analysis of isolated mRNA was used to determine the relative expression levels of *p15^{INK4b}*, *p16^{INK4a}*, *p14^{ARF}* and *GAPDH*. E) RT-qPCR analysis of gene expression in MRT cells reveals hSNF5-dependent induction of *p15^{INK4b}* and *p16^{INK4a}*, whereas *p14^{ARF}* transcription remains unaffected. Cells were collected 48 hours following transduction with lentiviruses expressing either GFP (yellow bars) or hSNF5 (blue bars). RT-qPCR analysis of isolated mRNA was used to determine the relative expression levels of *p15^{INK4b}*, *p16^{INK4a}*, *p14^{ARF}* and *GAPDH*. mRNA levels were plotted as percentage of *GAPDH* mRNA. The bar graphs represent the mean of three independent biological replicates, each analyzed by three separate qPCR reactions. Standard deviations are indicated.

Again cell differentiation was accompanied by a robust induction of $p15^{INK4b}$ and a particularly strong up-regulation of $p16^{INK4a}$. In contrast, $p14^{ARF}$ expression remained unaltered. As an alternative way to study the effects of cell differentiation, we isolated megakaryocyte and erythrocyte progenitor (MEP) cells from human fetal liver and induced differentiation towards erythrocytes (Figure 1E bottom). When we compared proliferating MEPs with their progenitors differentiating towards erythrocytes, we detected a clear induction of $p15^{INK4b}$ and $p16^{INK4a}$, but not of $p14^{ARF}$. We conclude that differentiation of human MEP and $CD34^-$ multi-potent progenitor cells is accompanied with selective up-regulation of $p15^{INK4b}$ and $p16^{INK4a}$.

As a model for senescence, we used human malignant rhabdoid tumor (MRT) cells that are caused by a loss of the hSNF5 subunit of the SWI/SNF chromatin remodeling complex. Re-expression of hSNF5 in MRT cells restores SWI/SNF recruitment to *INK4b* and *INK4a*, causing eviction of PRCs and loss of silencing (14). Consequently, these cells first undergo a G1/S cell cycle arrest and later become senescent (Figure 1F). In contrast to $p15^{INK4b}$ and $p16^{INK4a}$, $p14^{ARF}$ expression remained unaltered.

In conclusion, here we demonstrated coordinate induction of human $p15^{INK4b}$ and $p16^{INK4a}$, but not $p14^{ARF}$, during cellular aging, multi-potent progenitor cell differentiation or induction of senescence.

EZH2 is down-regulated during progenitor cell differentiation and aging

Because the PcG silencers EZH2 and BMI1 play important roles in repression of the *INK4b-ARF-INK4a* locus, we investigated their expression during aging and cellular differentiation. RT-qPCR and Western immunoblotting revealed clear down-regulation of EZH2 in aging HDFs whereas BMI1 levels remained stable (Figure 2A). When we compared proliferating MEPs with differentiating cells we again observed reduction of EZH2, but not of BMI1 (Figure 2B). Likewise, $CD34^+$ progenitor cells, isolated from umbilical cord blood, expressed much higher levels of EZH2 than mature $CD34^-$ cells (Figure 2). When $CD34^+$ cells were cultured for 6 weeks, they matured and lost CD34 expression. Concomitant with differentiation, EZH2 expression was strongly attenuated, whereas BMI1 levels remained stable. We conclude that during aging of HDFs and differentiation of hematopoietic progenitor cells, expression of the PRC2 subunit EZH2 is down-regulated, whereas levels of the PRC1 subunit BMI1 remain constant. Obviously, reduction of EZH2 provides an attractive explanation for de-repression of *INK4a* and *INK4b*. However, hSNF5-dependent induction of $p16^{INK4a}$ and $p15^{INK4b}$ in MRT cells does not involve down-regulation of EZH2 (Figure 2D). In MRT cells, re-expression of SNF5 enables SWI/SNF recruitment to *INK4a* and *INK4b* leading to eviction of PRCs and de-repression (14).

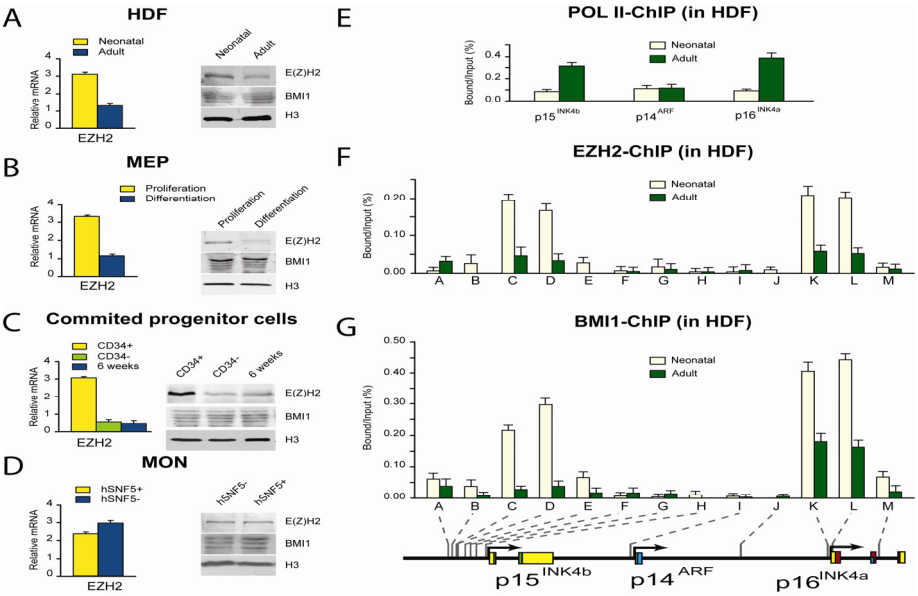

Figure 2. Induction of p15INK4b & p16INK4a is accompanied by down-regulation of E(z)h2
(A-C) RT-qPCR analysis of gene expression in Human Diploid Fibroblast, Megakaryocyte-Erythrocyte progenitor, Committed progenitor cells reveals reduction of *EZH2*, during aging and differentiation respectively (left side panel) in adult cells (blue bar) compared to neonatal cells (yellow bar). Western immunoblotting analysis of BMI1 and EZH2 expression in HDF, MEP and Committed progenitor cells revealed reduction of EZH2 during the aging and differentiation, while the BMI-1 level didn't change. Histone H3 serves as a loading control. (D) hSNF5 expression does not affect BMI1 and EZH2 levels. Western immunoblotting analysis of BMI and EZH2 expression in MON cells transduced by either GFP- or SNF5 expressing lentiviruses. Cell lysates were resolved by SDS-PAGE and analyzed by Western immunoblotting using antibodies against BMI1 and EZH2 respectively. Histone H3 serves as a loading control. (E) RNA pol II promoter binding was analyzed by ChIP-qPCR. Cross-linked chromatin was prepared from HDF- neonatal (light green bars), and HDF-adult (dark green bars). ChIPs with antibodies directed against RNA pol II were analyzed by qPCR using primer sets corresponding to the $p15^{INK4b}$, $p14^{ARF}$ and $p16^{INK4a}$ promoters. ChIP signal levels for each region are presented as percentage of input chromatin. (F-G) Down-regulation of E(z)h2 and reduced locus occupancy of PcG repressors. ChIPs using antibodies directed against (F) EZH2 and (G) BMI1. Cross-linked chromatin was isolated from HDF cells neonatal (light green bars) or adult (dark green bars). ChIPs were analyzed by qPCR using primer sets specific for the regions indicated by A-M along the *INK4b-ARF-INK4a* locus, revealing that PcG silencer binding peaks at the $p16^{INK4a}$ promoter and 3 kb upstream of $p15^{INK4b}$. During aging both PRC1 (BMI1) and PRC2 (EZH2) are removed or strongly reduced. QPCR primer sets correspond to the upstream of $p15^{INK4b}$ promoter (A-H), the $p14^{ARF}$ promoter (I), an intergenic control region (J), and various regions of the $p16^{INK4a}$ locus (sets K-M). Primer sets K and L cover the $p16^{INK4a}$ promoter. The positions of the amplified regions on the INK4b-ARF-INK4a locus are indicated at the bottom.

To examine the effects of EZH2 down-regulation in aging HDFs, we determined RNA Pol II, EZH2 and BMI1 occupancy of the *INK4b-ARF-INK4a* locus by chromatin immunoprecipitations (ChIPs) monitored by qPCR. Cross-linked chromatin was prepared from neonatal HDF (light yellow bars), and adult cells (dark green bars). ChIPs with antibodies directed against RNA pol II revealed increased recruitment upon aging, in agreement with enhanced transcription (Figure 2E). Next, we established the pattern of binding of PcG silencers to the *INK4b-ARF-INK4a* locus in neonatal HDFs by ChIPs using antibodies directed against EZH2 and BMI1 (Figure 2F and G). We observed strong binding of EZH2 and BMI1 to

two well defined regions: the *p16*^{INK4a} promoter region (primer sets K and L) and an area ~3kb upstream of the INK4b promoter (primer sets C and D). The peaks of PcG binding are confined to ~0.8 kb areas. More detailed mapping of binding to the *INK4a* locus revealed a pattern similar to what we published earlier for MRT cells (data not shown, (14). Outside the two domains upstream of *INK4b* and *INK4a*, PcG protein binding across the *INK4b-ARF-INK4a* locus was low. Although only EZH2 was down-regulated in aging HDFs, both EZH2 and BMI1 occupancy at *INK4a* and *INK4b* was strongly reduced. Together, these results show that attenuation of EZH2 is accompanied by a loss of both PRC1 and PRC2-binding, recruitment of RNA Pol II and induction of *INK4a* and *INK4b*. Importantly, *ARF* expression remained unaffected and is not co-regulated with *INK4a* and *INK4b* in the human cells studied here. Our results suggest a critical role for EZH2 in the selective regulation of *INK4a* and *INK4b* expression.

EZH2 is required for coordinate silencing of *p15*^{INK4b} and *p16*^{INK4a}

To test whether EZH2 is critical for silencing of *INK4a* and *INK4b*, we used a shRNA strategy to attenuate its levels in neonatal HDFs. Cells were transduced with lentiviruses expressing either shRNAs targeting *EZH2* mRNA or a scrambled control. Three days following transduction, EZH2 levels were effectively knocked down in cells treated with the appropriate shRNA (Figure 3A). However, BMI1 levels remained unaffected. Loss of EZH2 caused a strong induction of p16^{INK4a} and p14^{INK4b}, but not of ARF (Figure 3B). Likewise, RNA Pol II was selectively recruited to the *INK4a* and *INK4b* loci, as revealed by ChIP-qPCR (figure 3C). Depletion of EZH2 not only caused dramatically reduced binding of itself, but also of BMI1 to *INK4a* and *INK4b* (Figure 3 D and E). Taken together, these results suggest that EZH2 attenuation is sufficient for dissociation of PcG silencers from the *INK4b* and *INK4a* loci, RNA Pol II recruitment and induction of p16^{INK4a} and p14^{INK4b}.

A repressive chromatin loop, linking *INK4a* and *INK4b*, is released during aging, cellular differentiation, and senescence

Because of their coordinate regulation by PcG silencers, we wondered whether *INK4a* and *INK4b* might be in close physical proximity, in spite of being separated by ~35 kb of intervening DNA. We used chromatin conformation capture (3C) technology in combination with qPCR (5, 33) to investigate the three-dimensional conformation of the human *INK4b-ARF-INK4a* locus, during aging, differentiation and senescence. We first compared the higher-order chromatin structure in neonatal versus adult HDFs (Figure 4A). Cells were cross-linked with formaldehyde, followed by chromatin isolation, and restriction digestion with EcoR1. Samples were ligated under conditions that favor the union of DNA fragments that are physically connected and qPCR across junctions was used to determine the relative cross-

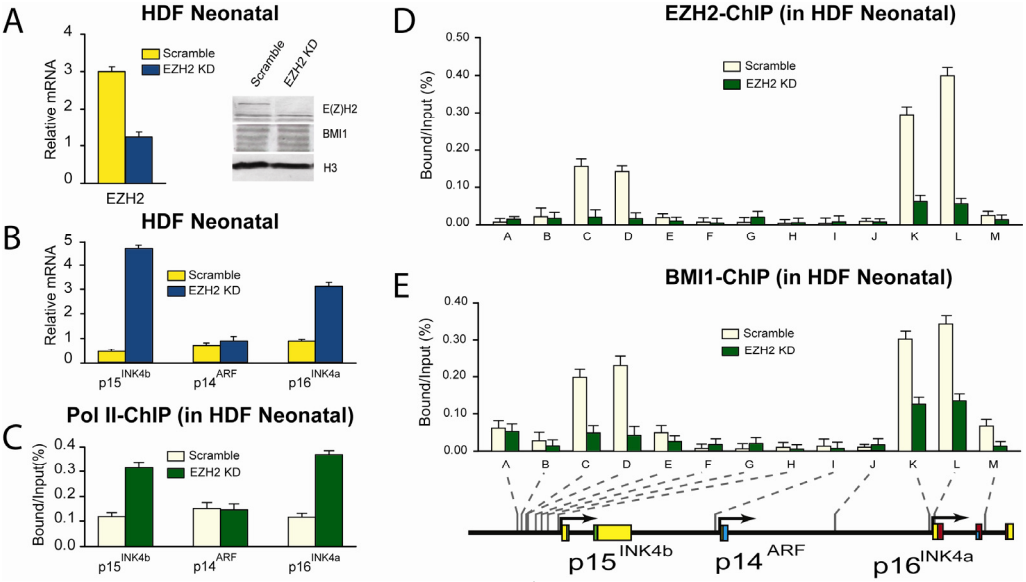

Figure 3. E(z)h2 is required for coordinate silencing of $p15^{INK4b}$ and $p16^{INK4a}$
(A) RT-qPCR analysis of gene expression and western blot analysis of the EZH2 protein levels in HDF-neonatal cell extracts prepared 3 days after EZH2 knock down using lentiviral transduction with viruses expressing shRNA targeting *EZH2* mRNA (Clone TRCN0000040073 and TRCN0000040075; Open Biosystems) As a control cells were trasnduced with scramble. Histone H3 serves as a loading control. (B) Loss of EZH2 causes transcriptional activation of $p15^{INK4b}$ and $p16^{INK4a}$. Relative expression levels of $p15^{INK4b}$, $p14^{ARF}$ and $p16^{INK4a}$ in these cells were determined by RT-qPCR of isolated mRNA, 72 hours following EZH2 knock down. The bar graphs represent the mean of three independent experiments, each analyzed in triplicate by RT-qPCR. (C) RNA pol II promoter binding was analyzed by ChIP-qPCR. Cross-linked chromatin was prepared from HDF-Neonatal control (light green bars), and HDF-neonatalEZH2 KD (dark green bars). All ChIP data presented in this study are the result of at least three independent experiments. (D-E) E(z)h2 depletion (KD) causes loss of PcG repressors on the INK4b and INK4a loci. ChIPs using antibodies directed against (D) EZH2 and (E) BMI1. Cross-linked chromatin was isolated from HDF neonatal cells transduced either with scramble (light green bars) or EZH2KD (dark green bars) lentiviral vectors. ChIPs were analyzed by qPCR using primer sets specific for the regions indicated by A-M along the *INK4b-ARF-INK4a* locus, revealing that PcG silencer binding peaks at the $p16^{INK4a}$ promoter and 3 kb upstream of $p15^{INK4b}$ and will be removed or reduced upon depletion of EZH2.Procedures were as described in the legend to Fig. 2.

linking frequency between restriction fragments. All 3C data presented here are the result of 3 fully independent biological replicate experiments. Cross-linking frequencies were determined of 10 suitable EcoRI fragments across almost 70 kb of DNA encompassing the *INK4b-ARF-INK4a* locus. The 'constant' primer and the TaqMan probe were designed in the EcoRI fragment -4 to -2 kb upstream of *INK4b*, harboring the PRC-binding sequences (Figure 4A). Plotting of the ligation frequencies to this "bait" fragment (grey bar) revealed a clear peak at fragment 9 corresponding to the *INK4a* promoter proximal region, overlapping the PRC-binding region. These experiments were complimented by 3C analysis using a "bait" fragment near the *INK4a* promoter. Now, we observed a peak at fragment 2, encompassing the PRC-binding domain upstream of the *INK4b* promoter (Figure 4B). We conclude that in neonatal HDFs, the repressed *INK4b-ARF-INK4a* locus has a looped structure. The loop is formed by interaction of the PRC-binding regions: one upstream of *INK4b* and the second formed by the *INK4a* promoter region. Within this higher-order chromatin structure, the almost 40 kb of

intervening DNA including the *ARF* promoter and first exon loops out. What structure is adopted by the *INK4b-ARF-INK4a* locus in adult HDFs, when both *INK4b* and *INK4a* are expressed? Strikingly, 3C-qPCR analysis in adult HDFs revealed a loss of long-range interaction between *INK4a* and *INK4b*, suggesting the locus adopted a linear conformation (Figure 4A-B). These results suggest that during aging, the repressive chromatin loop dissolves concomitant with EZH2 attenuation and increased transcription of *INK4a* and *INK4b*.

To study the effects of cellular differentiation, we undertook a similar 3C analysis of chromatin structure comparing undifferentiated with differentiating MEPs (Figure 4C and D). 3C-qPCR analysis revealed clear evidence for a chromatin loop between *INK4a* and *INK4b* in undifferentiated, proliferating MEPs. When these progenitor cells were induced to differentiate towards erythocytes, the silent chromatin loop dissolved, concomitant with *INK4a* and *INK4b* de-repression. Finally, we compared proliferating MON MRT cells, lacking hSNF5, with arrested cells after hSNF5 expression. As we have shown above (Figure 2D), in these cells EZH2 levels remain stable. Rather, PRCs are removed from INK4a and INK4b in a SWI/SNF-dependent manner, leading to comprehensive chromatin reprogramming (14). Following hSNF5 expression and PRC removal, the repressive chromatin loop is released and the *INK4b-ARF-INK4a* locus assumes a linear conformation (Figure 4E and F).

In summary, our results show that in young and progenitor cells the repressed *INK4b-ARF-INK4a* locus assumes a ~40 kb looped conformation. The chromatin loop links the PRC-binding regions of *INK4a* and *INK4b*, whilst excluding *ARF*. In aging or differentiating cells, the loop dissolves and expression of *INK4a* and *INK4b* is induced. The loss of looping is concomitant with loss of PRC-binding, which in aging HDFs and differentiating progenitor cells is caused by in down regulation of EZH2. Consequently, it is tempting to speculate that EZH2 is critical for loop formation. In MRT cells going into senescence, EZH2 levels remain stable, but the PRCs are removed from *INKa* and *INK4b* regulatory domains by SWI/SNF action. This duly leads to release of the repressive loop and gene activation, suggesting PRC-binding is required for looping.

EZH2 is required for chromatin looping

To test whether EZH2 is crucial for loop formation, we transduced neonatal HDFs with lentiviruses expressing either a shRNA targeting *EZH2* mRNA or a scrambled control. As shown above, depletion of EZH2 leads to a loss of PRC binding to *INK4a* and *INK4b* upstream regions (Figure 3). 3C-qPCR analysis revealed that loss of EZH2 also results in release of the repressive chromatin loop that links *INK4a* and *INK4b* (Figure 5A and B). In MRT cells, hSNF5 re-expression leads to SWI/SNF-mediated eviction of PRCs at *INK4a* and *INK4b*. This alternate mechanism of PRC removal also leads to loss of chromatin looping between *INK4a* and *INK4b* (Figure 4E and F). Nevertheless, in these cells looping is still EZH2-dependent. Depletion of EZH2 in the absence of hSNF5 expression, also led to loss of the repressive chromatin loop (Figure 5C and D). Taken together, these results support the notion that PRC binding is critical

for chromatin looping at the *INK4b-ARF-INK4a* locus. When PRC binding is lost, either due to diminished EZH2 levels in aging or differentiating cells or because of SWI/SNF action in MRT cells, the repressive chromatin loop is released, allowing up-regulation of *INK4a* and *INK4b*.

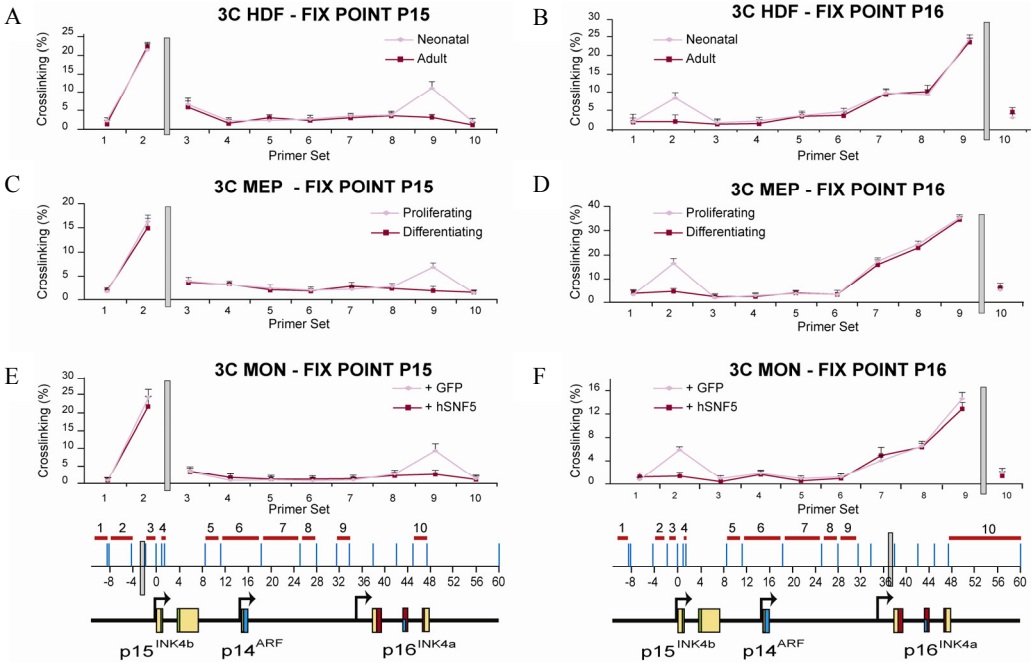

Figure 4. A repressive loop between p15INK4b & p16INK4b is resolved upon differentiation, aging or senescence
3C-qPCR analysis of long-distance interactions at the Human INK4-ARF locus. The relative level of each ligation product (fragments 1 to 10) has been plotted from position 21.932731 to 22.009.342 on chromosome 9 according to UCSC Genome Browser at http://genome.ucsc.edu/cgi-bin/hgTracks (see map below graphs). The 'constant' primer and the TaqMan probe were designed in the ECORI fragment (-4 to -2 kb upstream of INK4b or +36 kb to +37 kb downstream of INK4b) containing the polycomb binding region at INK4b and INK4a respectively (see Fig2.E-G). The locations of the constant fragment (gray segment) and candidate interacting fragments (red segments) are shown in the map. Restriction sites that will be used in the 3C assay are depicted as small vertical bars in red. The value of relative crosslinking frequency is plotted to y-axis and the locations of various EcoRI sites used for the 3C analysis are plotted on the X-axis. The data were normalized to ERCC3 for normalizing crosslinking frequency. Three independent assays were performed for each sample. 3C-qPCR assays were performed on (A-B) HDF-Neonatal (Light purple line) or HDF-Adult (dark purple line) , (C-D) MEP cells proliferative Light purple line)or differentiated cells Light purple line) and (E-F) MRT cells were collected 48 hours following transduction with lentiviruses expressing either GFP Light purple line) or hSNF5 Light purple line). Three independent assays were performed for each sample. *Error bars*, S.D. of three independent experiments.

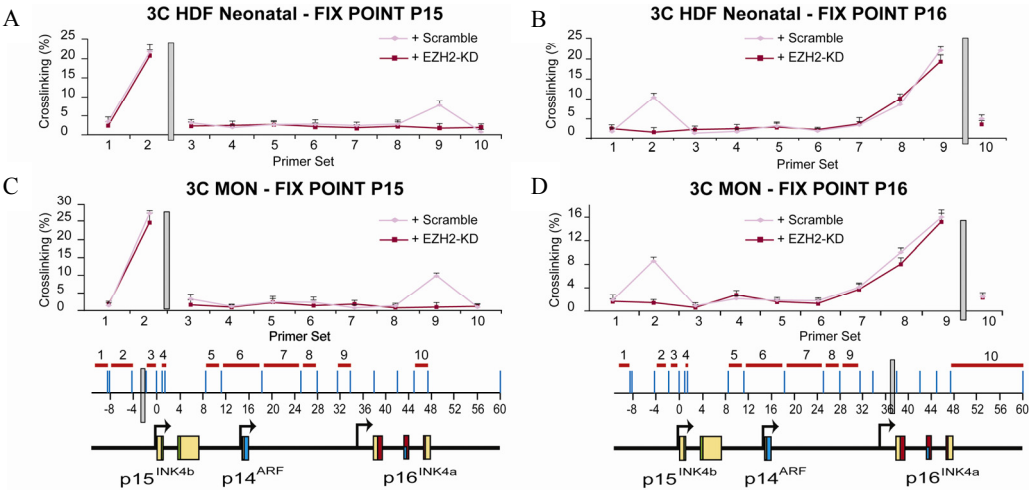

Figure 5. Looping between p15INK4b & p16INK4b is E(z)h2-dependent. 3C-qPCR assays were performed on (A-B) HDF-neonatal cells were collected 72 hours following transduction with lentiviruses expressing either scramble (light purple line) or shRNA targeting *EZH2* mRNA (dark purple line); and (C-D) MRT cells transduced with lentiviruses expressing either GFP (light purple line) or hSNF5 (dark purple line) and collected after 48 hours. Procedures were as described in the legend to Fig. 5.

DISCUSSION

Two classic problems in gene expression control are the mechanism of long range regulation and the regulation of multi-gene loci. Here, we studied how PcG silencers control the expression of the human *INK4b-ARF-INK4a* tumor suppressor locus during a variety of physiological processes. Our analysis led to the following conclusions: (1) During differentiation of human hematopoietic progenitor cells, in aging fibroblasts and following hSNF5-induced senescence of MRT cells, the *INK4b-ARF-INK4a* locus becomes differentially de-repressed. $p15^{INK4b}$ and $p16^{INK4a}$ are coordinately up-regulated, whereas $p14^{ARF}$ levels remain unaltered. (2) This is caused by a down-regulation of EZH2 in differentiating hematopoietic progenitor cells and aging fibroblasts, leading to loss of PRC-binding. (3) Our ChIP-qPCR analysis revealed non-homogeneous PRC binding to the *INK4b-ARF-INK4a* locus. EZH2 and BMI1 binding peaks at two well defined regions of ~800 bp: one overlapping the $p16^{INK4a}$ promoter region and the second area located ~3kb upstream of the $p15^{INK4b}$ promoter. (4) In MRT cells a different mechanism is operating. Re-expression of hSNF5 allows SWI/SNF to mediate PRC removal and loss of repression (14). (5) EZH2 is required for the formation of a ~40 kb chromatin loop linking *INK4b* and *INK4a*, but excluding *ARF*. Waning of EZH2 expression causes release of the repressive chromatin loop and up-regulation of $p15^{INK4b}$ and $p16^{INK4a}$. Thus, EZH2 levels determine the higher order chromatin structure and differential expression of the *INK4b-ARF-INK4a* locus, which in turn couples human progenitor cell differentiation to proliferation control. (6) Collectively, our findings support a looping

mechanism that couples *INK4b* and *INK4a* expression control, but are difficult to reconcile with models invoking continuous spreading of PcG silencers.

Our results and recent studies (3, 4, 7), emphasize a crucial role for EZH2 in orchestrating progenitor cell differentiation and proliferation control. Similar to our findings in human hematopoietic progenitor cells and aging fibroblast, Ezhkova et al (2009), observed de-repression of *INK4a* and *INK4b* due to EZH2 down-regulation, which controlled the balance between the proliferative basal layer of progenitor cells and non-proliferating differentiated epidermal cells. The importance of EZH2 levels in balancing progenitor cell proliferation and differentiation might have sinister consequences. EZH2 is over-expressed in a variety of tumors (32), thus potentially blocking the tumor suppression function of *INK4a* and *INK4b*. In these cells, EZH2 seems to promote de-differentiation and uncontrolled proliferation. This is the opposite of its function during normal development. Together with early studies in *Drosophila*, these observations emphasize the importance of PcG protein dosage and regulation. It is interesting to note that in MRT cells, EZH2 levels are not elevated. In these cells the SWI/SNF chromatin remodeler is crippled due to loss of hSNF5 and unable to evict PRCs from the *INK4b* and *INK4a* regulatory elements (14). Thus, loss of function of a trxG antagonist might have similar consequences as over-expression of a PcG silencer.

Previously, two studies promoted a continuous spreading of either heterochromatinization (10) or blanketing of the locus by PcG proteins (1). However, the data in the latter study actually revealed a clear peak of PRC binding at the *INK4a* promoter, which tapers off and is near background at the ARF gene. Based on the physiological processes studied here, we favor a discontinuous looping mechanism of *INK4b-ARF-INK4a* locus control over models invoking continuous spreading of silencers. Firstly, we observe two distinct peaks of PRC binding: ~3 kb upstream of *INK4b* and at the *INK4a* promoter. Outside these well defined areas PRC binding is near background levels, and we detected no significant PRC-binding at ARF. Secondly, during cell differentiation and aging, *INK4a* and *INK4b* are coordinately de-repressed through EZH2 attenuation, whereas ARF remained unaffected. Finally, the PRC-bound *INK4a* and *INK4b* regulatory regions are linked in nuclear space. Loss of PRC-binding causes a release of the chromatin loop and up-regulation of *INK4a* and *INK4b*. These findings for the *INK4b-ARF-INK4a* locus dove-tail well with other studies revealing PcG-mediated chromatin looping (19, 23, 34). We conclude that PcG proteins dynamically alter the higher order chromatin structure of the *INK4b-ARF-INK4a* locus to balance differentiation and proliferation of human cells.

EXPERIMENTAL PROCEDURES

Cell culture and lentiviral procedures

All tissue cultures were according to standard protocols. The human diploid embryonic fibroblast TIG3 were obtained from the Health Science Research Resource Bank (Osaka, Japan (http://cellbank.nibio.go.jp/celldata/jcrb0506.htm) and the Human diploid fibroblast Neonatal and Adult (purchased from Cascade Biologics) were grown in DMEM supplemented with 10% (v/v) FCS. The hSNF5 expressing lentiviral vector was generated by replacing the GFP encoding sequence of pRRLsin.sPPT.CMV.GFP.Wpre (8) with the hSNF5 cDNA (27). High titer vector stocks were produced in 293T cells by co-transfection of transfer vector constructs with the packaging constructs using standard transfection procedures (8). Mon cells were transduced with the appropriate vector. To knock down EZH2, the cells were transduced with lentiviruses expressing shRNA directed against *EZH2* (Clone TRCN0000040073 and TRCN0000040075; Expression Arrest™-The RNAi consortium (TRC) Human shRNA library purchased from Open Biosystems) for 3 days. In a control experiment, the cells were transduced with *scramble (non-targeting)* lentiviruses as described before.

Isolation of mononuclear cells from Human umbilical cord blood.

Human umbilical cord blood samples (UCB) were collected from umbilical cord vein after full-term delivery by the nursing staff of the department Obstetrics and Gynecology at the Sint Franciscus Hospital (Rotterdam, The Netherlands). Informed consent for taking the samples for clinical study was obtained. UCB was collected in sterile flasks containing 10 ml 1% heparin in H+H (Hanks + Hepes osmolarity 300), which had been stored at room temperature. Low-density cells were isolated from UCB by using Ficoll Hypaque density centrifugation (1.077g/cm^2, Lymphoprep, Nycomed Pharma, Oslo, Norway). The cell suspension were centrifuged at 600 g for 15 minutes, then mononuclear cell (MNC) band at the interface were removed, washed twice with Hanks Balanced Salt Solution (HBSS, Gibco, Breda, The Netherlands). The accumulated cells immediately used to CD34$^+$ isolation. The CD34$^+$ cells were isolated by indirect CD34$^+$ Microbead kit (Miltenyi Biotec). Isolated CD34+ cells had a purity of about 85-95%.
The CD34$^+$ cells were cultured in density of 1-3 x 10^4/ml in serum free medium. The medium was made of enriched DMEM which contains 1% (wt/vol) BSA, 0.3mg/L human transferrin, 0.1µmol/L sodium selenite, 1mg/L nucleosides (cytidine, adenosine, uridine, guanosine, 2'-deoxycytidine, 2'-deoxyaenosine, thymidine and 2'-deoxyguanosine, Sigma), 0.1mmol/L ß-mercaptoethanol, 15µmol/L linoleic acid and 15µmol /L cholesterol, 100 U/mL penicillin, and 100µg/mL streptomycin(24). The incubation condition was a humidified atmosphere of 10% CO2 and temperature of 37 °C. For stimulating cell expansion and proliferation, medium was supplemented with 100ng/ml stem cell factor (SCF), 100 ng/ml Flt3-L, and 20 ng/ml trombopoietin (TPO). The Cells have been kept in culture for 6 weeks and every week medium was refreshed.

Isolation of mononuclear cells from fetal liver.

Human fetal tissues were obtained from elective abortions of patients who had previously signed consent forms for research studies, under a protocol approved by the Medical Ethical Commissions of the Academic Medical Center of Amsterdam and the Erasmus University Medical Center of Rotterdam. Fetal livers of fetus from were sterilely dissected and teased into PBS containing 0.5 mg/ml collagenase Type IV (Sigma) using forceps and scissors. Cell suspensions were digested for 30 min at 37 °C with continuous stirring and were then filtered through a 70-μm nylon mesh. Briefly, fetal livers of 8-22 weeks of human embryos were resuspended in serum-free stem cell medium (StemSpan; Stem Cell Technologies, Vancouver, BC,Canada). For initial expansion, 5 $\times 10^6$ cells/mL were cultivated in serum-free medium (StemSpan; Stem Cell Technologies, Vancouver, BC, Canada) supplemented with Epo (2 U/mL Erypo Janssen- Cilag, Baar, Switzerland), the synthetic glucocorticoid Dex (1 μM; Sigma, St Louis, MO) SCF (100 ng/mL; R&D Systems, Minneapolis, MN), and lipids (40 ng /mL cholesterol-rich lipid mix; Sigma) for about 5 days, the cells were fed every day by partial medium changes. From day 5 on, a small population of expanding erythroid progenitors became visible in cytospins, around day 7 as an increasing population of large, non-adherent cells (~12 μm in diameter). The resulting proerythroblast culture was expanded by daily partial medium changes and addition of fresh factors, keeping cell density between 1.5–2 × 10 6 cells/ml. Proliferation kinetics and size distribution of the cell populations were monitored daily in an electronic cell counter (CASY-1, Schärfe-System, Reutlingen, Germany). To induce terminal differentiation, proliferating erythroblasts were washed in ice-cold PBS and reseeded at 1-1.5 x 10^6 cells/mL in StemSpan supplemented with Epo (0.5mg/ml human transferring Holo (1 mg/mL; SCIPAC Ltd, UK)(20). Differentiating erythroblasts were maintained at 2 to 3 x 10^6 cells/ml by daily cell counts and partial medium changes. We harvested the cells 48 hours after induction.

RNA purification and Real- time RT-PCR analysis

Total RNA was extracted from all cells using the SV Total RNA Isolation System (Promega). cDNA was synthesized from 1 □g of total RNA using random hexamers and Superscript™ II RNase H-Reverse Transcriptase (Invitrogen). Quantitative real-time PCR (MyIQ, Bio Rad) was performed using SYBR Green I. PCR primers were designed by Beacon designer (Premier Biosoft). The qPCR Core Kit (Invitrogen) was used with 400 nM of each primer under the following cycling conditions: 3 min. 95°C followed by 40 cycles of 10 seconds at 95°C and 45 seconds at 60°C. The *Gapdh* gene was used as an endogenous reference for normalization. Enrichment of specific DNA sequences was calculated using the comparative C_T method (21). PCR primer sequences are provided in Table 1.

Table1. Primers used for (A) ChIP, (B) mRNA expression, along the INK4-ARF locus

A: Primers used for ChIP (q PCR) along the INK4-ARF locus

Primer set	Location	Sequence
A	P15 ^{INK4b} (-3,982)	5′- AGTCCTAAGCCCAATACCTCAC
		5′- CTGCCTCTTCACATAGTCATCC
B	P15 ^{INK4b} (-3,575)	5′- ATCACGGAGCAATAAACCCAAC
		5′- CAAGAGAAACAGCGACCTAACC
C	P15 ^{INK4b} (-3,072)	5′- GGGTGGGCTGTTTCTGGAC
		5′- CCTCACGGGCAAGACCATC
D	P15 ^{INK4b} (-2,860)	5′- CCCACTATGTTCCCATCCACTTC
		5′- CCTCACGGGCAAGACCATC
E	P15 ^{INK4b} (-1,476)	5′- GACACATGCCACAGAGGAG
		5′- AGAAGACGAGAAGAGAAATCAAAC
F	P15 ^{INK4b} (-1,065)	5′- AGAAACTGAAGACTAGGAAATGGG
		5′- CTGGACAGGGAAGGGAACC
G	P15 ^{INK4b} (-1,065)	5′- ACTTGCGGTTCTCTTCCTATCC
		5′- TGTGGTGCTGGGCTTGTC
H	P15 ^{INK4b}-Pm	5′-GGCAGTGGTGAACATTCC
		5′-GCCCAAAGATGCTAGGAC
I	P14 ^{ARF}-Pm	5′-CGCCGTGTCCAGATGTCG
		5′-TGCTCTATCCGCCAATCAGG
J	P16 ^{INK4a} (-8.7 kb)	5′-ACTAGGCTTGTCCCACTTGC
		5′-TCAGTTCCTCTCTCCATTCTCC
K	P16 ^{INK4a} (-0.3 Kb)	5′-GGGCTCTCACAACTAGGAAAG
		5′-GGGTGTTTGGTGTCATAGGG
L	P16 ^{INK4a} (+85 bp)	5′-CCCCTTGCCTGGAAAGATAC
		5′-AGCCCCTCCTCTTTCTTCCT
M	P16 ^{INK4a} (+5.6 Kb)	5′- ACCAAGACTTCGCTGACC
		5′-CAAGGAGGACCATAATTCTACC

B: Primers used for mRNA expression (q PCR) of the INK4-ARF locus

P15 ^{INK4b}	5′- ATCACATGAGGTCAGGAGTTCG
	5′- CCAGGTTCAAGCGAGTCTCC
P14 ^{ARF}	5′- GGTTTTCGTGGTTCACATCC
	5′- CCTAGACGCTGGCTCCTC
P16 ^{INK4a}	5′-CCCCTTGCCTGGAAAGATAC
	5′-AGCCCCTCCTCTTTCTTCCT
GAPDH	5′- GCCAAAAGGGTCATCATCTC
	5′- GGTGCTAAGCAGTTGGTGGT

ChIP assays

ChIPs were performed as described by the Upstate protocol (http://www.upstate.com). Cross-linked chromatin was prepared from ~2x10^7 cells 48h following transduction with lentiviruses expressing either hSNF5 or GFP as a control for MRT cells or from HDF-Neonatal and adult. Cells were treated with 1% formaldehyde for 20 min at room temperature. Chromatin isolation, sonication yielding fragments of 300−600 bp and immunoprecipitations were performed according to protocol. All data presented are the result of at least 3 independent ChIP experiments. The following antibodies were used: BMI1 (Abcam; ab14389), EZH2 (Santa Cruz; Sc-25383), POL II (Santa Cruz; Sc-899). The abundance of specific DNA sequences in the immunoprecipitates was determined by qPCR and corrected for the independently determined amplification curves of each primer set. ChIP using species and isotype-matched immunoglobins directed against an unrelated protein (GST) were used to determine background levels analysed by qPCR as described above. Enrichment of specific DNA sequences was calculated using the comparative C_T method (21). PCR primer sequences are provided in Table 1. ChIP levels for each region are presented as percentage of input

chromatin. Statistical analysis of expression data and ChIP was performed using the R free software (http://www.r-project.org/).

Cell extracts and western blotting

Cell extracts were prepared in RIPA buffer (10 mM Tris-HCl, pH 7.5, 150 mM NaCl, 1% Nonidet P-40, 1% NaDOC, 0.1% SDS), assayed for protein concentration, 50 µg to 150 µg of extract was resolved by 6-20% (Bmi1), 6-8% (EZH2) and 6-12% SDS-PAGE, and transferred to 0.45 µm nitrocellulose membrane. We lysed 1 volume of committed progenitor cells directly in 1 volume of 2xLoading buffer (1xTris.Cl/SDS pH6.8, 20% glycerol, 4% SDS, O.2M DTT, 0.001% bromophenol blue) and resolved it by SDS-PAGE. The membranes were blocked for 1 hour in T-PBS with 5% milk and 0.1% Tween20 and incubated in primary- (overnight) and secondary (1 hour) antibody. Primary antibodies: SUZ12 (Abcam, ab12073), BMI1 (Abcam; ab14389), EZH2 (Santa Cruz; Sc-25383) and Histone H3 (Abcam; ab1791). Western blots were developed with the ECL detection kit (PIERCE) or visualized with the IRDye 680/800CW (LI-COR) and ODYSSEY Infrared Imaging System according to the supplier's instructions.

Chromatin Conformation Capture Assay

The 3C-qPCR assay was performed as described(11). We prepared nuclei from 10^7 MEPs, HDF (Neonatal- Adult) and Mon cells. Formaldehyde-fixed nuclei were digested with EcoRI overnight, followed by ligation with T4 DNA ligase at 16 °C for 4 h. Cross links were reversed and DNA was extensively purified. The PCR control template, primer efficiency and ligation efficiency were determined as described (11) by digesting and ligating a BAC clone, which encompassed the entire INK4-ARF locus. To correct for differences in quality and quantity of templates, ligation frequencies between the fragments were normalized to a fragment in the human *Ercc3* locus. Quantification of ligated products was performed by real-time qPCR with Taqman probe designed in the fragment that contains the polycomb binding region to INK4b and INK4a respectively (see Fig2.E-G). The primers and probes sequences are listed in table 2. The amplification conditions used in 3C assays are available on request. Crosslinking frequencies were calculated using the equation described previously (35) .

Table2. Primers used for 3C-qPCR analysis of (A) P15 ^{INK4b}, (B) P16 ^{INK4a} and (C) and ERCC3

A: Primers used for 3C-q PCR along the INK4-ARF locus, fixed fragment at P15^{INK4b}	
Constant primer	5'- CAGGTTGAGCAGGTTGGTTT
Probe	5'FAM- TCTAAAGCTTCACACTTGATCTTCCAAAGCCCCTT-3'BHQ^{R}
EcoRI Fragment number	**Forward primer Sequence**
1	5'- CCAACCTTAAACTACTGCTGAAAC
2	5'- GGAAGTCTGCCTATATGGGTTATC
3	5'- CTAAGGGGGTGGGGAGAC
4	5'- TGGTCATATTCAGTACTCACCTCA
5	5'- GTCCTGACTCCTACTCTGTTATCC
6	5'- CTGCCCAATACCTGTTCTCTTTC
7	5'- CCTTTCTTTCCTTAGGATGATGCC
8	5'- ATTATTCCTCCATTGCCTTTGCC
9	5'- GGAGACAGGACAGTATTTGAAGC
10	5'- GGGCAGCATTTGCTATCCTA
B: Primers used for 3C-q PCR along the INK4-ARF locus, fixed fragment at P16^{INK4a}	
Constant primer	5'- CTGCCCCTTTGCTATTTTGC
Probe	5'FAM- CCGAACTTCTGCGGAGCTGTCGTC-3'BHQ^{R}
EcoRI Fragment number	**Forward primer Sequence**
1	5'- GGCTCCCATCAACATATCTAACTC
2	5'- CAGGTTGAGCAGGTTGGTTT
3	5'- CTAAGGGGGTGGGGAGAC
4	5'- GAGACGGGATTCCTCAACCAC
5	5'- GTCCTGACTCCTACTCTGTTATCC
6	5'- CTGCCCAATACCTGTTCTCTTTC
7	5'- CCTTTCTTTCCTTAGGATGATGCC
8	5'- ATTATTCCTCCATTGCCTTTGCC
9	5'- AGTGGAGCCTACAGTAATCATTTG
10	5'- TCTTTGGCTTCTATTCCCTAGA
C: Primers used for 3C-q PCR along the ERCC3 locus	
Constant primer	5'- TCTTACCTGTTGGCCACTGACA
Probe	5'FAM- AGTTGTTCCTCCCAGGTCACATCCCAC-3'BHQ^{R}
Test primer	5'- GTCTGACCTTGCCCAGTGATAG

REFERENCES

1. **Bracken, A. P., D. Kleine-Kohlbrecher, N. Dietrich, D. Pasini, G. Gargiulo, C. Beekman, K. Theilgaard-Monch, S. Minucci, B. T. Porse, J.-C. Marine, K. H. Hansen, and K. Helin.** 2007. The Polycomb group proteins bind throughout the INK4A-ARF locus and are disassociated in senescent cells. Genes Dev **21:**525-530.
2. **Bruggeman, S., D. Hulsman, E. Tanger, B. Buckle T, M, , J. Zevenhoven, O. van Tellingen , and M. van Lohuizen.** 2007. Bmi1 controls tumor development in an Ink4a/Arf-independent manner in a mouse model for glioma. Cancer Cell **12:**328-41.
3. **Caretti, G., M. Di Padova, B. Micales, G. Lyons, and V. Sartorelli.** 2004. The Polycomb Ezh2 methyltransferase regulates muscle gene expression and skeletal muscle differentiation. Genes Dev **18:**2627-38.
4. **Chen, H., X. Gu, I. Su, R. Bottino, J. Contreras, A. Tarakhovsky, and S. Kim.** 2009. Polycomb protein Ezh2 regulates pancreatic beta-cell Ink4a/Arf expression and regeneration in diabetes mellitus. Genes Dev **23:**975-85.
5. **Dekker, J., K. Rippe, M. Dekker, and N. Kleckner.** 2002. Capturing Chromosome Conformation. Science **295:**1306-1311.
6. **Dietrich, N., A. P. Bracken, E. Trinh, C. K. Schjerling, H. Koseki, J. Rappsilber, K. Helin, and K. H. Hansen.** 2007. Bypass of senescence by the polycomb group protein CBX8 through direct binding to the INK4A-ARF locus. Embo J **26:**1637-1648.
7. **Ezhkova E, Pasolli HA, Parker JS, Stokes N, Su IH, Hannon G, Tarakhovsky A, and F. E.** 2009. Ezh2 Orchestrates Gene Expression for the Stepwise Differentiation of Tissue-Specific Stem Cells Cell **136:**1122-35.
8. **Follenzi, A., G. Sabatino, A. Lombardo, C. Boccaccio, and L. Naldini.** 2002. Efficient Gene Delivery and Targeted Expression to Hepatocytes In Vivo by Improved Lentiviral Vectors. Hum Gene Ther **13:**243-260.
9. **Gil, J., and G. Peters.** 2006. Regulation of the INK4b-ARF-INK4a tumour suppressor locus: all for one or one for all. Nat Rev Mol Cell Biol **7:**667-677.
10. **Gonzalez, S., P. Klatt, S. Delgado, E. Conde, F. Lopez-Rios, M. Sanchez-Cespedes, J. Mendez, F. Antequera, and M. Serrano.** 2006. Oncogenic activity of Cdc6 through repression of the INK4/ARF locus. Nature **440:**702-706.
11. **Hagege, H., P. Klous, C. Braem, E. Splinter, J. Dekker, G. Cathala, W. de Laat, and T. Forne.** 2007. Quantitative analysis of chromosome conformation capture assays (3C-qPCR). Nat. Protocols **2:**1722-1733.
12. **Jacobs, J. J. L., K. Kieboom, S. Marino, R. A. DePinho, and M. van Lohuizen.** 1999. The oncogene and Polycomb-group gene bmi-1 regulates cell proliferation and senescence through the ink4a locus. Nature **397:**164-168.
13. **Janzen, V., R. Forkert, H. E. Fleming, Y. Saito, M. T. Waring, D. M. Dombkowski, T. Cheng, R. A. DePinho, N. E. Sharpless, and D. T. Scadden.** 2006. Stem-cell ageing modified by the cyclin-dependent kinase inhibitor p16INK4a. Nature **443:**421-426.
14. **Kheradmand Kia, S., M. M. Gorski, S. Giannakopoulos, and C. P. Verrijzer.** 2008. SWI/SNF Mediates Polycomb Eviction and Epigenetic Reprogramming of the INK4b-ARF-INK4a Locus. MCB **28:**3457-3464.
15. **Kim, W. Y., and N. E. Sharpless.** 2006. The Regulation of INK4/ARF in Cancer and Aging Cell **127:**265-275.
16. **Kotake, Y., R. Cao, P. Viatour, J. Sage, Y. Zhang, and Y. Xiong.** 2007. pRB family proteins are required for H3K27 trimethylation and Polycomb repression complexes binding to and silencing p16INK4a tumor suppressor gene. Genes Dev **21:**49-54.
17. **Krishnamurthy, J., M. R. Ramsey, K. L. Ligon, C. Torrice, A. Koh, S. Bonner-Weir, and N. E. Sharpless.** 2006. p16INK4a induces an age-dependent decline in islet regenerative potential. Nature **443:**453-457.

18. **Lagarou, A., A. Mohd-Sarip, Y. M. Moshkin, G. E. Chalkley, K. Bezstarosti, J. Demmers, and C. P. Verrijzer.** 2008. dKDM2 couples histone H2A ubiquitylation to histone H3 demethylation during Polycomb group silencing. Genes Dev. **22:**2799-810.
19. **Lanzuolo, C., V. Roure, J. Dekker, F. Bantignies, and V. Orlando.** 2007. Polycomb response elements mediate the formation of chromosome higher-order structures in the bithorax complex. Nat Cell Biol **9:**1167-1174.
20. **Leberbauer, C., F. Boulme, G. Unfried, J. Huber, H. Beug, and E. W. Mullner.** 2005. Different steroids co-regulate long-term expansion versus terminal differentiation in primary human erythroid progenitors, p. 85-94, vol. 105.
21. **Livak, K. J., and T. D. Schmittgen.** 2001. Analysis of Relative Gene Expression Data Using Real-Time Quantitative PCR and the 2-[Delta][Delta]CT Method. Methods **25:**402-408.
22. **Lowe, S. W., and C. J. Sherr.** 2003. Tumor suppression by Ink4a-Arf: progress and puzzles. Current Opinion in Genetics & Development **13:**77-83.
23. **Mateos-Langerak, J., M. Bohn, W. de Leeuw, O. Giromus, E. M. M. Manders, P. J. Verschure, M. H. G. Indemans, H. J. Gierman, D. W. Heermann, R. van Driel, and S. Goetze.** 2009. Spatially confined folding of chromatin in the interphase nucleus, p. 3812-3817, vol. 106.
24. **Merchav, s., and G. Wagemaker.** 1984. Detection of murine bone marrow granulocyte/macrophage progenitor cells (GM-CFU) in serum-free cultures stimulated with purified M-CSF or GM-CSF. Int J Cell Cloning **2:**356-67.
25. **Molofsky, A. V., S. G. Slutsky, N. M. Joseph, S. He, R. Pardal, J. Krishnamurthy, N. E. Sharpless, and S. J. Morrison.** 2006. Increasing p16INK4a expression decreases forebrain progenitors and neurogenesis during ageing. Nature **443:**448-452.
26. **Müller, J., and P. Verrijzer.** 2009. Biochemical mechanisms of gene regulation by polycomb group protein complexes curr Opin Genet Dev **19:**150-8.
27. **Oruetxebarria, I., F. Venturini, T. Kekarainen, A. Houweling, L. M. Zuijderduijn, A. Mohd-Sarip, R. G. Vries, R. C. Hoeben, and C. P. Verrijzer.** 2004. P16INK4a is required for hSNF5 chromatin remodeler-induced cellular senescence in malignant rhabdoid tumor cells. J Biol Chem **279:**3807-16.
28. **Pasini D, Bracken AP, Hansen JB, Capillo M, and Helin K.** 2007. The polycomb group protein Suz12 is required for embryonic stem cell differentiation. Mol Cell Biol. **27:**3769-79.
29. **Pietersen, A., H. Horlings, M. Hauptmann, A. Langerod, A. Ajouaou, P. Cornelissen-Steijger, L. Wessels, J. Jonkers, M. Vijver, and M. van Lohuizen.** 2008. EZH2 and BMI1 inversely correlate with prognosis and TP53 mutation in breast cancer, p. R109, vol. 10.
30. **Pietersen, A. M., B. Evers, A. A. Prasad, E. Tanger, P. Cornelissen-Steijger, J. Jonkers, and M. van Lohuizen.** 2008. Bmi1 regulates stem cells and proliferation and differentiation of committed cells in mammary epithelium. Curr Biol **18:**1094-9.
31. **Pietersen, A. M., and M. van Lohuizen.** 2008. Stem cell regulation by polycomb repressors: postponing commitment. Curr Opin Cell Biol. **20:**201-7.
32. **Simon, J., and C. Lange.** 2008. Roles of the EZH2 histone methyltransferase in cancer epigenetics. Mutat Res. **647:**21-9.
33. **Simonis, M., J. Kooren, and W. de Laat.** 2007. An evaluation of 3C-based methods to capture DNA interactions. Nat methods **4:**895-901.
34. **Tiwari, V. K., K. M. McGarvey, J. D. F. Licchesi, J. E. Ohm, J. G. Herman, Sch, uuml, D. beler, and S. B. Baylin.** 2008. PcG Proteins, DNA Methylation, and Gene Repression by Chromatin Looping, p. e306, vol. 6.
35. **Tolhuis, B., R. Palstra, E. Splinter, F. Grosveld, and W. de Laat.** 2002. Looping and interaction between hypersensitive sites in the active beta-globin locus. Mol Cell **10:**1453-65.

Chapter6

Discussion and Future Prospects

Discussion and Future Prospect

Chromatin is a dynamic structure that modulates the access of regulatory factors to the genetic material of eukaryotes. The regulated alteration of chromatin structure, termed remodelling, can be accomplished by covalent modification of histones or by the action of ATP-dependent remodeling complexes. Remodelers are DNA-translocating motors that utilize the energy of ATP to disrupt histone-DNA contacts(14, 33, 44, 45, 62, 66, 67).

The multi-subunit SWI/SNF ATP-dependent chromatin remodelling complexes are highly conserved molecular motors that play crucial roles in diverse cellular processes, including expression and duplication of the genome. Human SNF5/INI1 is a universal SWI/SNF subunit and tumour-suppressor, lost in malignant rhabdoid tumours (MRTs), rare but highly aggressive paediatric cancers(3, 48, 49, 59).

Previously our group found that re-expression of hSNF5 in MRT cells caused an accumulation in G0/G1, cellular senescence and apoptosis. Cellular senescence is largely the result of direct transcriptional activation of the tumour-suppressor $p16^{INK4a}$ by hSNF5(41). hSNF5 acts as a transcriptional co-activator, which is required for the recruitment of the BRG1 containing SWI/SNF chromatin remodeling complex to the $p16^{INK4a}$ promoter. The increased $p16^{INK4a}$ levels result in inhibition of the cyclin D1-CDK4 complex, thus retaining pRb in its hypophosphorylated antiproliferative state (41). Loss of hSNF5 function in MRT cells promotes chromosomal instability as a result of compromised mitosis (61). Because cancers resulting from loss of hSNF5 are so extremely aggressive, insight in the pathways involved are critical to understanding these and might be relevant to understanding other forms of cancer.

In chapter 2, we performed genome-wide gene expression profiling to address the role of hSNF5 in tumorigenesis. We anticipate that this investigation will help us to gain insight into the corruption of cellular pathways resulting from loss of hSNF5 tumour suppressor in MRTs. Our genome wide expression analysis suggests that hSNF5 can function in both transcription activation and repression of the genome. Whole genome expression profiling of hSNF5 cells revealed expression change of many E2F targets, including mitotic control genes and pre-replication complex. This study identified hSNF5/INI1 target genes and provided evidence that hSNF5/INI1 may modulate cell cycle control through the regulation of the p16 INK4A-cyclinD/CDK4-pRb-E2F pathway. We have shown that the majority of the up-regulated genes encoded proteins with functions in extracellular matrix remodelling, adhesion or cell migration (*SERPINE2, ITGB5, MAP1B*), apoptosis (*DR6,FAS, CASP4, GAS6, ADAM19*), and cancer related pathway or other specialized functions (*CDKN2A, ETS2* and *TRIM22*).Those genes did not change or were down-regulated upon induction of mutant SNF5. shRNA knock down analysis of candidate effectors coupled with Chromatin immunoprecipitation studies (as we have done for ETS2, MAD2L1, TRIM22 and CDKN2A) will be done to determine the direct targets of SNF5 and to address the role of hSNF5 in tumourigenesis.

In Chapter 3 we report that cancer associated S284L substitution in hSNF5 causes polyploidy and aneuploidy due to failure in interaction between mitotic spindles and kinetochores, resulting in abrogation of chromosome segregation. In contrast re-expression of

wild type hSNF5 promotes accurate chromosome segregation and tightening of the mitotic check point. These observations suggest a critical function for hSNF5 in mitosis. This study once more draws attention to the fact that tetraploidization precedes aneuploidization(15, 54). Indeed tetraploid cells have a greater chance of aberrant cellular division than diploid cells. We have seen a distinct cleavage failure or untimely exit from mitosis. As well, abnormal mitotic spindle pole formation in cancer associated hSNF5 mutation results in tetraploid cells and doubled centrosome number. The relationship between centrosome aberration and aneuploidy and their function during cell cycle progression has been reviewed by many groups(4, 39) (53). Whole genome expression profiling showed that MAD2 and E2F1, which have been implicated in mitotic defects leading to aneuploidy(21), are both down-regulated following hSNF5 induction. These results suggested that misexpression of mitotic checkpoint components might cause the abnormal ploidy of MRT cells.

The SWI SNF related yeast RSC complex, containing the hSNF5 orthologue SNR1, has been implicated in kinetochore function, cohesion loading onto chromosomal arms, and 2 micron episome segregation (1, 22-24, 64). As hSWI/SNF5 colocalizes with kinetochore proteins, hSNF5 may be involved in establishment of a specialized centromeric chromatin structure or in the control of sister chromatid cohesion and segregation(65).

Using conditional siRNA approaches, we extended our analysis to non- MRT cells and again observed polyploidization due to the loss of hSNF5. We therefore propose that the mitotic functions of hSNF5 are general and not cell-type specific.

Inactivation of ATP- dependent chromatin remodeling factors has been implicated in the development of distinct types of tumors (29, 30, 43). In this chapter we describe a novel role for hSNF5 in maintenance of chromosomal stability. We propose that inactivation of hSNF5 promotes tumourigenesis through at least two distinct mechanisms: the previously described, compromised transcriptional activation of $p16^{Ink4a}$ mediated proliferation control(41), and defective mitosis resulting in polyploidization and numerical chromosome instability.

The aim of chapter 4 was to identify the mechanism of hSNF5-dependent transcriptional control of the INK4b-ARF-INK4a locus in MRT cells. The INK4b-ARF-INK4a locus is implicated in various types of cancer and encodes three distinct proteins, $p15^{INK4b}$, $p14^{ARF}$ and $p16^{INK4a}$ (reviewed in (19, 51)). The Ink4a-Arf locus responds to stress signals, limiting cell proliferation and modulating apoptosis (reviewed in (34)). hSNF5 acts as a transcriptional co-activator, which is required for the recruitment of the BRG1 containing SWI/SNF chromatin remodelling complex to the and $p16^{INK4a}$ promoter but not $p14^{ARF}$. Our results suggest that, at least in these MRT cells, hSNF5 is critical for the recruitment of the SWI/SNF complex to the activated $p16^{INK4a}$ promoter as well as the $p15^{INK4b}$ promoter.

It is still of interest to identify the other DNA binding regulators that activate $p16^{INK4a}$ through association with the hSNF5 chromatin-remodelling factor. The SWI/SNF complexes lack sequence specific DNA binding, and are therefore thought to be recruited to specific promoters via interactions with DNA binding proteins. ETS2 is a transcriptional activator of $p16^{INK4a}$ which has been shown to bind to the $p16^{INK4a}$ promoter(40). ChIP data revealed that

ETS2 and SNF5 are co-recruited to the P16 promoter in MRT cells (Figure1). shRNA knock down analysis of ETS2, and studies of $p16^{INK4a}$ activation upon induction of hSNF5 will be useful to address the co-recruitment of hSNF5 and ETS2 to $p16^{INK4a}$ promoter and examine role of ETS2 and hSNF5 in activation of $p16^{INK4a}$.

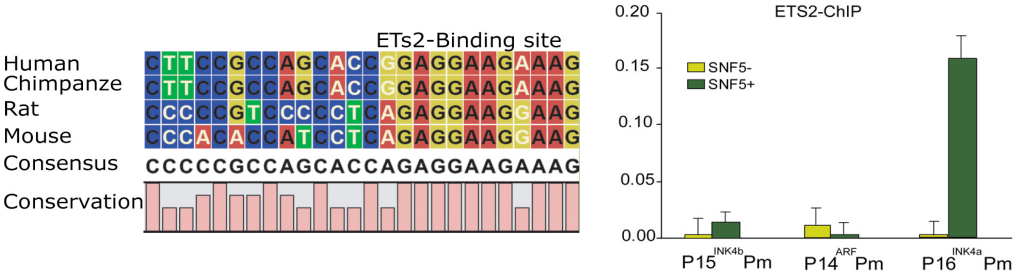

Figure1. hSNF5 and ETS2 are co-recruited to the p16INK4a Promoter.
(A) Conservation of ETS2 binding site at p16INK4a promoter during evolution **(B)** ETS2 binding to the p16INK4a promoter is hSNF5-dependent, as revealed by ChIP-qPCR using antibodies directed against ETS2. ChIPs using antibodies directed against ETS2. Cross-linked chromatin was prepared from MRT cells lacking hSNF5, but expressing GFP (light green bars), or cells expressing hSNF5 (dark green bars).

Previously, a number of reports have demonstrated a role for Polycomb silencers, including PRC1 and PRC2 upstream of $p15^{INK4b}$, $p14^{ARF}$ and $p16^{INK4a}$ (6, 10, 18, 25) . Therefore, it appears that SWI/SNF and PcG proteins act antagonistically on this locus. However, while PcG proteins suppress the INK4a/ARF locus, hSNF5 selectively activates $p15^{INK4b}$ and $p16^{INK4a}$. Our results now clearly establish that PRC1 and PRC2 mainly act upstream of $p16^{INK4a}$ and specifically localize within a region spanning approximately 800 bp, even though H3K27 trimethylation covers a larger domain. Interestingly, restoration of SWI/SNF in MRT cells causes removal of Polycomb silencers (PRC1 and PRC2) from the $p16^{INK4a}$ promoter. This is not consistent with a model in which PRC1 blocks SWI/SNF mediated chromatin remodeling as has been previously reported from experiments conducted in vitro (50). Instead, our data suggest that silencing by PcG complexes is a less rigid more dynamic process subject to removal in response to SWI/SNF expression.

We found that concomitant with the decrease in H3-K27me3, the active H3-K4me3 mark is strongly induced at $p16^{INK4a}$ and $p15^{INK4b}$. The prominent H3-K4me3 methyltransferase MLL1 is the human homologue of *Drosophila* trx, the founding member of the trxG (7). ChIPs revealed that hSNF5 expression triggers MLL1 binding to the INK4b and INK4a loci. Because *MLL1* translocations are associated with highly aggressive lymphoid and myeloid infant leukemia (7), it will be of interest to investigate whether the oncogenic MLL1 fusion proteins are defective in $p16^{INK4a}$ activation. Collectively, our results show that during hSNF5-mediated $p16^{INK4a}$ activation, the trxG activators SWI/SNF and MLL1 replace the PcG silencers PRC1 and PRC2. We conclude that the antagonism between PcG and trxG proteins is not limited to fly development but also operates in human cancer cells.

Notably these findings and our latest finding suggest that, at least in MRT cells and neonatal fibroblast the mechanisms that control the activation or suppression of the INK4b-

ARF-INK4a locus are not the same for all three genes within the locus. As we have shown in chapter 4 and 5, *p16*^{INK4a} and *p15*^{INK4b} are both induced upon induction of hSNF5 or during aging and differentiation, while *p14*^{Arf} remains unchanged. This contrasts existing models in which the control of all genes within this locus is proposed to occur through a region 1 kb upstream of p15 termed regulatory domain (RD)(20).

Hypermethylation of CpG island sequences are a nearly universal somatic genome alteration in cancer. DNA methylation, occurring on cytosine bases in CpG dinucleotides, is an important epigenetic mechanism of gene regulation in eukaryotic cells. The CpG island of the p16 ^{INK4a} promoter is hypermethylated in various cancers (38). Alterations of SWI/SNF remodeling complex activity in various mammalian cells and organs have been implicated in transcriptional silencing through site-specific genomic methylation(2, 12, 17). Our results demonstrate that hSNF5, a core subunit of SWI/SNF induces demethylation of p16^{INK4a} to promote transcriptional activation.

DNMT3b is involved in de-novo methylation during development. Our data also reveals that induction of hSNF5 causes removal of DNMT3b from the p16 ^{INK4a} promoter, an observation, which may explain alterations of methylation in this region. Higher expression of DNMT3b has been demonstrated in human oesophageal squamous cell carcinoma, which is correlated with low expression of p16 ^{INK4a} (52). Disruption of DNMT1 and DNMT3b resulted in demethylation of the p16 ^{INK4a} in other human cancer cells (42). DNMT3b has also been shown to interact with hSNF2H (ISWI), another ATP-dependent chromatin-remodelling enzyme(16).

EZH2 has been shown to serve as a recruitment platform for DNA methyltransferases(60) Our results demonstrate that re-expression of hSNF5 in MRT cells results in not only removal of Polycomb silencers (PRC1 and PRC2) but also of DNA methyltransferases from the p16^{INK4a} promoter. This is in agreement with two recently published observations which claimed that aberrant silencing in cancer cells is caused by de novo meyhylation of the Polycomb-marked genes by DNA methyltransferases (46, 63).

The main conclusion from our work is a model for reactivation of the p16^{INK4a} –Rb pathway by the SWI/SNF complex in MRT cells, which emphasizes the close interconnectivity of epigenetic pathways; i.e. polycomb silencing, histone methylation, DNA methylation and ATP-dependent chromatin remodeling.

In chapter5 we have tried to delineate the mechanism behind INK4/ARF transcription during differentiation, aging and cancer. In order to answer this question we analyzed the spatial organization of the INK4/ARF locus *in vitro* to detect the frequency of possible interactions between these genomic loci by 3C (Capturing Chromosome Conformation) technology(11). 3C analysis revealed that at least in Mon cells, Neonatal fibroblasts and Megakaryocyte-Erythrocyte progenitor cells, there is a physical and spatial interaction between p15^{INK4b} and p16^{INK4a} but not p14^{ARF}. Importantly, p15^{INK4b} loses its physical interaction with p16^{INK4a} upon induction of hSNF5, upon aging, as well as differentiation. We examined whether PcG complexes mediate this long-range gene silencing.

Mammalian Polycomb group (PcG) proteins are essential transcription silencers that control multiple developmental processes, including stem cell self-renewal and differentiation, and have been implicated in several types of cancers (5, 32, 35, 58). However, it is not clear how PcG proteins and specifically those bound to downstream regions exert their repression over target genes. Long-range chromatin interactions by chromatin looping are thought to be one of the potential mechanisms to explain PcG action over broad distances in *cis* (8, 9, 26, 47). The first direct evidence comes from work in *Drosophila* showing that all major PcG-bound elements at the BX-C multi-gene locus—including PREs and core promoters—physically associate by chromatin long-range interactions in the repressed state (31). Recently it has been shown that the PcGs and histone marks help to silence target genes via the looping process in human cells (56, 57). Previously we showed that restoration of SWI/SNF causes removal of Polycomb silencers from the $p16^{INK4a}$ locus(27). Further we showed that PcGs also bind to 3 kb upstream of $p15^{INK4b}$ in the repressed state and are removed upon induction of hSNF5 during aging and differentiation. Notably, we showed that YY1 and PcG silencers concomitantly bind to the Ink4a/b locus. Strikingly, induction of hSNF5 leads to the removal of YY1 and PcG proteins (Fig2). YY1 is the human homolog of Drosophila Pleiohomeotic (PHO) - a key sequence specific DNA binding recruiter of PcG complex.

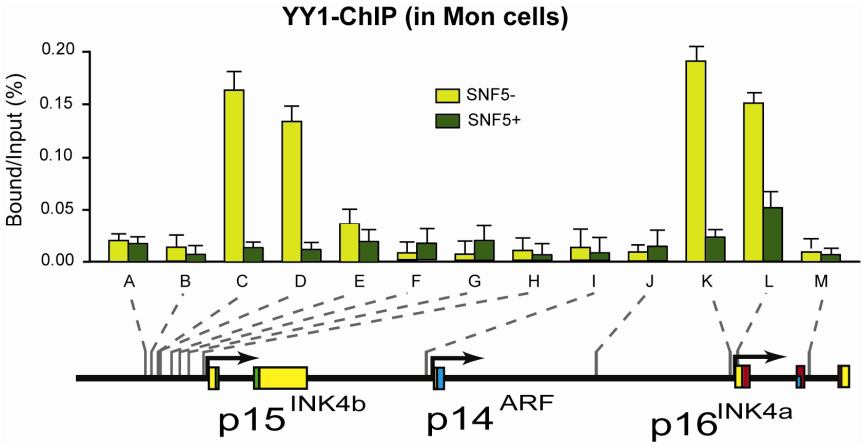

Figure2. Restoration of SWI/SNF Causes Removal of YY1 from $p15^{INK4b}$ and $p16^{INK4a}$ Promoters.
Restoration of SWI/SNF Causes Removal of YY1 from INK4a/b locus. ChIPs using antibodies directed against YY1. Cross-linked chromatin was prepared from MRT cells lacking hSNF5, but expressing GFP (light green bars), or cells expressing hSNF5 (dark green bars). ChIPs were analyzed by qPCR using primer sets specific for the regions indicated by A-M along the *INK4b-ARF-INK4a* locus, revealing that YY1 binding peaks at the $p16^{INK4a}$ promoter and 3 kb upstream of $p15^{INK4b}$. Upon induction of hSNF5 YY1 is removed or strongly reduced. QPCR primer sets correspond to the upstream of $p15^{INK4b}$ promoter (A-H), the $p14^{ARF}$ promoter (I), an intergenic control region (J), and various regions of the $p16^{INK4a}$ locus (sets K-M). Primer sets K and L cover the $p16^{INK4a}$ promoter. The positions of the amplified regions on the INK4b-ARF-INK4a locus are indicated at the bottom.

To test if PcG proteins can silence the locus through the looping process, we applied RNA interference to deplete Ezh2, the catalytic component of the Polycomb repressive complex2

(PRC2) in Mon cells and Neonatal fibroblasts. We found that the loop resolved and transcription was activated in response to Ezh2 depletion. Our data provide strong evidence that PcGs play a role in generating the repressive loop at the INK4/ARF locus. In conclusion, we found that coordinate induction of $p15^{INK4b}$ and $p16^{INK4a}$ but not $p14^{ARF}$ during differentiation or aging is accompanied by down-regulation of EZH2 and reduced locus occupancy of PcG repressors. EZH2 is required for coordinate silencing of $p15^{INK4b}$ and $p16^{INK4a}$. EZH2 depletion (KD) causes loss of PcG repressors on the INK4b and INK4a loci and resolution of the repressive loop. Therefore looping between $p15^{INK4b}$ and $p16^{INK4a}$ is EZH2-dependent. It has been shown that depletion of EZH2 subunit of PRC2 in response to stress causes the loss of H3K27me3, displacement of BMI1 subunit of the Polycomb-Repressive Complex1 (PRC1) and transcription activation of INK4a (6). In agreement with this we showed that depletion of EZH2 during aging and differentiation causes displacement of BMI1 and activation of Ink4a and Ink4b (this thesis).

It is well established that the *Ink4/Arf* locus is activated during organismal aging in both rodents and humans, and the levels of $p16^{Ink4a}$ constitute an impressively good overall biomarker of aging (28). It has been shown that $p16^{Ink4a}$ both serves as a brake for the proliferation of cancer cells, and also limits the long-term renewal of stem cells (Reviewed in (13)). EZH2 is accumulated in the undifferentiated progenitor cell population such as hematopoietic cells (55). In agreement, we showed that depletion of EZH2 during aging and differentiation results in resolution of the repressive loop in MEP, HDF and MRT cells and thus regulates the expression of $p16^{Ink4a}$.

Finally, the PRC-bound *INK4a* and *INK4b* regulatory regions are linked in nuclear space. Loss of PRC-binding causes a release of the chromatin loop and up-regulation of *INK4a* and *INK4b*. These findings for the *INK4b-ARF-INK4a* locus dove-tail well with other studies revealing PcG-mediated chromatin looping (31, 36, 37). We conclude that PcG proteins dynamically alter the higher order chromatin structure of the *INK4b-ARF-INK4a* locus to balance differentiation and proliferation of human cells.

References

1. **Baetz, K. K., N. J. Krogan, A. Emili, J. Greenblatt, and P. Hieter.** 2004. The ctf13-30/CTF13 genomic haploinsufficiency modifier screen identifies the yeast chromatin remodeling complex RSC, which is required for the establishment of sister chromatid cohesion. Mol Cell Biol **24:**1232-44.
2. **Banine, F., C. Bartlett, R. Gunawardena, C. Muchardt, M. Yaniv, E. S. Knudsen, B. E. Weissman, and L. S. Sherman.** 2005. SWI/SNF Chromatin-Remodeling Factors Induce Changes in DNA Methylation to Promote Transcriptional Activation, p. 3542-3547, vol. 65.
3. **Biegel, J. A., J. Y. Zhou, L. B. Rorke, C. Stenstrom, L. M. Wainwright, and B. Fogelgren.** 1999. Germ-line and acquired mutations of INI1 in atypical teratoid and rhabdoid tumors. Cancer Res **59:**74-9.
4. **Borel, F., O. D. Lohez, F. o. B. Lacroix, and R. L. Margolis.** 2002. Multiple centrosomes arise from tetraploidy checkpoint failure and mitotic centrosome clusters in p53 and RB pocket protein-compromised cells, p. 9819-9824, vol. 99.
5. **Boyer, L. A., K. Plath, J. Zeitlinger, T. Brambrink, L. A. Medeiros, T. I. Lee, S. S. Levine, M. Wernig, A. Tajonar, M. K. Ray, G. W. Bell, A. P. Otte, M. Vidal, D. K. Gifford, R. A. Young, and R. Jaenisch.** 2006. Polycomb complexes repress developmental regulators in murine embryonic stem cells. Nature **441:**349-353.
6. **Bracken, A. P., D. Kleine-Kohlbrecher, N. Dietrich, D. Pasini, G. Gargiulo, C. Beekman, K. Theilgaard-Monch, S. Minucci, B. T. Porse, J.-C. Marine, K. H. Hansen, and K. Helin.** 2007. The Polycomb group proteins bind throughout the INK4A-ARF locus and are disassociated in senescent cells. Genes Dev **21:**525-530.
7. **Canaani, and N. T. E, Rozovskaia T, Smith ST, Mori T, Croce CM, Mazo A.** 2004. ALL-1/MLL1, a homologue of Drosophila TRITHORAX, modifies chromatin and is directly involved in infant acute leukaemia. Br J Cancer **90:**Br J Cancer. 2004 Feb 23;90(4):756-60.
8. **Cleard, F., Y. Moshkin, F. Karch, and R. K. Maeda.** 2006. Probing long-distance regulatory interactions in the Drosophila melanogaster bithorax complex using Dam identification. Nat Genet **38:**931-935.
9. **Comet, I., E. Savitskaya, B. Schuettengruber, N. Nègre, S. Lavrov, A. Parshikov, F. Juge, E. Gracheva, P. Georgiev, and G. Cavalli.** 2006. PRE-Mediated Bypass of Two Su(Hw) Insulators Targets PcG Proteins to a Downstream Promoter. **11:**117-124.
10. **Core N, J. F., Boned A, Djabali M. .** 2004. Disruption of E2F signaling suppresses the INK4a-induced proliferative defect in M33-deficient mice. Oncogene. **23:**7660-7668.
11. **Dekker, J., K. Rippe, M. Dekker, and N. Kleckner.** 2002. Capturing Chromosome Conformation. Science **295:**1306-1311.
12. **Dennis, K., T. Fan, T. Geiman, Q. Yan, and K. Muegge.** 2001. Lsh, a member of the SNF2 family, is required for genome-wide methylation, p. 2940-2944, vol. 15.
13. **Finkel, T., M. Serrano, and M. A. Blasco.** 2007. The common biology of cancer and ageing. Nature **448:**767-774.
14. **Fyodorov, D. V., and J. T. Kadonaga.** 2002. Dynamics of ATP-dependent chromatin assembly by ACF. Nature **418:**897-900.
15. **Ganem, N. J., Z. Storchova, and D. Pellman.** 2007. Tetraploidy, aneuploidy and cancer. Current Opinion in Genetics & Development **17:**157-162.

16. **Geiman, T. M., U. T. Sankpal, A. K. Robertson, Y. Zhao, Y. Zhao, and K. D. Robertson.** 2004. DNMT3B interacts with hSNF2H chromatin remodeling enzyme, HDACs 1 and 2, and components of the histone methylation system. Biochemical and Biophysical Research Communications **318:**544-555.
17. **Gibbons, R. J., T. L. McDowell, S. Raman, D. M. O'Rourke, D. Garrick, H. Ayyub, and D. R. Higgs.** 2000. Mutations in ATRX, encoding a SWI/SNF-like protein, cause diverse changes in the pattern of DNA methylation. Nat Genet **24:**368-371.
18. **Gil, J., D. Bernard, D. Martinez, and D. Beach.** 2004. Polycomb CBX7 has a unifying role in cellular lifespan. Nat Cell Biol **6:**67-72.
19. **Gil, J., and G. Peters.** 2006. Regulation of the INK4b-ARF-INK4a tumour suppressor locus: all for one or one for all. Nat Rev Mol Cell Biol **7:**667-677.
20. **Gonzalez, S., P. Klatt, S. Delgado, E. Conde, F. Lopez-Rios, M. Sanchez-Cespedes, J. Mendez, F. Antequera, and M. Serrano.** 2006. Oncogenic activity of Cdc6 through repression of the INK4/ARF locus. Nature **440:**702-706.
21. **Hernando, E., Z. Nahle, G. Juan, E. Diaz-Rodriguez, M. Alaminos, M. Hemann, L. Michel, V. Mittal, W. Gerald, R. Benezra, S. W. Lowe, and C. Cordon-Cardo.** 2004. Rb inactivation promotes genomic instability by uncoupling cell cycle progression from mitotic control. Nature **430:**797-802.
22. **Hsu, J. M., J. Huang, P. B. Meluh, and B. C. Laurent.** 2003. The yeast RSC chromatin-remodeling complex is required for kinetochore function in chromosome segregation. Mol Cell Biol **23:**3202-15.
23. **Huang, J., J. M. Hsu, and B. C. Laurent.** 2004. The RSC nucleosome-remodeling complex is required for Cohesin's association with chromosome arms. Mol Cell **13:**739-50.
24. **Huang, J., and B. C. Laurent.** 2004. A Role for the RSC chromatin remodeler in regulating cohesion of sister chromatid arms. Cell Cycle **3:**973-5.
25. **Jacobs, J. J. L., K. Kieboom, S. Marino, R. A. DePinho, and M. van Lohuizen.** 1999. The oncogene and Polycomb-group gene bmi-1 regulates cell proliferation and senescence through the ink4a locus. Nature **397:**164-168.
26. **Kadaukea, S. a. B., G. A.** 2009. Chromatin loops in gene regulation Biochimica et Biophysica Acta (BBA) - Gene Regulatory Mechanisms **1789:**17-25.
27. **Kheradmand Kia, S., Gorski, M.M., Giannakopoulos, S., Verrijzer, C.P.** 2008. SWI/SNF Mediates Polycomb Eviction and Epigenetic Reprogramming of the INK4b-ARF-INK4a Locus. MCB **28:**3457-3464.
28. **Kim, W. Y., and N. E. Sharpless.** 2006. The Regulation of INK4/ARF in Cancer and Aging. **127:**265-275.
29. **Klochendler-Yeivin, A., C. Muchardt, and M. Yaniv.** 2002. SWI/SNF chromatin remodeling and cancer. Curr Opin Genet Dev **12:**73-9.
30. **Ko, M., D. H. Sohn, H. Chung, and R. H. Seong.** 2008. Chromatin remodeling, development and disease. Mutat res. **647:**59-67.
31. **Lanzuolo, C., V. Roure, J. Dekker, F. Bantignies, and V. Orlando.** 2007. Polycomb response elements mediate the formation of chromosome higher-order structures in the bithorax complex. Nat Cell Biol **9:**1167-1174.
32. **Lee, T. I., R. G. Jenner, L. A. Boyer, M. G. Guenther, S. S. Levine, R. M. Kumar, B. Chevalier, S. E. Johnstone, M. F. Cole, K.-i. Isono, H. Koseki, T. Fuchikami, K. Abe, H. L. Murray, J. P. Zucker, B. Yuan, G. W. Bell, E. Herbolsheimer, N. M. Hannett, K. Sun, D. T. Odom, A. P. Otte, T. L. Volkert, D. P. Bartel, D. A. Melton, D. K. Gifford, R. Jaenisch, and R. A. Young.** 2006. Control of Developmental Regulators by Polycomb in Human Embryonic Stem Cells. **125:**301-313.

33. **Lia, G., E. Praly, H. Ferreira, C. Stockdale, Y. C. Tse-Dinh, D. Dunlap, V. Croquette, D. Bensimon, and T. Owen-Hughes.** 2006. Direct observation of DNA distortion by the RSC complex. Mol Cell **21:**417-25.
34. **Lowe, S. W., and C. J. Sherr.** 2003. Tumor suppression by Ink4a-Arf: progress and puzzles. Current Opinion in Genetics & Development **13:**77-83.
35. **Lund, A. H., and M. van Lohuizen.** 2004. Epigenetics and cancer. Genes Dev **18:** 2315-2335.
36. **Mateos-Langerak, J., M. Bohn, W. de Leeuw, O. Giromus, E. M. M. Manders, P. J. Verschure, M. H. G. Indemans, H. J. Gierman, D. W. Heermann, R. van Driel, and S. Goetze.** 2009. Spatially confined folding of chromatin in the interphase nucleus, p. 3812-3817, vol. 106.
37. **Merchav, s., and G. Wagemaker.** 1984. Detection of murine bone marrow granulocyte/macrophage progenitor cells (GM-CFU) in serum-free cultures stimulated with purified M-CSF or GM-CSF. Int J Cell Cloning **2:**356-67.
38. **Merlo A, H. J., Mao L, Lee DJ, Gabrielson E, Burger PC, Baylin SB, Sidransky D. .** 1995. 5' CpG island methylation is associated with transcriptional silencing of the tumour suppressor p16/CDKN2/MTS1 in human cancers. Nat Med. **1:**686-92.
39. **Nigg, E. A.** 2002. Centrosome aberrations: cause or consequence of cancer progression? Nat Rev Cancer **2:**815-825.
40. **Ohtani, N., Z. Zebedee, T. J. G. Huot, J. A. Stinson, M. Sugimoto, Y. Ohashi, A. D. Sharrocks, G. Peters, and E. Hara.** 2001. Opposing effects of Ets and Id proteins on p16INK4a expression during cellular senescence. Nature **409:**1067-1070.
41. **Oruetxebarria, I., F. Venturini, T. Kekarainen, A. Houweling, L. M. Zuijderduijn, A. Mohd-Sarip, R. G. Vries, R. C. Hoeben, and C. P. Verrijzer.** 2004. P16INK4a is required for hSNF5 chromatin remodeler-induced cellular senescence in malignant rhabdoid tumor cells. J Biol Chem **279:**3807-16.
42. **Rhee, I., K. E. Bachman, B. H. Park, K.-W. Jair, R.-W. C. Yen, K. E. Schuebel, H. Cui, A. P. Feinberg, C. Lengauer, K. W. Kinzler, S. B. Baylin, and B. Vogelstein.** 2002. DNMT1 and DNMT3b cooperate to silence genes in human cancer cells. Nature **416:**552-556.
43. **Roberts, C. W., and S. H. Orkin.** 2004. The SWI/SNF complex--chromatin and cancer. Nat Rev Cancer **4:**133-42.
44. **Saha, A., J. Wittmeyer, and B. R. Cairns.** 2002. Chromatin remodeling by RSC involves ATP-dependent DNA translocation. Genes Dev **16:**2120-34.
45. **Saha, A., J. Wittmeyer, and B. R. Cairns.** 2005. Chromatin remodeling through directional DNA translocation from an internal nucleosomal site. Nat Struct Mol Biol **12:**747-55.
46. **Schlesinger, Y., R. Straussman, I. Keshet, S. Farkash, M. Hecht, J. Zimmerman, E. Eden, Z. Yakhini, E. Ben-Shushan, B. E. Reubinoff, Y. Bergman, I. Simon, and H. Cedar.** 2007. Polycomb-mediated methylation on Lys27 of histone H3 pre-marks genes for de novo methylation in cancer. Nat Genet **39:**232-236.
47. **Schwartz, Y. B., and V. Pirrotta.** 2007. Polycomb silencing mechanisms and the management of genomic programmes. Nat Rev Genet **8:**9-22.
48. **Sevenet, N., A. Lellouch-Tubiana, D. Schofield, K. Hoang-Xuan, M. Gessler, D. Birnbaum, C. Jeanpierre, A. Jouvet, and O. Delattre.** 1999. Spectrum of hSNF5/INI1 somatic mutations in human cancer and genotype-phenotype correlations. Hum Mol Genet **8:**2359-68.

49. **Sevenet, N., E. Sheridan, D. Amram, P. Schneider, R. Handgretinger, and O. Delattre.** 1999. Constitutional mutations of the hSNF5/INI1 gene predispose to a variety of cancers. Am J Hum Genet **65:**1342-8.
50. **Shao, Z., F. Raible, R. Mollaaghababa, J. R. Guyon, C.-t. Wu, W. Bender, and R. E. Kingston.** 1999. Stabilization of Chromatin Structure by PRC1, a Polycomb Complex. Cell **98:**37-46.
51. **Sharpless, N. E.** 2005. INK4a/ARF: A multifunctional tumor suppressor locus. Mutation Research/Fundamental and Molecular Mechanisms of Mutagenesis **576:**22-38.
52. **Simao Tde A, S. G., Ribeiro FS, Cidade DA, Andreollo NA, Lopes LR, Macedo JM, Acatauassu R, Teixeira AM, Felzenszwalb I, Pinto LF, Albano RM. .** 2006. Lower expression of p14ARF and p16INK4a correlates with higher DNMT3B expression in human oesophageal squamous cell carcinomas Hum Exp Toxicol. 2006 Sep;25(9):515-22 **25:**515-22.
53. **Sluder, G., and J. J. Nordberg.** 2004. The good, the bad and the ugly: the practical consequences of centrosome amplification. Current Opinion in Cell Biology **16:**49-54.
54. **Storchova, Z., and D. Pellman.** 2004. From polyploidy to aneuploidy, genome instability and cancer. Nat Rev Mol Cell Biol **5:**45-54.
55. **Su, I. H., A. Basavaraj, A. H. Krutchinsky, O. Hobert, A. Ullrich, B. T. Chait, and A. Tarakhovsky.** 2003. Ezh2 controls B cell development through histone H3 methylation and Igh rearrangement. Nat Immunol. **4:**124-31.
56. **Tiwari, V. K., Cope,L. , McGarvey, K.M., Ohm, J.E.and Baylin, S.B. .** 2008. A novel 6C assay uncovers Polycomb-mediated higher order chromatin conformations. Genome Res. 2008. 18: 1171-1179 **18:**1171-1179.
57. **Tiwari, V. K., K. M. McGarvey, J. D. F. Licchesi, J. E. Ohm, J. G. Herman, Sch, uuml, D. beler, and S. B. Baylin.** 2008. PcG Proteins, DNA Methylation, and Gene Repression by Chromatin Looping, p. e306, vol. 6.
58. **Valk-Lingbeek, M. E., S. W. M. Bruggeman, and M. van Lohuizen.** 2004. Stem Cells and Cancer: The Polycomb Connection. **118:**409-418.
59. **Versteege, I., N. Sevenet, J. Lange, M. F. Rousseau-Merck, P. Ambros, R. Handgretinger, A. Aurias, and O. Delattre.** 1998. Truncating mutations of hSNF5/INI1 in aggressive paediatric cancer. Nature **394:**203-6.
60. **Vire, E., C. Brenner, R. Deplus, L. Blanchon, M. Fraga, C. Didelot, L. Morey, A. Van Eynde, D. Bernard, J.-M. Vanderwinden, M. Bollen, M. Esteller, L. Di Croce, Y. de Launoit, and F. Fuks.** 2006. The Polycomb group protein EZH2 directly controls DNA methylation. Nature **439:**871-874.
61. **Vries, R. G., V. Bezrookove, L. M. Zuijderduijn, S. K. Kia, A. Houweling, I. Oruetxebarria, A. K. Raap, and C. P. Verrijzer.** 2005. Cancer-associated mutations in chromatin remodeler hSNF5 promote chromosomal instability by compromising the mitotic checkpoint. Genes Dev **19:**665-70.
62. **Whitehouse, I., C. Stockdale, A. Flaus, M. D. Szczelkun, and T. Owen-Hughes.** 2003. Evidence for DNA translocation by the ISWI chromatin-remodeling enzyme. Mol Cell Biol **23:**1935-45.
63. **Widschwendter, M., H. Fiegl, D. Egle, E. Mueller-Holzner, G. Spizzo, C. Marth, D. J. Weisenberger, M. Campan, J. Young, I. Jacobs, and P. W. Laird.** 2007. Epigenetic stem cell signature in cancer. Nat Genet **39:**157-158.
64. **Wong, M. C., S. R. Scott-Drew, M. J. Hayes, P. J. Howard, and J. A. Murray.** 2002. RSC2, encoding a component of the RSC nucleosome remodeling complex, is essential for 2 microm plasmid maintenance in Saccharomyces cerevisiae. Mol Cell Biol **22:**4218-29.

65. **Xue, Y., J. C. Canman, C. S. Lee, Z. Nie, D. Yang, G. T. Moreno, M. K. Young, E. D. Salmon, and W. Wang.** 2000. The human SWI/SNF-B chromatin-remodeling complex is related to yeast rsc and localizes at kinetochores of mitotic chromosomes. Proc Natl Acad Sci U S A **97:**13015-20.

66. **Zhang, Y., C. L. Smith, A. Saha, S. W. Grill, S. Mihardja, S. B. Smith, B. R. Cairns, C. L. Peterson, and C. Bustamante.** 2006. DNA translocation and loop formation mechanism of chromatin remodeling by SWI/SNF and RSC. Mol Cell **24:**559-68.

67. **Zofall, M., J. Persinger, S. R. Kassabov, and B. Bartholomew.** 2006. Chromatin remodeling by ISW2 and SWI/SNF requires DNA translocation inside the nucleosome. Nat Struct Mol Biol **13:**339-46.

Chromatin is a highly dynamic structure that plays a key role in the orchestration of gene expression patterns during cellular differentiation and development. The regulated alteration of chromatin structure, termed remodeling can be accomplished by covalent modification of histones or by the action of ATP-dependent remodeling complexes.

hSNF5/INI1 is a subunit of the ATP-dependent hSWI-SNF chromatin-remodelling complex. This gene is a tumour suppressor gene frequently mutated in malignant rhabdoid tumours (MRT). We have developed MRT-derived G401 cell lines lacking genomic hSNF5 gene, which can express wild type or mutant hSNF5 (S284L) upon induction. We also transduced wild type hSNF5 to parental malignant rhabdoid MON cell lines lacking endogenous hSNF5. In chapter2 we studied time course variation (24h, 48h and 5 days) of 22,500 genes/expressed sequence tags upon hSNF5/INI1 or mutant hSNF5 (S284L) induction or transfection. Our genome wide expression suggests that hSNF5 can function in both transcription activation and repression of genes. Whole genome expression profiling of hSNF5 cells revealed expression change of many E2F targets, including mitotic control genes and pre-replication complex. This study identifies hSNF5/INI1 target genes and provides evidence that hSNF5/INI1 may modulate cell cycle control through the regulation of the p16 INK4A-cyclinD/CDK4-pRb-E2F pathway.

In chapter3, we report that loss of hSNF5 function in MRT-derived cells leads to polyploidization and chromosomal instability. Re-expression of hSNF5 restored the coupling between cell cycle progression and ploidy checkpoints. In contrast, cancer-associated hSNF5 mutants harbouring specific single amino acid substitutions exacerbated poly- and aneuploidization, due to abrogated chromosome segregation. We found that hSNF5 activates the mitotic checkpoint through the p16INK4a-cyclinD/CDK4-pRb-E2F pathway. These results establish that poly- and aneuploidy of tumour cells can result from mutations in a chromatin remodeler.

In chapter4, we investigated how the balance between Polycomb group (PcG) silencing and SWI/SNF activation affects epigenetic control of the *INK4b-ARF-INK4a* locus in MRT cells. hSNF5 re-expression in MRT cells caused SWI/SNF recruitment and activation of $p15^{INK4b}$ and $p16^{INK4a}$, but not of $p14^{ARF}$. Gene activation by hSNF5 is strictly dependent on the SWI/SNF motor subunit BRG1. SWI/SNF mediates eviction of the PRC1 and PRC2 PcG silencers and extensive chromatin reprogramming. Concomitant with PcG complex removal, the mixed lineage leukemia 1 (MLL1) protein is recruited and active histone marks supplant repressive ones. Strikingly, loss of PcG complexes is accompanied by DNA methyltransferase DNMT3B dissociation and reduced DNA methylation. Thus, various chromatin states can be modulated by SWI/SNF action. Collectively, these findings emphasize the close interconnectivity and dynamics of diverse chromatin modifications in cancer and gene control.

In chapter5 we have tried to delineate the mechanism behind the INK4/ARF transcription during differentiation, aging and cancer. We analyzed the spatial organization of the INK4/ARF locus *in vitro* to detect the frequency of possible interactions between these genomic loci by 3C (Capturing Chromosome Conformation) technology. 3C analysis revealed that at least in Mon cells, Neonatal fibroblasts and Megakaryocyte-Erythrocyte progenitor cells, there is a physical and spatial interaction between $p15^{INK4b}$ and $p16^{INK4a}$ but not $p14^{ARF}$. Importantly, $p15^{INK4b}$ loses its physical interaction with $p16^{INK4a}$ upon induction of hSNF5, upon aging as well as differentiation. We applied RNA interference to deplete EZH2, the catalytic component of the Polycomb Repressive Complex2 (PRC2) in Mon cells and Neonatal fibroblasts, and we found EZH2 mediates this long-range gene silencing. Our data provide strong evidence that PcGs play a role in generating the repressive loop at the INK4/ARF locus. In conclusion we found that coordinate induction of $p15^{INK4b}$ and $p16^{INK4a}$ but not $p14^{ARF}$ during differentiation or aging is accompanied by down-regulation of EZH2 and reduced locus occupancy of PcG repressors. EZH2 depletion causes loss of PcG repressors on the INK4b and INK4a loci and resolution of the repressive loop. Therefore looping between $p15^{INK4b}$ and $p16^{INK4a}$ is EZH2-dependent.

Chromatine is een zeer dynamische structuur die een belangrijke functie rol spelt bij de regulatie van genexpressive gedurende cellulaire differentiatie en ontwikkeling. De gereguleerde verandering van de chromatine structuur, remodeling genoemd, kan worden gerealiseerd door covalente modificaties van de histonen of door de activiteit van ATP afhankelijke remodeling complexen.

hSNF5/INI1 maakt deel uit van het ATP afhankelijke hSWI-SNF chromatine remodelling complex. Het gen is een tumor suppressor dat vaak is gemuteerd in Malignant Rhabdoid Tumours (MRT). We hebben een MRT afgeleide cel lijn, G401 waarin het hSNF5 gen mist, die een wild type of mutante hSNF5 tot expressie kan brengen na inductie. We hebben ook wild type hSNF5 ingebracht in de malignant rhabdoid MON cel lijn. In hoofdstuk 2 hebben we een tijd reeks gedaan (1, 2, en 5 dagen) waarin we de genexpressie van 22500 genen hebben bekeken na inductie of transfectie van hSNF5 en de mutant hSNF5 (S284L). Onze genomische expressie studie suggereert dat hSNF5 een functie heeft in zowel transcriptie aktivatie als repressie. Het genomische expressie profiel van de hSNF5 geïnduceerde cellen liet een verandering zien in het expressie patroon van veel E2F gereguleerde genen, waaronder genen belangrijk tijdens de mitose and genen van het pre-replicatie complex. Deze studie heeft hSNF5/INI1 gereguleerde genen geïdentificeerd en laat zien dat hSNF5/INI1 de cel cyclus kan contoleren door de regulatie van de p16 INK4A-cyclinD/CDK4-pRb-E2F route.

In hoofdstuk 3 laten we zien dat het verlies van de functie van hSNF5 in MRT afgeleide cellen leidt tot polyploidi en chromosomale instabiliteit. Hernieuwde expressie van hSNF5 herstelt de koppeling tussen de cel cyclus progressie en ploidi controle punten. In tegenstelling hiertoe leidde kanker geassocieerde mutaties tot een verergering van de aneuploidi en polyploidi door een verstoring van de chromosoom segregatie. We vonden dat hSNF5 de mitotische controle punten activeerde via de p16 INK4a-cyclinD/CDK4-pRb-E2F signaal route. Deze resultaten laten zien dat poly- en anueploidy het resultaat kunnen zijn van mutatie in een chromatine remodeller.

In hoofdstuk 4 onderzoeken we hoe de balance tussen inactivatie van genexpressie door de Polycomb groep (PcG) en activatie door SWI/SNF activiteit de epigenetische controle van de *INK4b-ARF-INK4a* locus in MRT celllen beinvloed. Hernieuwde expressie van hSNF5 in MRT cellen veroorzaakte het recruiteren van SWI/SNF en de activatie van $p15^{INK4b}$ en $p16^{INK4a}$, maar niet van $p14^{ARF}$. De activatie door hSNF5 is volkomen afhankelijk van de SWI/SNF katalitische eiwit BRG1. SWI/SNF medieerd de verwijdering van PcG repressoren en veroorzaakt uitgebreide chromatine herprogrameringen. Tegelijkertijd met de verwijdering van het PcG complex, word het Mixed Lineage Leukemia 1 (MLL1) eiwit gerecuiteerd en worden zo repressieve histonen labels vervangen door actitieve markeringen. Verassend is dat het verlies van PcG complexen vergezeld word door de dissociatie van de DNA

methyltranferase DNMT3B en verlaagde DNA methylering. Samengevat, SWI-SNF activiteit moduleert het chromatine in verschillende stadia. Deze resultaten benadrukken de verbondenheid en dynamiek van de verschillende chromatine modificaties in gen regulatie tijdens kanker.

In hoofdstuk 5 hebben we geprobeerd het mechanisme dat tengrondslag ligt aan de regulatie van INK4A-ARF expressie tijdens differentiatie, kanker en veroudering op te helderen. We hebben de ruimtelijke organisatie van de INK4/ARF locus *in vitro* geanalyseerd om de frequentie van de interactie tussen de verschillende regios van de INK4A/ARF locus te bepalen met behulp van 3C technologie (Capturing Chromosome Conformation) technologie. 3C analyse liet zien dat er in Mon cellen, Neonatale fibroblasten en de Megakaryocyte-Erythrocyte voorlopers een directe fysieke interactie is tussen $p15^{INK4b}$ en $p16^{INK4a}$, maar niet met $p14^{ARF}$. Belangrijk is dat deze interactie verloren gaat na inductie van hSNF5 in MRT cellen, bij differentiatie en veroudering. We hebben RNA interferentie toegepast om Ezh2, de katalitische component van het Polycomb Repressieve Complex 2 (PRC2) te verwijderen in Mon cellen en Neonatale fibroblasten. Wij vonden hierbij dat EZH2 noodzakelijk is voor de repressieve chromatine loop. Deze resultaten vormen sterke aanwijzingen dat PcG eiwitten, en met name EZH2, een belangrijke rol spelen bij het vormen van een repressieve verbinding in de INK4/ARF locus. Concluderend hebben wij beschreven dat gecoördineerde inductie van $p15^{INK4b}$ en $p16^{INK4a}$ maar niet $p14^{ARF}$ gedurende differentiatie of veroudering vergezeld gaat met velaging van EZH2 en een verlies van PcG repressors op de locus. Dus is de verbinding tussen $p15^{INK4b}$ and $p16^{INK4a}$ afhankelijk van E(z)h2. Wij concluderen dat een PcG eiwit afhankelijke chromatiene loop een belangrijke rol speeld bij het koppelen van cel differentiatie en proliferatie.

Curriculum Vitae

Personal Details

Name: Sima Kheradmand Kia
Birth date: 26-11-1969
Birthplace: Tehran, Iran

Education and Research experience

1989-1993 B.Sc. Biology, major of Zoology, Shahid Beheshti University, Tehran, Iran

1993-1999 Research assistant, Biotechnology department, Pasture Institute, Tehran, Iran (Mutation analysis, Carrier Detection and Prenatal Diagnosis of DMD/BMD), Supervisor: Dr. S. Zeinali and Prof. dr. D.D. Farhud

1996-1998 M.Sc. Human Genetics, School of public Health, Tehran University of Medical Sciences & Health Services, Tehran-Iran.

1999-2002 Instructor and Researcher, faculty of Paramedicine, Iran University of Medical Sciences and Health Services, Tehran, Iran

2002-2004 Post-graduate program in Human Genetics, Department of Human Genetics, Leiden University, The Netherlands.

2004-2008 PhD Student, Department of Biochemistry, Erasmus University Medical Centre, Rotterdam, The Netherlands. (Prof.dr. C.P. Verrijzer)

2009-Present Postdoctoral fellow, Department of Clinical Genetics, Erasmus University Medical Centre, Rotterdam, The Netherlands (Dr. G. Mancini)

List of publications

Kheradmand Kia, S., P. Solaimani, E. Farahbakhshian, F. Pourfarzad, M. von lindern, and C.P. Verrijzer. 2009. An EZH2-Dependent Repressive Chromatin Loop Controls *INK4a* and *INK4b* Expression during Human Cell Differentiation, Aging and Senescence (Manuscript submitted)

Kheradmand Kia, S., M. M. Gorski, S. Giannakopoulos, and C. P. Verrijzer. 2008. SWI/SNF Mediates Polycomb Eviction and Epigenetic Reprogramming of the INK4b-ARF-INK4a Locus. Mol cell Biol **28**: 3457-3464.

Vries, R. G. J., V. Bezrookove, L. M. P. Zuijderduijn, S. Kherdmand Kia, A. Houweling, I. Oruetxebarria, A. K. Raap, and C. P. Verrijzer. 2005. Cancer-associated mutations in chromatin remodeler hSNF5 promote chromosomal instability by compromising the mitotic checkpoint. Genes Dev **19**. 665-670.

Vanmolkot, K. R. J., E. E. Kors, U. Turk, D. Turkdogan, A. Keyser, L. A. M. Broos, S. Kheradmand Kia, J. J. M. W. van den Heuvel, D. F. Black, J. Haan, R. R. Frants, V. Barone, M. D. Ferrari, G. Casari, J. B. Koenderink, and A. M. J. M. van den Maagdenberg. 2006. Two de novo mutations in the Na,K-ATPase gene ATP1A2 associated with pure familial hemiplegic migraine. Eur J Hum Genet **14**:555-560.

Hottenga, J. J., K. R. J. Vanmolkot, E. E. Kors, S. Kheradmand Kia, P. de Jong, J. Haan, G. M. Terwindt, R. R. Frants, M. D. Ferrari, and A. van den Maagdenberg. 2005. The 3p21.1-p21.3 hereditary vascular retinopathy locus increases the risk for Raynaud's phenomenon and migraine. Cephalalgia **25**: 1168-1172, vol. 25.

Kors*, E. E., K. R. J. Vanmolkot*, J. Haan, S. Kheradmand Kia, H. Stroink, L. A. E. M. Laan, D. S. Gill, J. Pascual, A. M. J. M. van den Maagdenberg, R. R. Frants, and M. D. Ferrari. 2004. Alternating Hemiplegia of Childhood: No Mutations in the Second Familial Hemiplegic Migraine Gene ATP1A2. Neuropediatrics **35 (5)**:293-296.

Erasmus MC
Universitair Medisch Centrum Rotterdam

PhD Portfolio Summary

Summary of PhD training and teaching activities

Name PhD student: Sima Kheradmand Kia Erasmus MC Department: Biochemistry Research School: Medical Genetic center (MGC) graduate school	PhD period: 15-06-2004 until 29-12-2008 Promotor: C.P. Verrijzer

1. PhD training	
	Year
General academic skills	
- Gene expression Data analysis System (Rosetta Resolver), Rosetta Resolver group, Amsterdam	2004
In-depth courses (e.g. Research school, Medical Training)	
- Analysis of microarray data	2004
- Browsing genes and genome with ensembl	2004
- Molecular Medicine	2005
- Basic and translational Oncology	2006
- Epigenetics and chromatine	2008
Presentations	
- 17th MGC symposium, September, Rotterdam	2007
- Winter School of the International Graduiertenkolleg "Transcriptional Control in Developmental processes". Kleinwalsertal	2007
- BSIK-SCDD Annual Members Meeting	
- BSIK-SCDD Annual Members Meeting	2007 2009
International conferences	
- International Symposium " Stem Cells, Development and Regulation"	2007-8
- Stem Cell, Punta Cana	2007
Seminars and workshops	
- MGC Promovendi Workshop	2005-6
- Dutch Chromatin community meeting	2005
2. Teaching activities	
Supervising Master's theses	
- Mechanism of INK4A regulation in human malignant rhabdoid tumor cells	2007-8

It was a long journey from Iran to finishing my thesis in Rotterdam and there are so many people who have contributed significantly to my work and my life here, I will attempt to remember you all within the next page!!. Peter, I would like to start with you, thank you for everything. I will never forget the day after my first interview when I told you that, I am pregnant and I want to do my PhD in your lab. It was a strange feeling both scary and exciting when I signed my contract in the hospital as I was concerned about my capability to be a good mother and efficient PhD student. However the last 4 years have flown by and we are nearing the end now. Thank you to accept me from a multidisciplinary, high profiling and what ever they called lab to your scientific, friendly, international and high quality lab. Thank you for your trust and for all of your scientific guidance, encouragement and your unending support. It was a great pleasure and honour to work with you, I have learnt a lot.

Dear Tokameh and Rob thank you for introducing me to Peter, your scientific support, your faith in me and most of all your friendship.
Rob thank you for INI project. Thank you also for your friendship and supporting us whenever we needed. Tokameh thank you for reading and editing my thesis, for gossiping and I hope to see you all soon in Rotterdam. We have had so many good times together.

I would like to thank my reading committee (Sjaak, Frank and Riccardo) for reading my thesis in such a short time.

I am deeply indebted to Marieke von Lidern for her collaboration and scientific discussion.

Many thanks to Lobke for the beginning of INI-project, even though we only had a limited time but it was unforgettable.

Grazia, thank you for your trust in me and patience while I finished up my thesis.

Thanks to all present and former lab members Gil (you are the best lab supervisor), Jan, Karin, Prashanth (special thanks for all fly-duty, your help saved a lot of time for Jasmin), Anna, Stavrus, Yuri, Elena, Ashok, Natasha, Ulko, Marcin, Tsung wai, Olaf, Erick Jan, Lisette, Adrie , Jeroen, Adone and Willem (You are a lab member too, even though you won't believe that!). Adone, we had a nice time in Punta Cana together. I wish you three, all the best in Singapore.
Parham, it was a great pleasure to meet you and work with you. Thank you. You are talented and I am sure you are going to have a bright scientific future. I hope you enjoy your new project in Stem cell group.

Petra and Wouter thank you for your time and teaching me the 3C method.

Dear Marjan and Hossein Najmabadi, Thank you so much for your best friendship and help during my master and PhD. It is a great pleasure and honour to have you in my committee.
Many Thanks to Ton and Pim (from Pc-support), Melle and Arthur, Angela, Marieke, Jasperina, Corina, Cecile, Rita, Tom (For helping me with the layout). I would like to thank Ali Imam for all scientific and cultural discution.
Elnaz, my paranymph, thank you for all cells and gossip and your never ending friendship. You are one of my best friends in the Netherlands.
Maryam, thank you for every thing, for being my sister in Leiden, without you it was difficult to be away from all my family. We had a lot of fun and some stressful moments together. Thank you for being an aunt for Jasmin and a true friend to me.
Gelare, Negin, Matt and Stefan, who made Jasmin feel at home thank you for all your friendship and help. I would also like to thank Family Arastafar and Saeedavi for their help during my PhD period.
Special thank to Anke and Max, our first land lord and lady in Leiden, for all Sinterklaas cadeautjes, teaching us Dutch culture and nice evenings we had together.
Ghazelle, I really appreciate your patient and your art. I am so sorry to change your painting many times and only thing I can say is, it is beautiful. Alex Pezeshkmehr thank you for designing the invitation card.
Thanks to Iranian community, who made this time wonderful, Omid, Payman, Vilo, Parisa, Ali, Ali Reza, Amir Hossein, Mehrnaz, Saeed, Sahar (I won't forget all your help), Babak, Medya, Mahban, Payam, Ronak, Ghazal and Farhad.
Maziaar, you are the best captain in the world! Farzin (Kabir), Hossein Deylami, Hossein Hojabr and Azam, you are always my best friends.
My special thank to Dr. Behrooz Broumand for all his effort, knowledge, support and his encouragement. I owe not only my health to you but also my scientific carrier. I gratefully acknowledge Dr. Paul Van der Boog for monitoring of my health in the Netherland.
Maman and Baba, Thank you, I love you, without your support and your love it was not possible to make it. Simin (I don't know how can I say thank you, your help and your support is always endless), Mohammad, Saman, Parastoo, Saeedeh , Bahman, Arian and Shirin thank you, your kindness, your love and all your support gave me a lot of energy to continue even it was hard to be far away from you. Hengameh, without your phone call and your mails, your friendship, your magic AASH and voice and of course fruitful gossips I would not have made it to this point! I am so glad that you want to join my party.
Many thanks to my parents in law (Zarrindokht & Saeed) for being wonderful grandparents to Jasmin, and for all their help during my PhD. Hossein, Jamileh, Mohsen and Nahid, I wish you all the best.

My dearest Farzin and my lovely Jasmin without your love and your help this thesis would not have been possible. Thank you so much specially for last two months for all your support during this period. My little Jasmin hope we can spend more time together after that.

5-azadC	5-aza-2-deoxycytidine
3C	Chromatin Conformation Capture
ADAM19	A disintegrin and Metallopeptidase Domain 19
ANGPT2	Angiopoietin 2
AT/RT	Teratoid/Rhabdoid Tumour
BAF	BRG1/Brm-Associated Factor
BMI1	B lymphoma Mo-MLV Insertion region1
BRCA1	Breast Cancer1
BRG1	Brahma-Related Gene1
CASP4	Caspase 4
CCNF	CyclinF
CDC25A	Cell Division Cycle 25 Homolog A
CDK	Cyclin-Dependent Kinase
CENPA	Centromere Protein A
CENPE	Centromere Protein E
ChIP	Chromatin Immunoprecipitation
CMP	Common Myeloid Progenitors
DNMT	DNA (cytosine-5-)-Methyltransferase 1
E2F1	E2F transcription factor 1
ETS2	V-ETS Avian Erythroblastosis Viruse26 Oncogene Homolog2
EZH	Enhancer of Zeste
FACS	Fluorescence Activated Cell Sorting
FAS	TNF receptorsuper family,member6
FOXO	Forkheadbox
GAS6	Growth Arrest Specific 6
BRM	Brahma
HDAC	Histone Deacetylase
HDFs	Human Diploid Fibroblasts
HEFs	Human Embryonic Fibroblasts
INI1	Integrase Interactor 1
Arf	Alternative translational Reading Frame
LOH	Loss of Heterozygosity
MAD2	Mitotic Arrest Deficient 2
MRT	Malignant Rhabdoid Tumours
MAP1	B Microtubule-Associated Protein 1B
MeDIP	Methylated DNA Immunoprecipitation
MEP	MegakaryocyteErythroid Progenitor
MLL	Mixed-Lineage Leukaemia
MPP	Multipotent Progenitors
PcG	Polycomb Group proteins
PHO	Pleiohomeotic
PhoRC	Pleiohomeotic Repressive complex
POLD3	Polymerase (DNA-directed) Delta3, accessory subunit
PRC1	Protein Regulatorof Cytokinesis1
PRC2	Protein Regulator of Ctokinesis2
Rb	Retinoblastoma
SERPINE2	Serpin Peptidase Inhibitor, clade E, member2
shRNA	Small hairpin RNA
SMARCB1	SWI/SNF related, Matrix Associated, Actin dependent Regulator of Chromatin, subfamily B, member1

SNF	Sucrose Non-Fermenting
SNR1	Snf5-Related1
ST-HSC	Short Term-Hematopoietic Stem Cells
SWI	Switching defective
TRIM22	Tripartite Motif-containing22
TrxG	Trithorax Group
YY1	Yin and Yang1 protein